ENVIRONMENTAL RESEARCH

RESEARCH AND TECHNOLOGY BRANCH

Environment
Ontario

ISBN 0-7729-8793-9

92-01666/

THE DEVELOPMENT OF A LONG-RANGE TRANSPORT MODEL WITH A NESTED FINE RESOLUTION GRID

R. A. C. PROJECT NO. 475C

Prepared for Environment Ontario by:

Dr. M. Niewiadomski and L. Shenfeld
The MEP Company

SEPTEMBER 1991

Cette publication technique n'est disponible qu'en anglais.

Copyright: Queen's printer for Ontario,
1991
This publication may be reproduced for
non-commercial purposes with appropriate
attribution.

PIBS 1681
log 91-9200-475

ACKNOWLEDGEMENT AND DISCLAIMER

This report was prepared for the Ontario Ministry of the Environment. The views and ideas expressed in this report are those of the author and do not necessarily reflect the views and policies of the Ministry of the Environment, nor does mention of trade names or commercial products constitute endorsement or recommendation for use. The Ministry, however, encourages the distribution of information and strongly supports technology transfer and diffusion.

Any person who wishes to republish part or all of this report should apply for permission to do so to the Research and Technology Branch, Ontario Ministry of the Environment, 135 St. Clair Avenue West, Toronto, Ontario, M4V 1P5, Canada.

Copyright: Queen's Printer for Ontario
This publication may be reproduced for non-commercial purposes with appropriate attribution.

ABSTRACT

A mesoscale meteorological model, Gesima and the long range transport Acid Deposition and Oxidant model (ADOM) have been interfaced to obtain a nested, mesoscale air pollution modelling system. The system can simulate the transport, chemical transformations and deposition of a wide range of atmospheric pollutants with a horizontal resolution as fine as 5 km. In this study the model has been applied to simulate a high ozone episode in Southern Ontario, for a Toronto centered domain of 340 x 340 km, with horizontal resolution of 20 km. The analysis of results focuses on areal distribution of ozone and the time series of ozone in selected locations, Guelph, Toronto and Oshawa. The results are shown to be in fairly good agreement with observations.

EXECUTIVE SUMMARY

Two existing numerical models: a German mesoscale meteorological model, Gesima and the long range transport Acid Deposition and Oxidant Model (ADOM) have been enhanced, adapted and interfaced to obtain a nested modelling system for simulations of the transport, chemical transformations and deposition of atmospheric pollutants.

The Gesima and a modified, mesoscale version of ADOM are 'nested' in the large scale ADOM domain. The role of Gesima is to provide the fine resolution fields of meteorological parameters, which for the 'regular', large scale/coarse resolution runs of ADOM are derived from the output of the spectral diagnostic model of the CMC at Dorval. The large scale ADOM provides the initial and boundary conditions for the mesoscale run. The interactions between Gesima and the large scale and mesoscale versions of ADOM are schematically represented in Figure 1.

To allow the nesting of Gesima in the large scale flow a 'nudging' technique has been introduced, with weak, artificial tendency terms forcing the mesoscale solutions towards the evolving large scale values.

The role of interfacing software developed under this project is to extract the input data necessary for the mesoscale run of ADOM from the output of Gesima and the large scale ADOM. Software has also been developed to process other input data for Gesima and mesoscale ADOM, such as the topography and land use information.

In order to test and validate the system, a simulation of a high ozone episode in Southern Ontario has been performed. The test run was carried out with horizontal resolution of 20 km in a Toronto centered area of 340 x 340 km. A period of 4 days, starting on August 1, 1988 was simulated.

The analysis of results of this run focuses on the areal distribution of ozone and nitric oxides and their diurnal variations in selected locations. The horizontal cross-sections of the ozone and NOx concentrations, presented in Figs. 17 to 92 show pronounced mesoscale variability, which cannot be simulated using the regional scale air pollution models such as the large scale ADOM. The modelled time series of ozone were in selected locations, Guelph, Toronto and Oshawa compared to the available observational data (see Figs. 113 - 116), and are in fairly good agreement with observations, especially near ground level.

TABLE OF CONTENTS

Page

1. INTRODUCTION 1

2. GESIMA AND ITS MODIFICATIONS 5

   2.1 Description 5
   2.2 Initialization 6
   2.3 Lateral boundary conditions 7
   2.4 Nudging 8

3. THE MESOSCALE ADOM 9

4. SIMULATION OF THE HIGH OZONE EPISODE (August 1-4, 1988) 10

   4.1 Introduction 10
   4.2 The nested grid, and the domain of simulations 11
   4.3 Topography of the domain and the land use data 13
   4.4 Gesima simulations 14
   4.5 ADOM simulations 15

5. RESULTS 16

   5.1 Gesima results 16
   5.2 Areal distribution of ozone 17
   5.3 Diurnal variations 19
   5.4 Comparison with observations 20

6. CONCLUSIONS 22

7. ACKNOWLEDGEMENTS 23

8. REFERENCES 24

Figures 1 to 116

THE DEVELOPMENT OF A LONG RANGE TRANSPORT MODEL WITH A NESTED FINE RESOLUTION GRID

1. INTRODUCTION

This report describes the development and testing of a nested grid, mesoscale air pollution modelling system, carried out under a contract with the Ontario Ministry of the Environment. The test run of the system concerns a high ozone episode over Southern Ontario in August 1988.

The system described here is capable of simulating the transport, chemical transformation and deposition of a wide range of air pollutants, with horizontal resolution of 5 to 20 km. The size of the domain of simulation can vary, depending on resolution, from about 100 x 100 km to 500 x 500 km. The described test run of the system for the Toronto area, was carried out in a domain of 340 x 340 km, with horizontal resolution of 20 km.

The resolution and the size of the domain place this system in the mesoscale, i.e. between the urban scale air quality models and the large scale models of long range transport of atmospheric pollutants (LRTAP). The mesoscale modelling capability is necessary to address the urban NOx/VOC issue with a view to understanding and eventually to controlling the precursor emissions and to quantify the subgrid scale variability of pollutant concentrations simulated by the LRTAP models.

The approach was to adapt, enhance and interface two models: a large scale Acid Deposition and Oxidant Model (ADOM), and a mesoscale meteorological model 'Gesima'. Gesima and the modified, mesoscale version of ADOM are then 'nested' in the large scale ADOM domain. Thus, the modelling system developed in this study consists of three main parts: the large scale ADOM, Gesima, and the mesoscale version of ADOM developed under this contract. The programs interfacing these three parts are also an important part of the system. The interactions between the system components are schematically represented in Figure 1.

The original, large scale version of ADOM uses the coarse resolution meteorological fields from the Canadian Meteorological Centre (CMC) spectral diagnostic model. The mesoscale ADOM requires three-dimensional fields of meteorological parameters like horizontal and vertical wind velocity, temperature, humidity, turbulent diffusion parameters etc., with a fine horizontal resolution. Such fields are generated in this project by Gesima. The role of the large scale ADOM, is to provide the initial and boundary conditions for the mesoscale simulations.

The development of the system and the performing of a test run for the Toronto area involved several tasks which are covered in detail in the following sections. The major tasks are:

- modifications of the mesoscale model Gesima, allowing 'nested' simulations and interfacing with mesoscale ADOM.
- adaptation of ADOM, to mesoscale application.
- development of the Gesima/mesoscale ADOM interface, to extract the data required by ADOM from the Gesima output.
- development of the large scale ADOM/mesoscale ADOM interface, to extract initial and boundary conditions values for the mesoscale run from the output of the large scale ADOM.
- assembling and processing the input data for the Gesima run, including the topography, land use data, and the meteorological data for the initial and boundary conditions, and for the large scale 'nudging' fields.
- assembling and processing the fine resolution input data for the mesoscale ADOM, including the emissions from point and area sources and geophysical data.
- performing the 'production runs' of Gesima and mesoscale ADOM. The large scale ADOM was not run under this project, the results of an earlier run were used instead.

This project is a continuation of the research performed by M. Niewiadomski at the University of Toronto, under a postdoctoral fellowship from the Ontario Ministry of the Environment. Under that project (Niewiadomski et al., 1989, Niewiadomski, 1989, 1990a) Gesima was run on a smaller domain in the Toronto area, with a horizontal resolution of 5 km. Early versions of subroutines preparing the Gesima output in a form suitable for the mesoscale ADOM were developed, but neither the development of the full Gesima/ADOM and the mesoscale ADOM/large scale ADOM interfaces nor the running of the mesoscale ADOM were attempted. A separate task for this project was to rewrite all the JCL codes developed previously, since in the summer of 1990 the CRAY operating system used at the Ontario Centre for Large Scale Computation (CLSC) changed from COS to UNICOS.

A short description of the objectives and approach of this project and main features of Gesima and ADOM were presented at the Technology Transfer Conference in November 1990 (Niewiadomski 1990b). The application of Gesima and its modifications developed for this project, especially in areas of initialization and 'nudging' techniques were also presented and discussed during the author's visit at GKSS in Geesthacht, Germany in April 1991. The 'nudging' procedures generated some interest among the German scientists and may be implemented in the future at that centre.

The following sections provide a general information about ADOM and Gesima models and their interfaces, describe a test run of the system and discuss the results.

2. GESIMA AND ITS MODIFICATIONS

2.1 Description

Gesima (GEesthacht SImulation Model of the Atmosphere) is a sophisticated, meteorological mesoscale model developed at the GKSS Forschungszentrum, a research centre in Geesthacht, Germany, sponsored by the German federal government.

The model solves the non-hydrostatic, anelastic equations of motion in terrain-following coordinates using a predictor-corrector scheme (for the detailed description of the dynamics and numerics of the model see Kapitza, 1987). The dynamic pressure is computed using a conjugated gradients method (Kapitza and Eppel, 1987). The turbulent diffusion is parameterized according to the mixing length approach. A sophisticated surface layer module is used for computing the heat and moisture balance at the ground level, taking into account the shortwave and longwave radiation, heat and moisture fluxes in soil etc. The model also includes a cloud module computing mixing ratios of cloud water, rain and cloud ice/snow (combined in one variable) using the 'bulk microphysics' approach (see Levkov et al, 1989a,b).

The version of the model, obtained from GKSS in November 1990, had been significantly restructured and improved over the older version that was previously used. These changes, include both coding and formulational enhancements and significantly improved the performance and reliability of Gesima. The model has been recently successfully applied to study sea-breeze the in Northern Germany (Jacob et al, 1990) and the boundary layer structure over Denmark (Mengelkamp 1991).

Information on Gesima and its modules can be found in the papers cited above. The full documentation of the model is currently being prepared and will be available from the GKSS in the near future. This section describes the most important extensions and modifications of Gesima developed under this project and enabling its application in the Toronto area, 'nesting' in large scale fields and its interfacing with ADOM.

2.2 Initialization

The original Gesima is initialized by horizontally uniform profiles of all parameters. Since, for this project more detailed information from the CMC spectral model was available, those data were used as initial fields of wind, temperature and humidity.

2.3 Lateral boundary conditions

Gesima can use several types of boundary conditions, including fixed value at the boundary, first or second derivative set to zero, or the Orlanski type (where the 'fixed' inflow value is modified according to the internal flow). No 'nesting' subroutines or the time dependent boundary conditions are available in the original model.

When the model is used over prolonged time period, only the fixed and Orlanski type conditions can accommodate evolving data from outside the domain, provided that the 'fixed' (i.e. not dependent on the internal conditions) inflow boundary values do in fact vary in time and space, according to the outer meteorological fields. A procedure for introducing time and space dependent inflow boundary values of all parameters has been developed under this project.

During the initial testing of the model, it has been discovered that the 'fixed' or Orlanski type boundary conditions for temperature (i.e. the only types that can accommodate the time dependent data from outer model) cause numerical instability in Gesima and produce unreasonable results, especially in the wind field. This led to the introduction of the concept of 'nudging' (see section 2.4) as an alternative way of introducing the time dependent information from the outer model to the mesoscale domain.

Despite of the introduction of 'nudging' for temperature, humidity and wind fields, the time dependent boundary conditions can still be used for all of the variables except temperature. In the present experiment however, the time dependent boundary conditions were determined only for humidity and cloud parameters.

2.4 Nudging

As mentioned above, the preliminary experiments showed, that it is impossible, due to numerical instabilities, to introduce in Gesima the time dependent inflow boundary conditions for temperature. This led to the introduction of the Newtonian relaxation or "nudging" technique, not only for the temperature but also for wind and humidity.

The concept of nudging (see for example Hoke and Anthes, 1976; Stauffer and Seaman, 1990; Seaman and Cole, 1991) involves introduction of additional, artificial tendency terms to the prognostic equations of the model, which force the solution of the mesoscale model toward the observed or modelled large scale conditions. This approach allows to combine the fine scale variability, with the large scale tendencies which cannot be simulated by the mesoscale model itself, and seems to be more efficient and reasonable than introducing those tendencies by means of the time dependent boundary conditions alone.

These artificial tendencies - the nudging terms, applied at each time step, are proportional to the difference between the values of large scale field at given grid point and the actual solution of the mesoscale model. The coefficient of proportionality - the nudging coefficient, can be a function of height and has values of the order of 0.0001/sec.

3. THE MESOSCALE ADOM

Compared to Gesima, the ADOM model is better known in Canada and relatively better documented (see for example Scire et al., 1986; Venkatram et al., 1988), so this section focuses only on its modifications for the mesoscale application. Since the model is written in a general way, in principle no special, mesoscale version of ADOM is necessary, and its run in a mesoscale domain should involve only the redefining of some control parameters (e.g. those specifying the grid) and, of course, providing appropriate input data.

However, the model has never been tested before in a nested, mesoscale grid, so it was expected, that many corrections or modifications would be required to make it behave properly in such a mesoscale run. Surprisingly, only a few modifications were necessary, including new subroutines for the time dependent boundary conditions.

The ADOM input data include meteorological fields, pollutant emissions and their initial and boundary concentrations, geophysical information, as well as some parameters controlling the execution of the model.

4. SIMULATION OF THE HIGH OZONE EPISODE (August 1 - 4, 1988)

4.1 Introduction

This section describes the test run of the system, i.e. its domain, sources of the input data and the procedures of operation. The episode for this study, August 1 - 4, 1988 was chosen because of the high ozone concentrations observed at that time in Southern Ontario, and the availability of the results of the large scale ADOM simulation and the observational data. The model was run for a Toronto centred area. A simulation for the same period in the Windsor area is planned for the phase II of this project.

A preliminary analysis of the results of this simulation is provided in Section 5. It discusses some Gesima results and focuses on the evolution of the ozone concentrations in some selected locations and its areal distribution in the whole domain.

4.2 The nested grid, and the domain of simulations

The large scale ADOM is routinely run on a 33 x 33 grid based on a polar stereographic projection with nominal horizontal resolution of 127 km (true at 60° N). That domain covers most of eastern North America. In the Toronto area, south of 60° N, the actual size of this 127 km grid is about 115 km.

In this simulation, the 'nested' grid of Gesima and mesoscale ADOM covers 9 cells of the large grid, including the Toronto cell and the 8 cells around it (that is the cells 15,17; 16,17; 17,17; 15,18; 16,18; 17,18; 15,19; 16,19 and 17,19 of the large scale ADOM grid). Thus, the mesoscale domain covers an area of about 120,000 km^2, with Metropolitan Toronto area located about 25 km south of its centre. This domain of 9 large cells is divided into 17 x 17 mesoscale cells, so that the horizontal resolution is about 20 km. A map of the area covered by the mesoscale domain, and its location on the large scale grid are shown in Figures 2 and 3, respectively.

The mesoscale domain applies to both Gesima and the mesoscale ADOM. However, while the whole domain of Gesima is subject of dynamic simulations (the boundary rows and columns numbered 0 and 18 lie outside the main 17 x 17 domain), in ADOM the boundary cells, with pollutant concentrations predetermined according to the boundary conditions, are located inside the main domain. Thus, the domain of simulation of ADOM is actually smaller than that of Gesima. This problem can be overcome in future simulations by redefining the domain of ADOM, (e.g. to a 19 x 19 domain) with the boundary cells outside the domain of Gesima.

The basic vertical structure of the large scale ADOM, with 12 variable depth layers has been retained for the mesoscale version of the model. The same structure was adopted for the Gesima simulations. The tops of the ADOM layers are located at 56.2, 135.8, 250.7, 416.3, 655.3, 1000.0, 1497.2, 2214.5, 3249.2, 4741.6, 6894.5, and 10000.0 metres above the ground level. The vertical resolution of the upper layers of ADOM is however too coarse for Gesima, so the 4 top layers of ADOM were split in two. In effect, 16 rather than 12 vertical layers are used in Gesima, with tops at 56.2, 135.8, 250.7, 416.3, 655.3, 1000.0, 1497.2, 2214.5, 2731.8, 3249.2, 3995.4, 4741.6, 5818.1, 6894.5, 8447.3, and 10000.0 m. The Gesima/ADOM interface averages the data from those split layers before using them in appropriate layers of ADOM.

Note that the above heights of the layer tops give only the reference values, since both Gesima and ADOM use terrain following height transformations, and the real thickness and top height of each layer depend on the location inside the domain. Although the two models use different height transformations, no attempt has been made to include in the Gesima/ADOM interface the adjustment of the Gesima output to slightly different depths of ADOM cells. It is believed, that in relatively flat terrain of southern Ontario, errors resulting from this inconsistency of vertical grids will be negligible. The implementation of a grid adjustment scheme is planned for the Phase II of the project.

4.3 Topography of the domain and the land use data

A significant amount of time and effort was spent to develop software extracting the necessary data from a magnetic tape obtained form the Surveys and Mappings Branch of the Energy Mines and Resources Canada, which contained in a digital form all cartographic information for a 1:250000 map. The task, while not impossible, proved however too cumbersome and time consuming as it involved extracting the coded contours of elevation from thousands of other cartographical features and converting the contours to the mean elevation in a given grid cell. The elevations for each of the 289 cells of the Toronto domain were instead subjectively read from topographical maps and manually entered in the data file. This procedure proved much faster than developing objective software. The contours of elevation in the mesoscale domain, obtained from these data are shown in Fig. 4.

Land use information for both Gesima and ADOM runs was extracted from an EPA database. The data contain percentages of coverage of a given grid cell by various land use categories. The grid has resolution of 1/6 deg latitude and 1/4 deg longitude.

4.4 Gesima simulations

Gesima was run for a period of 96 hours starting on August 1, 1988 at 00:00 GMT (July 31, 20:00 EDT). The time step of 45 sec was used throughout that period. Fields of wind velocity, temperature and humidity were subjected to 'nudging' (see Section 2.4). The nudging coefficient did not depend on height and was kept equal to 0.0001 s^{-1} for all these fields except the temperature, for which the coefficient was increased to 0.0005 s^{-1} in a part of the period of simulations.

The fields of velocity, temperature, humidity and cloud water were disposed to the front end computer and briefly analyzed in 3 hour intervals. The 'restart' files were stored on magnetic tape in 6 hour intervals. The simulations can be repeated with modified input parameters starting from any of those files. The same restart files can be used for the detailed analysis of any of the Gesima variables.

With the 45 sec time step, Gesima consumed from 100 to 270 CPU seconds of the CLSC CRAY computer, depending of the time of day and the meteorological situation. The total computer time of the 4 day simulation was about 4.5 CPU hours, i.e. roughly one hour per day.

4.5 ADOM simulations

As mentioned above, the large scale ADOM was not run under this project. The output files, from a previous simulation for the same period, were obtained from the O.M.E. These files, together with the output of Gesima were processed by the interfacing programs described in Section 3 and provided the input data for the mesoscale ADOM simulations.

Since the mesoscale ADOM requires Gesima output data, the ADOM run started one hour later then that of Gesima, at 01:00 GMT, on August 1, 1988 and continued for 95 hours. Thus the first ADOM results, after one hour of simulation, are available for 22:00 EDT on 31 July and the last one at 20:00 EDT on August 4, 1988. The simulations proceeded in separate runs for each day of the period. While the concentrations of all simulated pollutants stored on magnetic tape in OCON files are available for further analysis in hourly intervals, only 4 sets of restart files ORES and output files PRTOUT are available.

The mesoscale ADOM requires much less computer time to run than Gesima. The simulations consumed about 1300 CPU seconds per day. Thus the whole 4 day GESIMA/ADOM mesoscale simulation takes about 6 CRAY hours plus some overhead for processing the input and output data.

5. RESULTS

5.1 Gesima results

As mentioned above, the 3-D fields of wind velocity, temperature, humidity and cloud water were disposed to the front end computer in 3 hour intervals. The mean, maximal and minimal values at each level were computed from these data and compared to the mean, maximal and minimal values in the 'nudging' fields derived from the output of large scale CMC diagnostic model, to check if the modelled values stay within a reasonable range. Such comparison led to the mentioned above increase in the nudging coefficient for the temperature. The disposed 3-D fields allowed also to plot some two-dimensional, horizontal cross-sections, for wind velocity and other parameters. As an example, the wind velocity field at 12:00 GMT on August 1, 1988 is discussed below.

The contours of W-E (u) and S-N (v) components of wind velocity are shown in Figs. 5 and 6 for layer 1, Figs. 7 and 8 for layer 6 and Figs. 9 and 10 for layer 10 of the model (elevations of the tops of each layer of the Gesima domain are listed in Section 4.2). For comparison, corresponding 'nudging' velocities, derived from the large scale data are shown in Figs. 11 to 16. As can be seen, the wind field, while retaining the mean characteristics of the large scale winds, shows pronounced small scale variability, especially at the lower levels. Although the slightly increased wind velocity gradient over the NW shore of Lake Ontario can be seen in Figs. 5 and 6, the occurrence of lake-breezes is not clearly indicated. The 20 km horizontal resolution is likely too crude to simulate the local lake effects.

A comprehensive analysis of the Gesima results is planned for the Phase II of this project, which will include numerical evaluations of the effects of nudging coefficients on the modelled fields of wind and other parameters.

5.2 Areal distribution of ozone

Contours of the horizontal ozone distribution in the domain, as modelled by mesoscale ADOM, are shown in six hour intervals in Figs. 17 to 64. Data from three ADOM layers are included, level 1 denotes the first layer with mean elevation at about 25 m above the ground, while level 4 corresponds to about 330 m and level 7 to about 1250 m above the ground level. Elevations of the tops of all ADOM layers were listed in Section 4.2.

To explain the modelled areal distribution of ozone during the day and night, the concentrations of nitric oxide (NO) and nitrogen dioxide (NO_2) for levels 1 and 4, in 12 hour intervals are shown in Figs. 65 to 96.

The concentrations of NO and NO_2 and some other strong sources peak over the area of Metropolitan Toronto and become transported by the wind over the area. It may be noted, that at the surface, the ozone is scavenged to near zero level at night (see Fig. 64 for 02:00 a.m. EDT, Aug. 1) in the area influenced by the NO_x emissions, but remains over 30 ppb over the eastern area.

Evolution of the meteorological situation over Southern Ontario and surrounding areas during the period studied is shown in the surface synoptic maps included at the end of this report (Figs. 97 to 112).

The strong west to east gradient of ozone concentrations west of Toronto, which is shown in Fig. 70 at 14:00 EDT for the layer 1, can be explained by the synoptic meteorological conditions. The leading edge of the warm air mass which contained high ozone levels, moved eastward across Southern Ontario on Aug. 1 (see Figs. 97 to 102) reaching the Toronto area during the evening. Highest ozone concentrations on Aug. 1 are shown to occur in the south and western portion of the modelled area where it has been transported in the warm air mass into the Province.

5.3 Diurnal variations

The diurnal variations of the modelled ozone concentration is easier to analyze by concentration vs time graphics. Such plots have been prepared for a few selected locations and are discussed below.

To show the ozone level as determined by the large scale ADOM, an output has been produced for a cell on the western boundary of the modelled area, where the pollutant concentrations follow the boundary conditions, determined according to the large scale ADOM results.

It may be noted (see Fig. 113), that the large scale ADOM has produced the first peak of surface ozone on Aug. 1 at 18:00 EDT (78 ppb), the second peak at 15:00 EDT on Aug. 2 (72 ppb), a minor peak (50 ppb) 04:00 Aug. 3, which accompanied a major peak (128 ppb) aloft, another peak (100 ppb) on Aug.3 at 20:00 EDT and a peak of 70 ppb on Aug. 4 at 15:00 EDT. The timing of some of the peak ozone levels at the surface at the western edge of the area are difficult to explain from meteorology during the period.

For a location near Guelph, the model output at three elevations for ozone, nitric oxide and nitrogen dioxide is shown in Figs. 114, 115 and 116. It may be noted that the first peak in surface ozone occurs at 21:00 EDT on Aug. 1, possibly with the arrival of the warm polluted air, ozone then peaks at the more expected times of 15:00 EDT on Aug. 2, 14:00 EDT on Aug. 3 and maintains persisting high concentrations, near 80 ppb, from 13:00 to the end of simulations at 20:00 EDT on Aug. 4, 1988. It may be noted, that ozone at elevated levels peaked at almost the same times as at the surface, except during the early morning of Aug. 4 when ozone peaked aloft at the time when ozone at the surface was at a minimum.

5.4 Comparison with observations

In order to validate the ozone levels as computed by the ADOM/Gesima approach, the discussed above concentrations at the lowest model cell in the Guelph area are compared in Fig. 117 to the levels measured at the AQI station in Guelph. Similar comparisons are shown in Fig. 118 for the surface of the Toronto cell of the model and measurements at 26 Breadalbane in Toronto, in Fig. 119 for the level 4 elevation in Toronto and the measurements at the CN Tower, and in Fig. 120 for the surface modelled concentrations in the Oshawa area and the observations at the AQI station in Oshawa. Note, that due to the unavailability of the observed data for some hours, the periods shown in Figs. 117 to 120 may differ from those discussed in Section 5.3 and between each other.

Analyzing these figures, one should keep in mind, that while the measurements were taken at specified points, the modelled concentrations represent averages from a mesoscale ADOM cell of the size 20 x 20 km and the depth of 56 m for the 'level' 1 and 165 m for 'level' 4. Even so, the modelled and observed ozone concentrations are in fairly good agreement, especially for the surface locations in Toronto and Oshawa (Figs. 118, 120).

The times of maximum and minimum modelled concentrations coincide with those observed at the surface in Toronto and Oshawa (except for the secondary peaks in observed concentrations during the early morning of Aug 4, both in Toronto and Oshawa, which are not reflected in the model results). For the Guelph location (Fig. 117) the modelled peak occurs 3 hours after the observed one on Aug. 1, coincides on Aug. 2 and roughly on Aug. 4 and advances the observed peak by about 3 hours on Aug. 3.

The values of the modelled ozone concentrations are also in fairly good agreement with the observed ones, although the model does not predict the highest measured concentrations (e.g. 112

ppb observed in Toronto on Aug. 2 at 14:00 EDT versus 68 ppb modelled). These discrepancies can be partly attributed to a significant area and depth represented by an ADOM cell, compared to the point measurements.

The upper level data, both modelled and observed, have a much less regular diurnal variability (see Fig. 119). The modelled concentrations roughly agree with the observed ones, the biggest discrepancies being the peaks in the model results at 03:00 EDT on Aug. 2 and at 08:00 EDT on Aug 4 during the secondary and primary minima in observations.

6. CONCLUSIONS

A mesoscale modelling system for transport, chemical transformations and deposition of atmospheric pollutant has been designed, programmed and tested in one case study over Southern Ontario.

The system is capable to simulate the distribution of various air pollutants with the spatial resolution of 20 km or less. It can detect local effects in this scale, that are impossible to simulate with large scale models like the original version of ADOM.

The preliminary analysis of the simulation of the early August 1988 high ozone episode over Southern Ontario, showed reasonably good agreement of the model results with observations.

More comprehensive analysis of results of several case studies, and further improvements of the system are planned for the Phase II of this project.

7. ACKNOWLEDGEMENTS

We would like to thank the following Ministry of the Environment, Air Resources Branch personnel; Drs. P.K. Misra, C. Fung and R. Bloxom, for their assistance in this study.

8. REFERENCES

Hoke J.E. and R.A. Anthes (1976) The initialization of numerical models by dynamic initialization technique. Mon. Wea. Rev. 104, 1551 - 1556.

Jacob D., W. Koch, L., Levkov and D.P. Eppel (1990) Cloud formation within a sea-breeze circulation system. Proc. 4-th Conf on Mesoscale Processes, Boulder, Colorado June 25-29, 1990.

Kapitza H. (1987) Das dynamische Gerust eines nicht-hydrostatischen Mesoskalen-Modells der atmospharischen Zirculation. GKSS 87/E/35.

Kapitza H. and D. Eppel (1987) A 3-D Poisson solver based on conjugate gradients compared to standard iterative methods and its performance on vector computers. J. Comput. Phys. 68, 474 - 484.

Levkov L., D. Jacob, D. Eppel and H. Grassl (1989a) Framework of cloud parameterization including ice for 3-D mesoscale models. GKSS 89/E/7.

Levkov L., D. Jacob, D. Eppel and H. Grassl (1989b) Test of a parameterization scheme for cloud microphysical processes in a 3-D mesoscale model. Atmos. Research, 24, 193 - 208.

Mengelkamp H. T. (1991) Boundary layer structure over an inhomogeneous surface: simulation with a non-hydrostatic mesoscale model. Boundary Layer Meteorology, in press.

Niewiadomski M. (1989) Adaptation of a mesoscale atmospheric model to studies of air pollution in the Toronto area. Proc. Technology Transfer Conf. Toronto, November 20 - 21, 1989, 254 - 256.

Niewiadomski M. (1990a) Adaptation of a mesoscale atmospheric model to studies of air pollution in the Toronto area. Report for the Ontario Ministry of the Environment.

Niewiadomski M. (1990b) Mesoscale and long range transport models are combined to model pollutants from local and distant sources. Proc. Technology Transfer Conf. Toronto, November 19 - 20, 1990, 206 - 209.

Niewiadomski M., L. Levkov, D. Jacob and D. Eppel (1989) Three-dimensional numerical simulations of pollutant transport and acid rain formation in a mesoscale field of convective clouds. Proc. 6-th Joint AMS/APCA Conference on Applications of Air Pollution Meteorology, Anaheim, CA, pp. J26 - J30.

Scire J.S., F.W. Lurmann, P. Karamchandani, A. Venkatram, R. Yamartino, J. Young and J. Pleim (1986) ADOM/TADAP development program, Vol. 9: ADOM/TADAP user's guide. Report for the Ontario Ministry of the Environment, the Umweltbundesamt (Germany) and Environment Canada by the ERT Company, Newbury Park, California.

Seaman N.L. and C.D. Cole (1991) Application of four-dimensional data assimilation for generating three-day episodic meteorological fields over the Los Angeles basin suitable for air quality modeling. Proc. 7-th Joint AMS/APCA Conference on Applications of Air Pollution Meteorology, New Orleans, Louisiana, Jan. 13-18, 1991, pp 320 - 323.

Stauffer D.R. and N.L. Seaman (1990) Use of four-dimensional data assimilation in a limited-area mesoscale model. Part I: Experiments with synoptic scale data. Mon. Wea. Rev., 118, 1250 - 1277.

Venkatram A. (1981). Estimation of turbulence velocity scales in the stable and the unstable boundary layer for dispersion applications. In Air Pollution Modeling and Its Application I, C.D. Wispelaere Ed., Plenum Press, New York, 1981, pp 169 -179.

Venkatram A., P.K. Karamchandani and P.K. Misra (1988) Testing a comprehensive acid deposition model. Atmospheric Environment 22, 737 - 747.

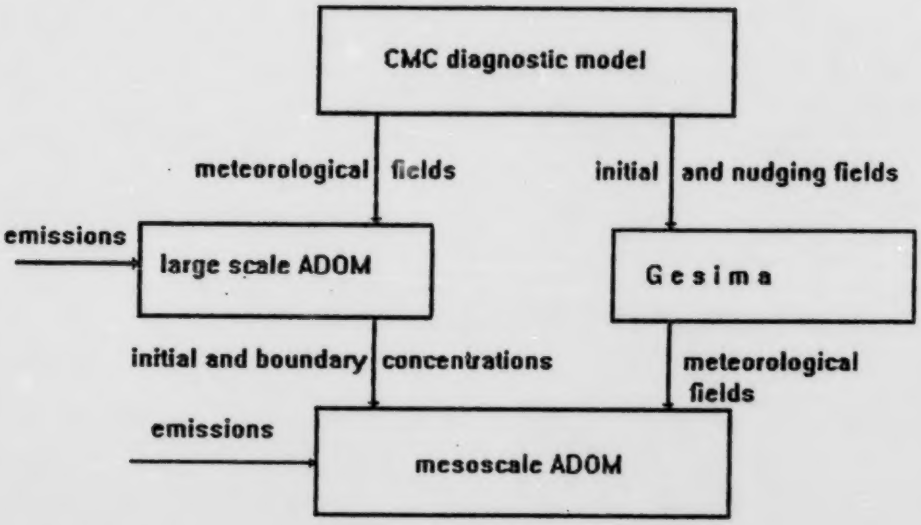
CMC diagnostic model
meteorological fields
initial and nudging fields
emissions
large scale ADOM
Gesima
initial and boundary concentrations
meteorological fields
emissions
mesoscale ADOM

Figure 1: Components and scheme of operation of the nested mesoscale modelling system.

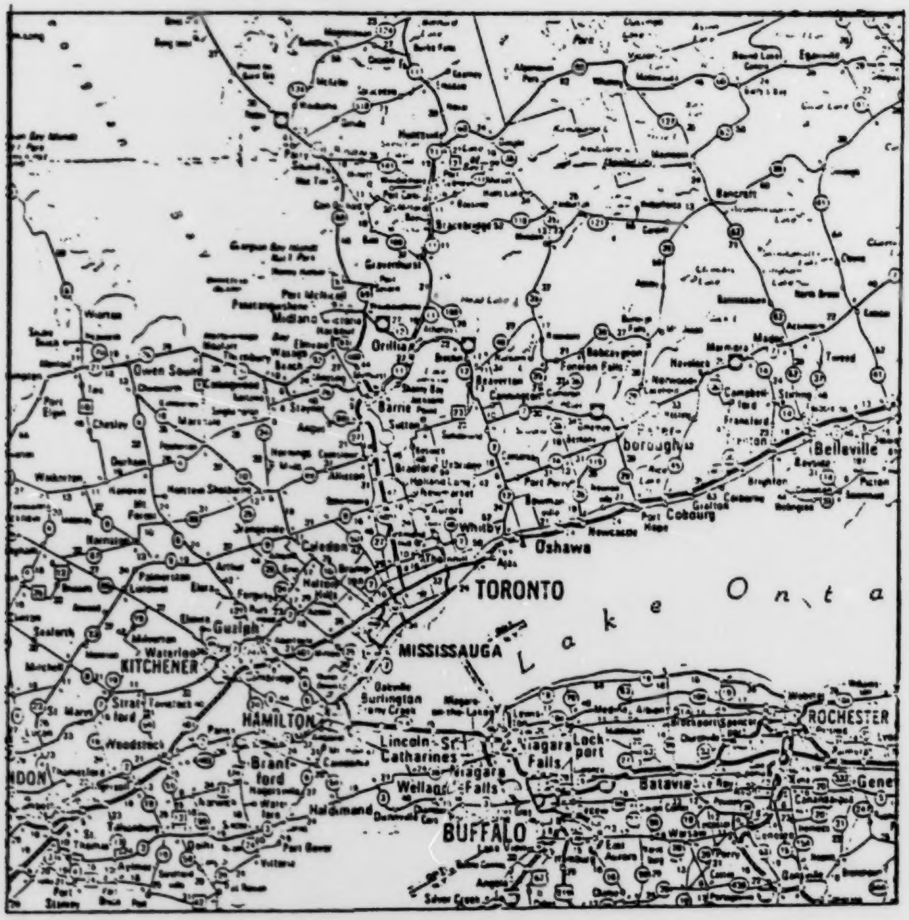
TORONTO
MISSISSAUGA
Lake Ontario
HAMILTON
KITCHENER
Guelph
Waterloo
BUFFALO
ROCHESTER
Oshawa
Whitby
Belleville
Peterborough
Cobourg
Barrie
Orillia
Owen Sound
Niagara Falls
St. Catharines
Welland
Lockport
Batavia
Brantford
Stratford
Woodstock
Burlington
Oakville
Midland
Gravenhurst
Bracebridge
Caledon
Haldimand
Lincoln

Figure 2: The mesoscale domain.

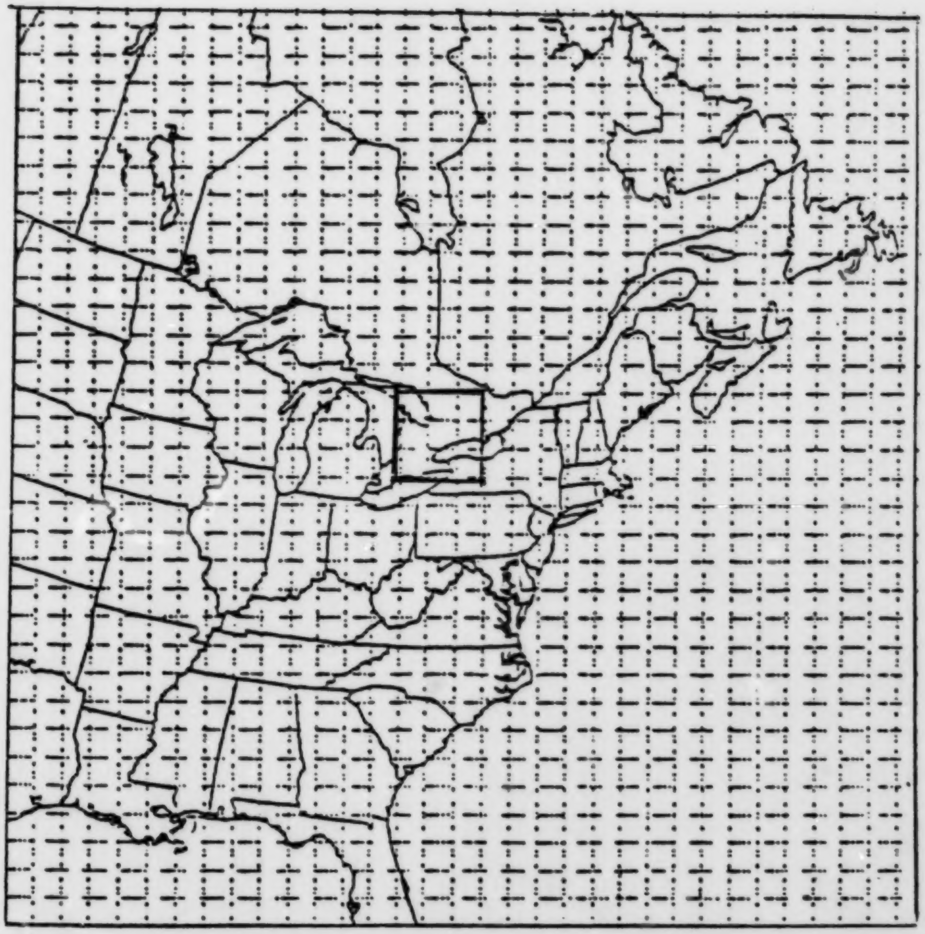

Figure 3: Domain of the large scale ADOM and location of the mesoscale domain.

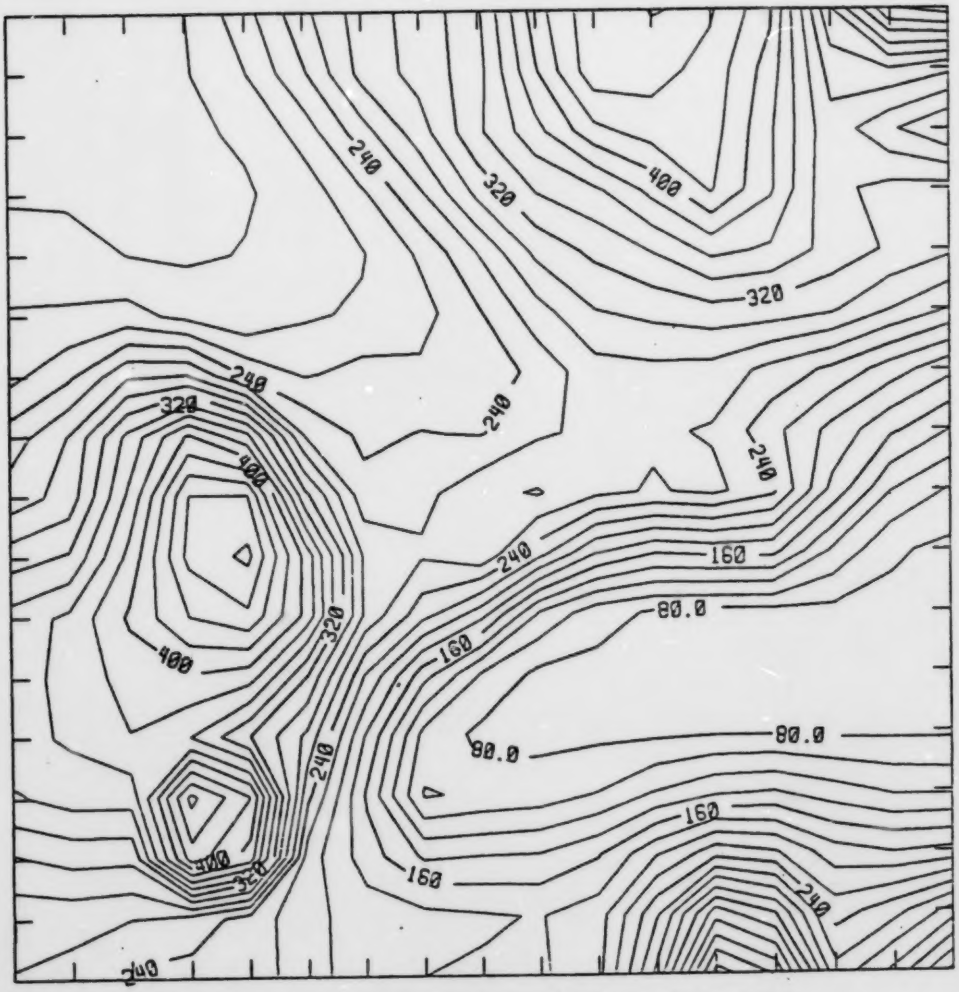
240
320
400
320
240
320
400
240
240
400
160
80.0
160
320
400
160
240
80.0
80.0
160
400
320
160
240
240

CONTOUR FROM 60.000 TO 400.00 CONTOUR INTERVAL OF 20.000 PT(3,3)= 305.00

Figure 4: The mesoscale domain, contours of elevation.

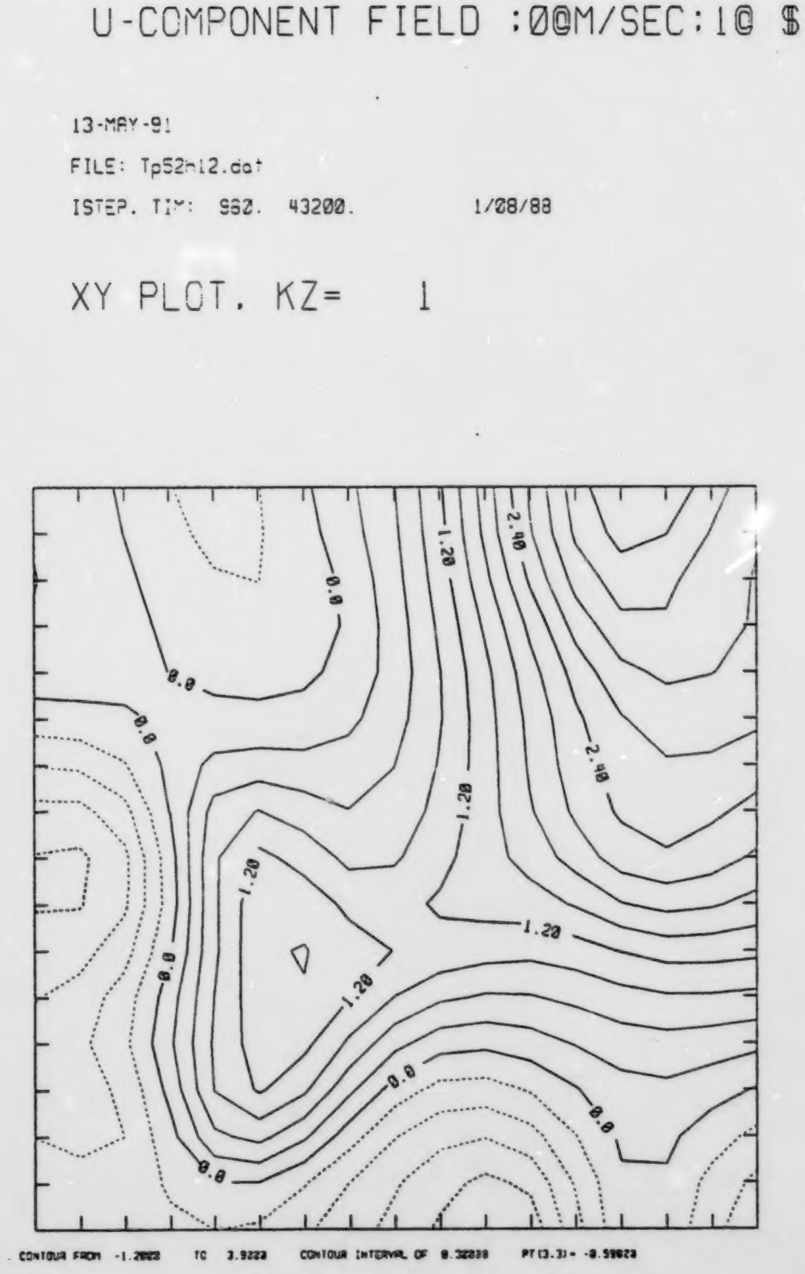
U-COMPONENT FIELD :0@M/SEC:1@ $
13-MAY-91
FILE: Tp52h12.dat
ISTEP, TIM: 962. 43200. 1/08/88
XY PLOT, KZ= 1
0.0
1.20
2.40
CONTOUR FROM -1.2000 TO 3.9000 CONTOUR INTERVAL OF 0.30000 PT(3,3)= -0.59020

Figure 5

V-COMPONENT FIELD :0@M/SEC:1@ $

13-MAY-91
FILE: Tp53h12.dat
ISTEP. TIM: 960. 43200.   1/08/66

XY PLOT. KZ= 1

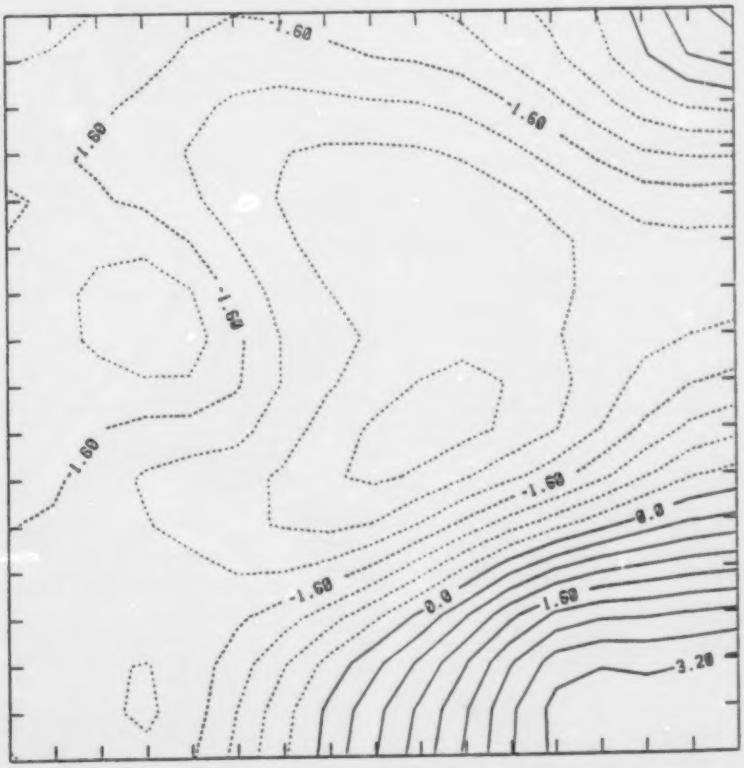

Figure 6

U-COMPONENT FIELD :0@M/SEC:10 $

13-MAY-91

FILE: Tp52h12.dat

ISTEP. TIM: 960. 43200. 1/08/88

XY PLOT. KZ= 6

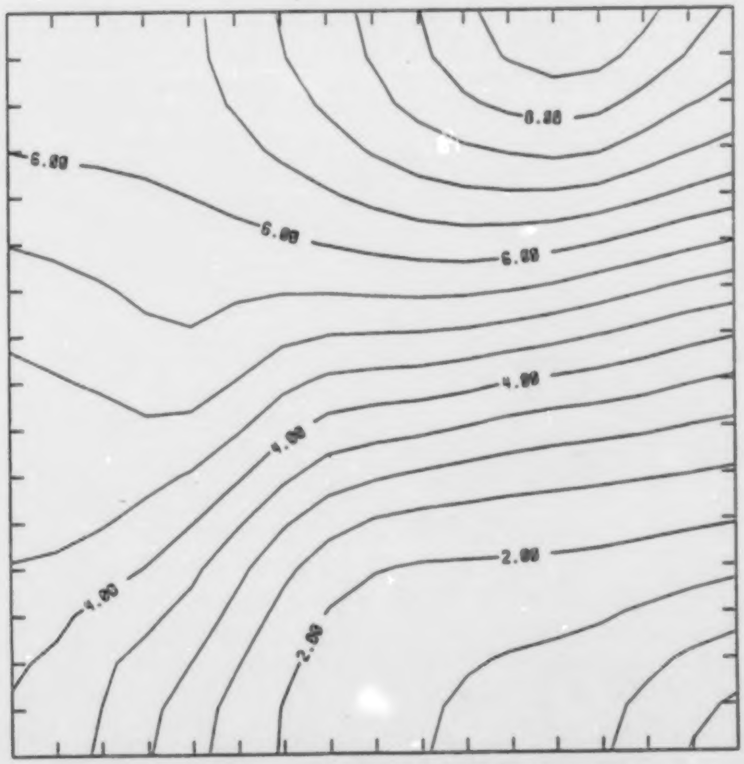

CONTOUR FROM 0.00000E+00 TO 8.5820 CONTOUR INTERVAL OF 0.50000 PT(3,3)= 3.5980

Figure 7

V-COMPONENT FIELD :00M/SEC:10 $

13-MAY-91

FILE: Tp53h12.dat

ISTEP. TIM: 960. 43200.   1/08/88

XY PLOT. KZ=   6

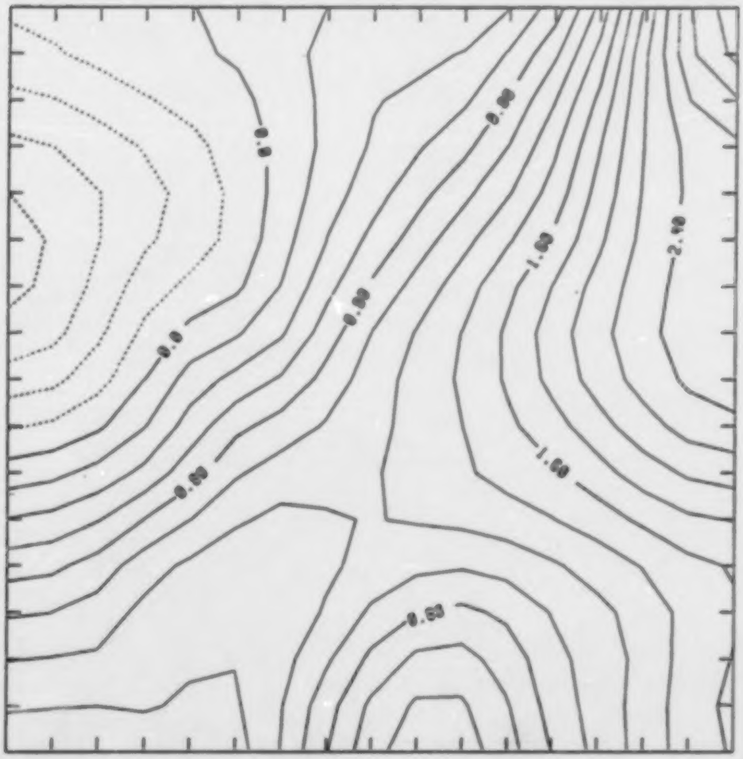

CONTOUR FROM -0.80000   TO   3.2000   CONTOUR INTERVAL OF 0.20000   PT(3,3)= 1.2338

Figure 8

U-COMPONENT FIELD :00M/SEC:10 $

13-MAY-91

FILE: Tp52h12.dat

ISTEP, TIM: 960. 43200.   1/08/88

XY PLOT, KZ= 10

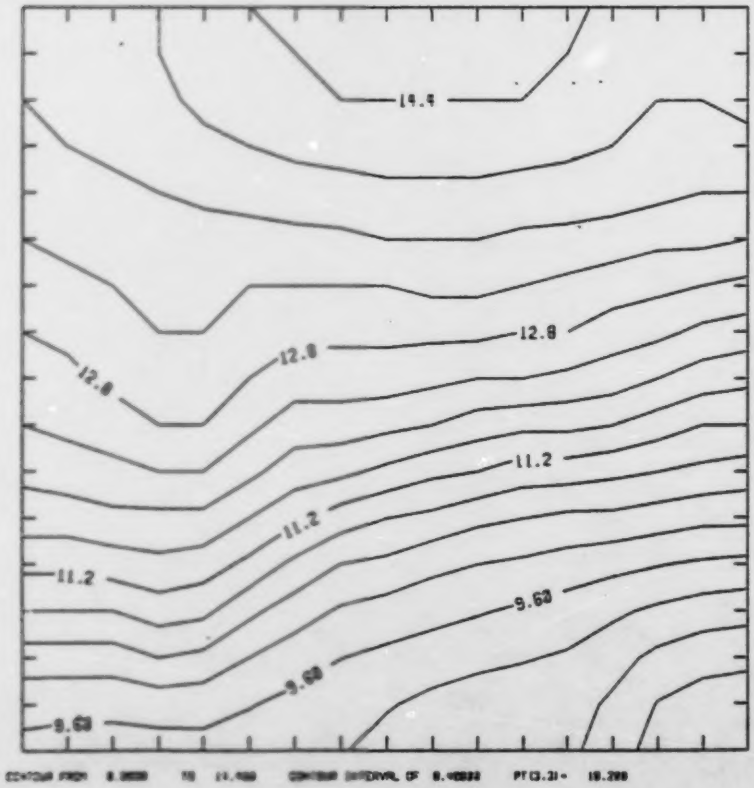

Figure 9

V-COMPONENT FIELD :00M/SEC:10 $

13-MAY-91

FILE: Tp53h12.dat

ISTEP. TIM: 960. 43200. 1/08/88

XY PLOT. KZ= 10

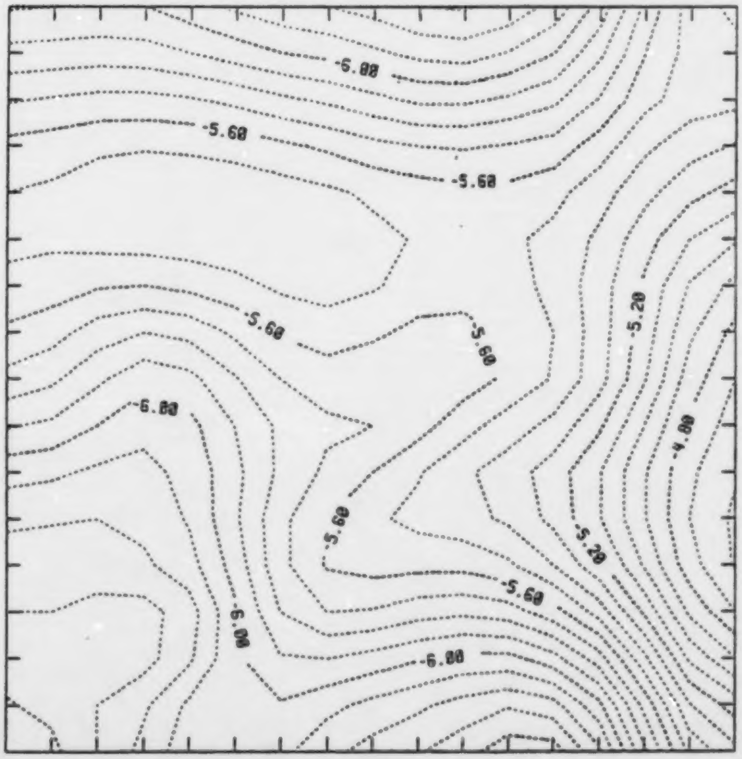

CONTOUR FROM -6.4000 TO -4.5200 CONTOUR INTERVAL OF 0.10000 PT(3,3)= -6.3200

Figure 10

U-COMPONENT FIELD :00M/SEC:10 $

10-MAY-91

FILE: Tp52nh12.dat

ISTEP. TIM: 0. 0. nudging field

XY PLOT. KZ= 1

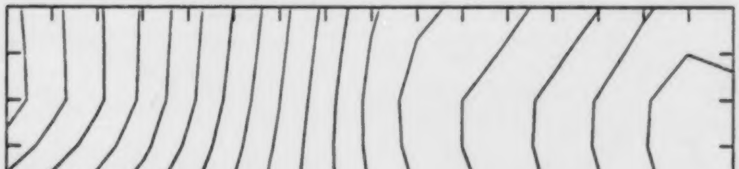

Figure 11

V-COMPONENT FIELD :00M/SEC:10 $

10-MAY-91

FILE: Tp53nh12.dat

ISTEP. TIM: 0. 0. nudging field

XY PLOT. KZ= 1

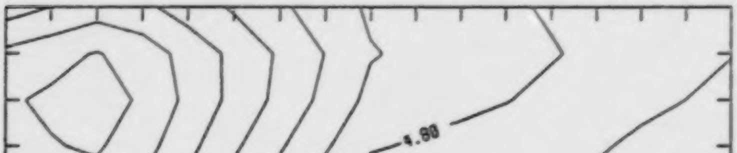

Figure 12

U-COMPONENT FIELD :0@M/SEC:1@ $

10-MAY-91

FILE: Tp52nh12.dat

ISTEP. TIM: 0. 0.   nudging field

XY PLOT. KZ=   6

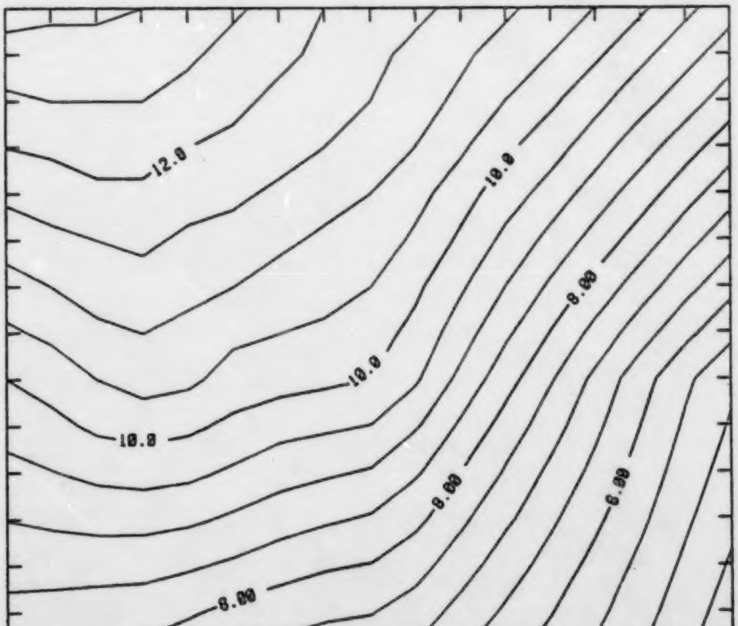

Figure 13

V-COMPONENT FIELD :0@M/SEC:1@ $

10-MAY-91

FILE: Tp53nh12.dat

ISTEP. TIM: 0. 0. nudging field

XY PLOT. KZ= 6

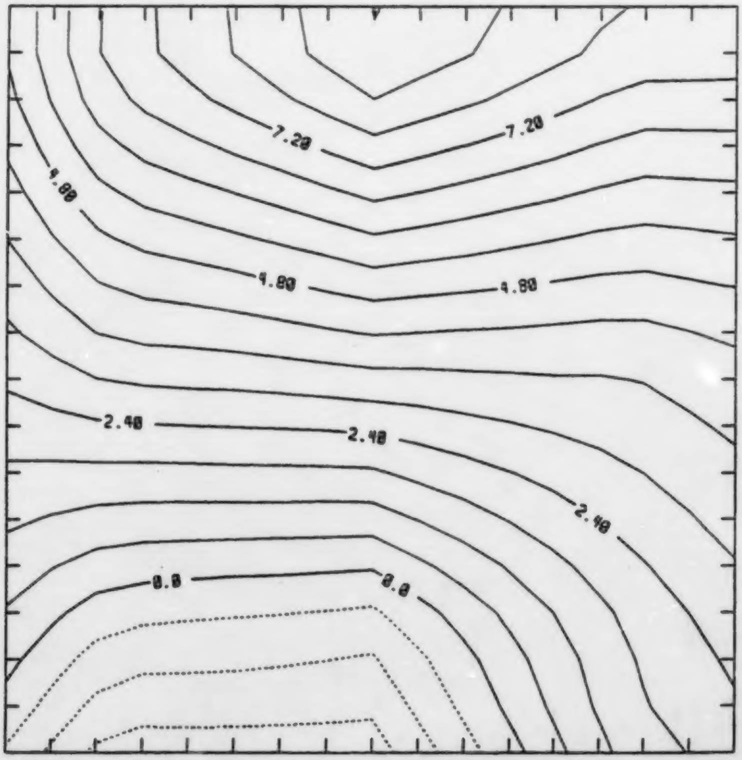

CONTOUR FROM -1.0000 TO 9.0000 CONTOUR INTERVAL OF 0.60000 PT(3,3)= -0.02700

Figure 14

U-COMPONENT FIELD :0@M/SEC:1@ $

10-MAY-91

FILE: Tp52nh12.dat

ISTEP. TIM: 0. 0.   nudging field

XY PLOT. KZ= 10

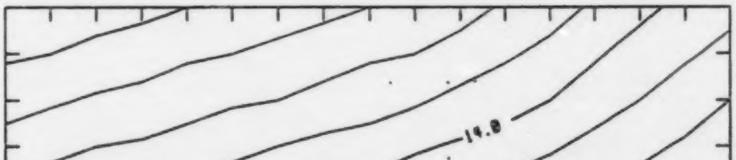

CONTOUR FROM 5.6000 TO 17.500 CONTOUR INTERVAL OF 0.70000 PT(3,3)= 8.1200

Figure 15

V-COMPONENT FIELD :00M/SEC:10 $

10-MAY-91

FILE: Tp53nh12.dat

ISTEP. TIM: 0. 0.   nudging field

XY PLOT. KZ= 10

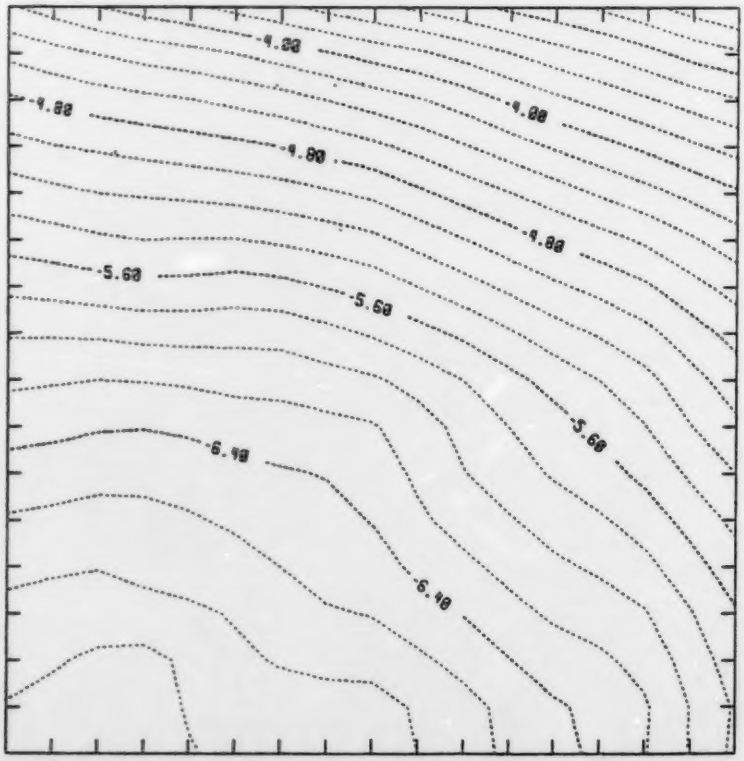

CONTOUR FROM -7.0000 TO -2.4000 CONTOUR INTERVAL OF 0.20000 PT(3,3)= -7.0300

Figure 16

03 concentration (ppb)
1 Aug 1988 2:00 a.m

LEVEL = 1 03

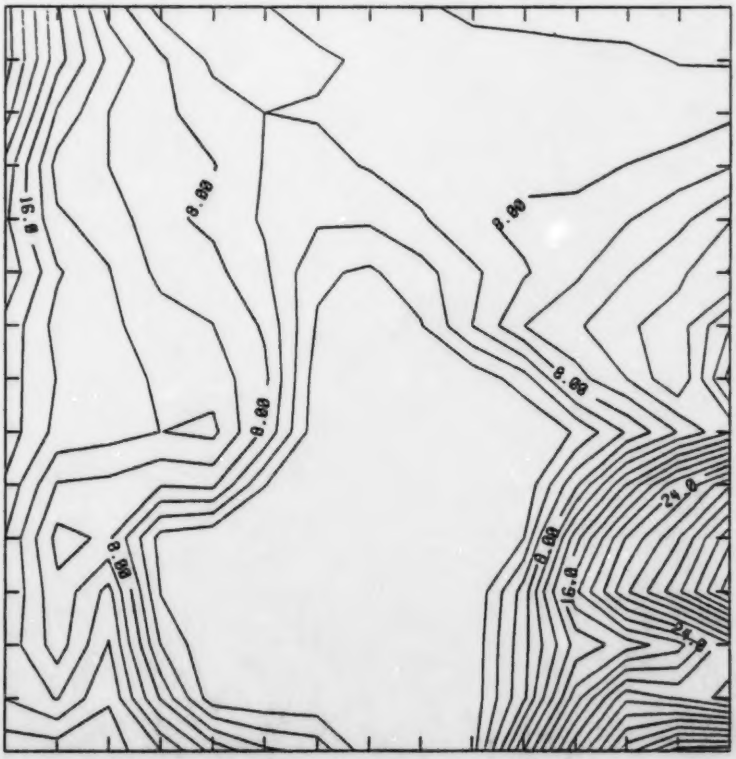

CONTOUR FROM 0.20000E-23 TO 40.000 CONTOUR INTERVAL OF 2.0000 PT(3,3)= 14.149

Figure 17

O3 concentration (ppb)
1 Aug 1988 2:00 a.m

LEVEL = 1 O3

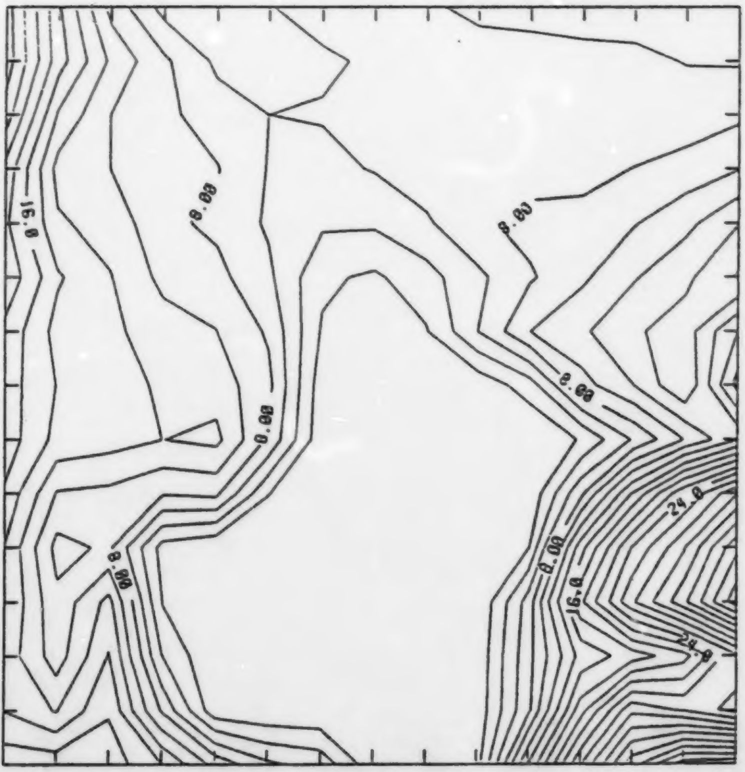

CONTOUR FROM 0.20000E-22 TO 48.000 CONTOUR INTERVAL OF 2.0000 PT(3,3)= 19.149

Figure 17

O3 concentration (ppb)
1 Aug 1988 2:00 a.m

LEVEL = 4 O3

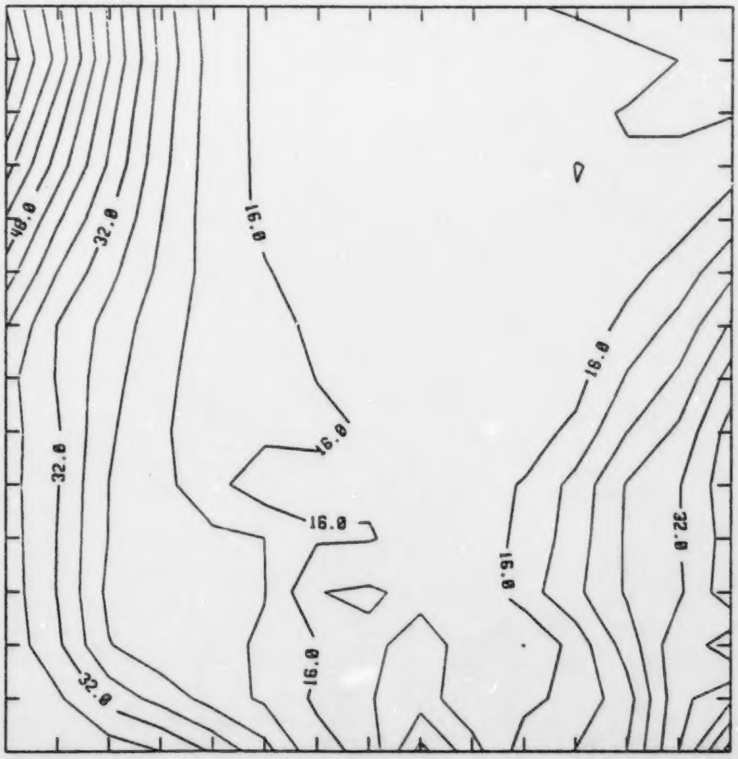

CONTOUR FROM 0.83096E+00 TO 64.229 CONTOUR INTERVAL OF 4.0000 PT(3,3)= 24.284

Figure 18

O3 concentration (ppb)
1 Aug 1988 2:00 a.m.

LEVEL = 7 O3

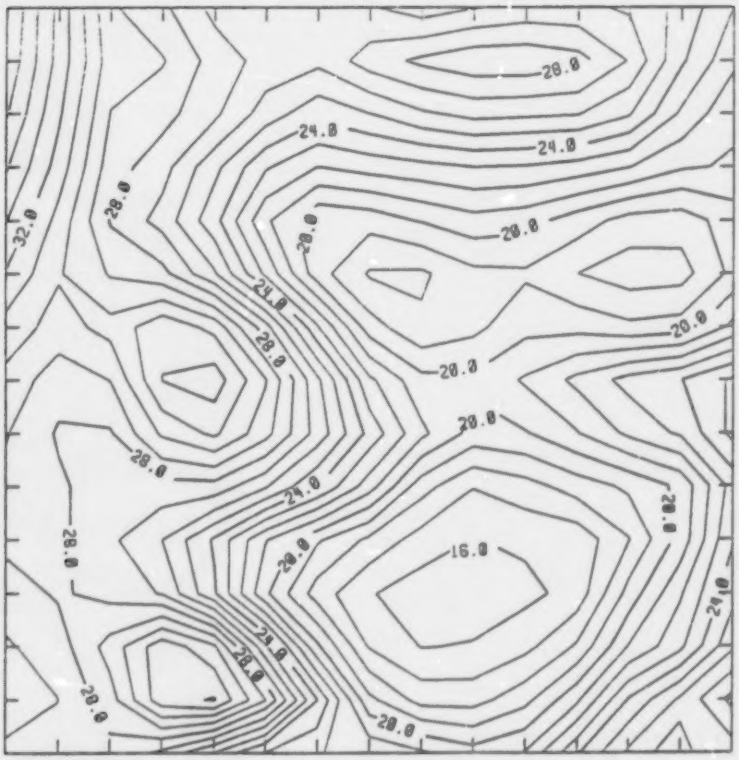

Figure 19

O3 concentration (ppb)

1 Aug 1988 8:00 a.m.

LEVEL = 1 O3

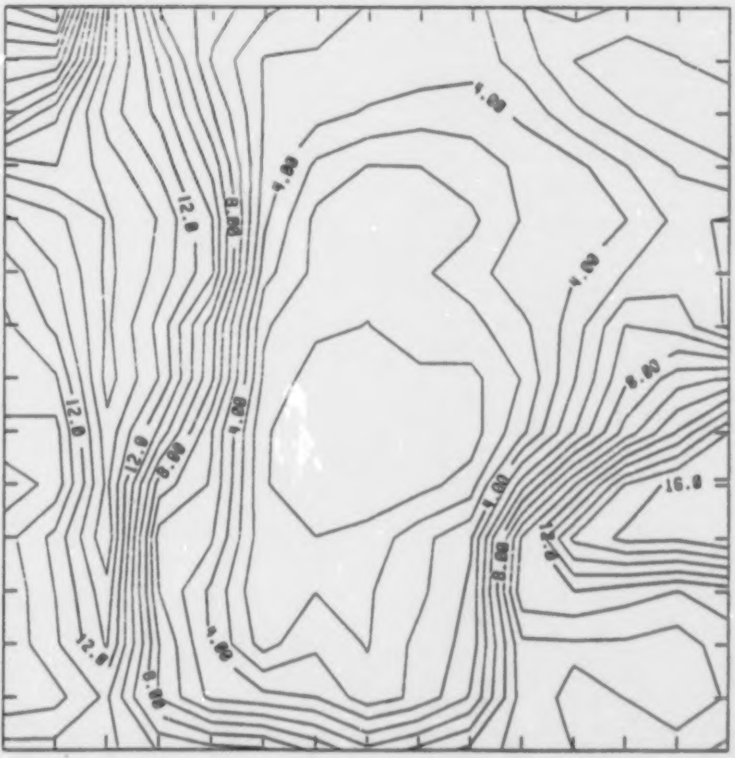

CONTOUR FROM 0.00000E+00 TO 20.000 CONTOUR INTERVAL OF 1.0000 PT(3,3)= 13.125

Figure 20

O3 concentration (ppb)

1 Aug 1988 8:00 a.m.

LEVEL = 4 O3

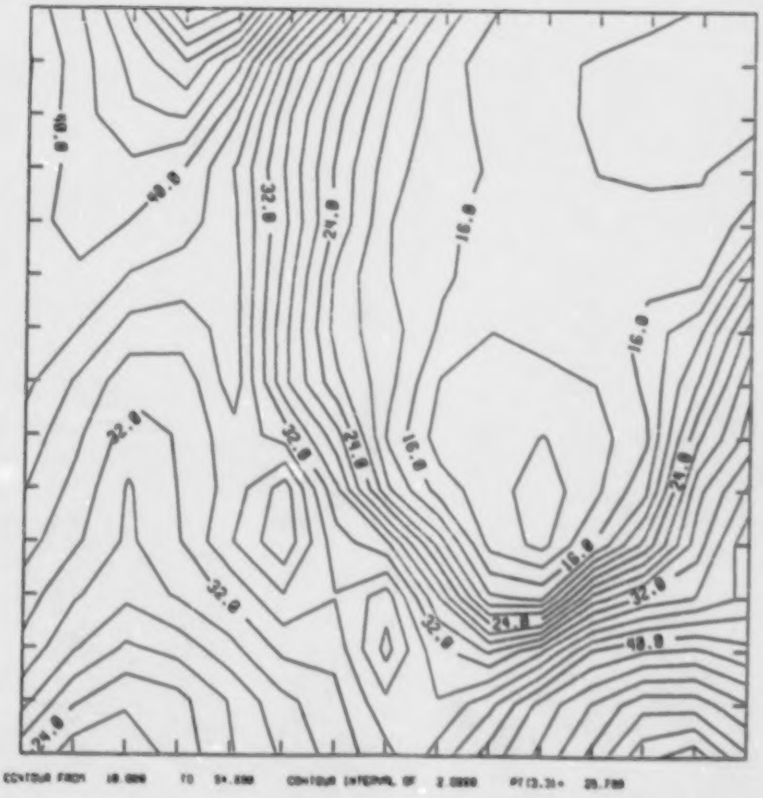

Figure 21

O3 concentration (ppt)
1 Aug 1988 8:00 a.m.)

LEVEL = 7 O3

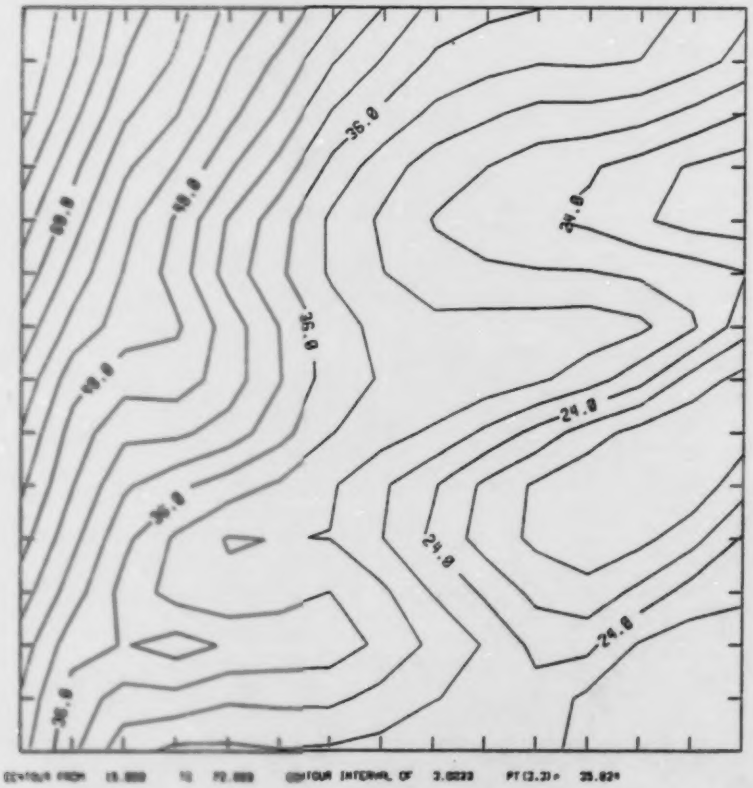

Figure 22

O3 concentration (ppb)
1 Aug 1988 2:00 p.m.

LEVEL = 1 O3

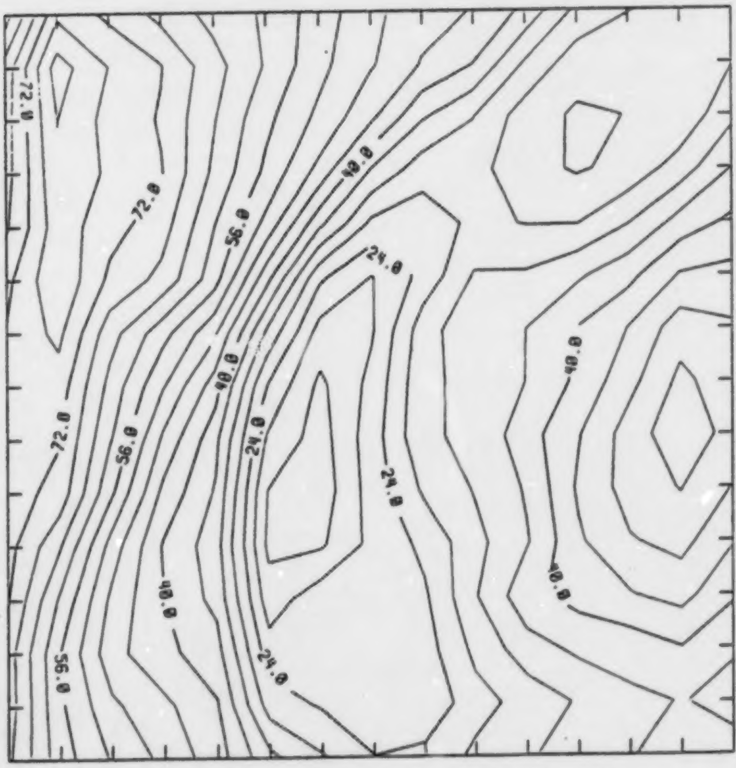

CONTOUR FROM 12.000 TO 80.000 CONTOUR INTERVAL OF 4.0000 PT(3,3)= 45.337

Figure 23

O3 conc. (ppb)
01/08/88 2:00 p.m.

LEVEL = 4 O3

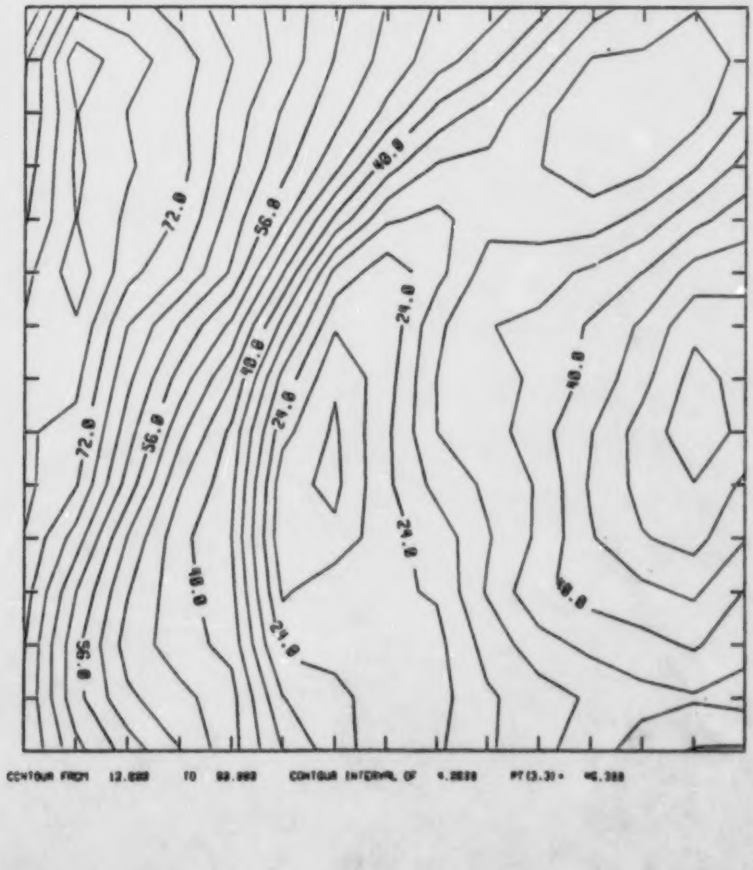

Figure 24

O3 conc. (ppb)

01/08/88 2:00 p.m.

LEVEL = 7 O3

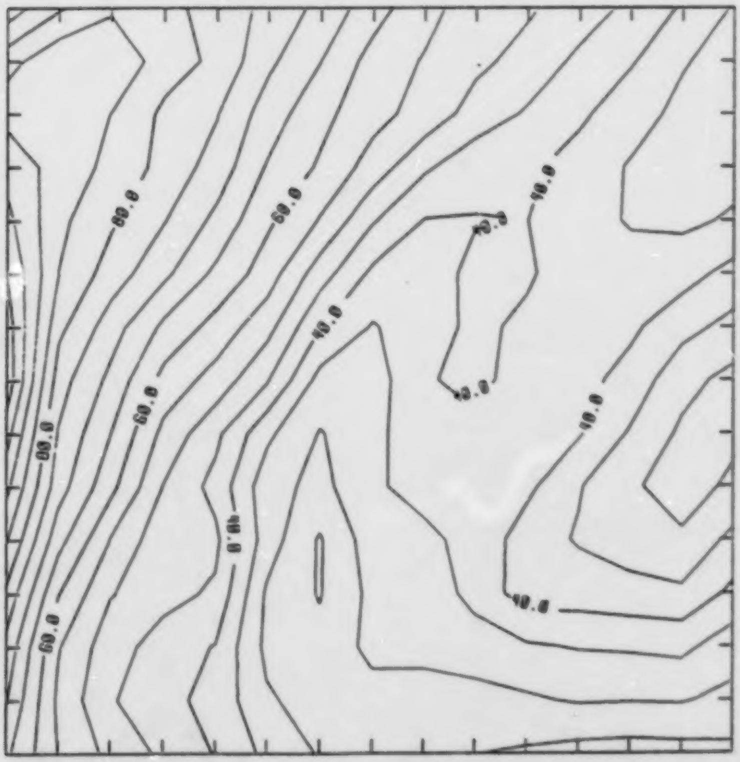

Figure 25

O3 conc. (ppb)

01/08/88 8:00 p.m.

LEVEL = 1 O3

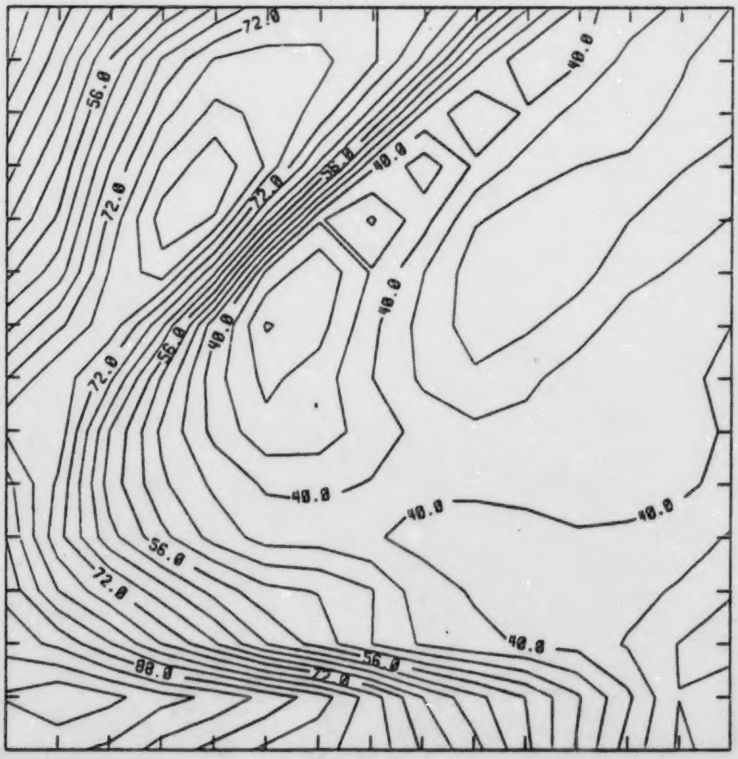

CONTOUR FROM 24.000 TO 100.00 CONTOUR INTERVAL OF 4.0000 PT(3,3)= 64.282

Figure 26

O3 conc. (ppb)

01/08/88 8:00 p.m.

LEVEL = 4 O3

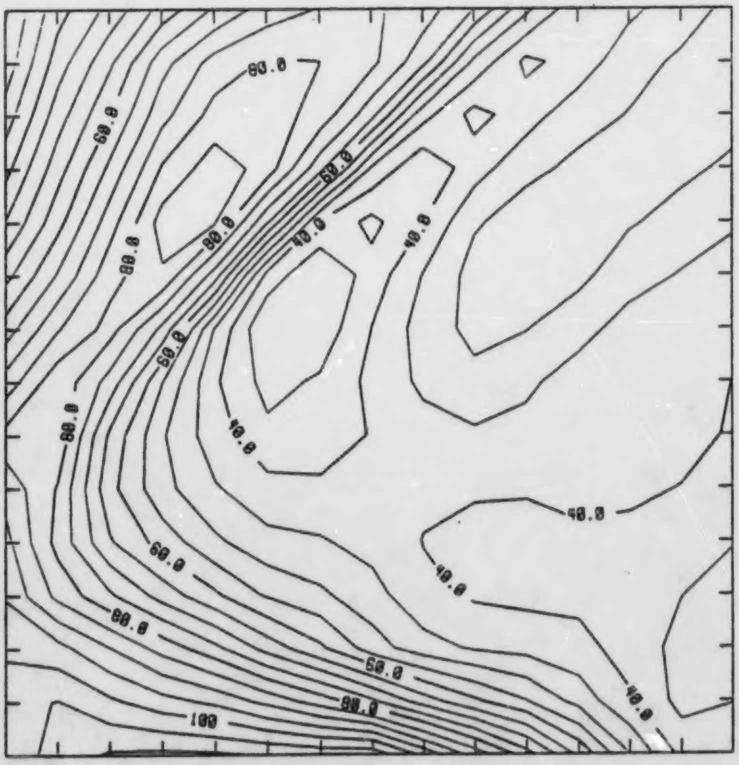

CONTOUR FROM 20.000 TO 110.00 CONTOUR INTERVAL OF 5.0000 PT(3,3)= 98.313

Figure 27

O3 conc. (ppb)

01/08/88 8:00 p.m.

LEVEL = 7 O3

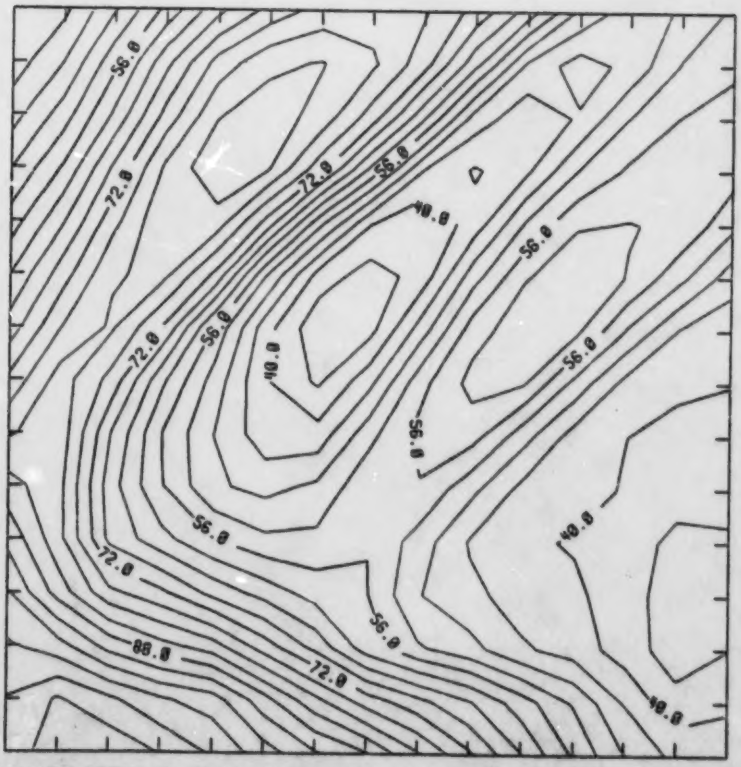

CONTOUR FROM 32.000 TO 100.00 CONTOUR INTERVAL OF 4.0000 PT(3,3)= 88.313

Figure 28

O3 conc. (ppb)

02/08/88 2:00 a.m.

LEVEL = 1 O3

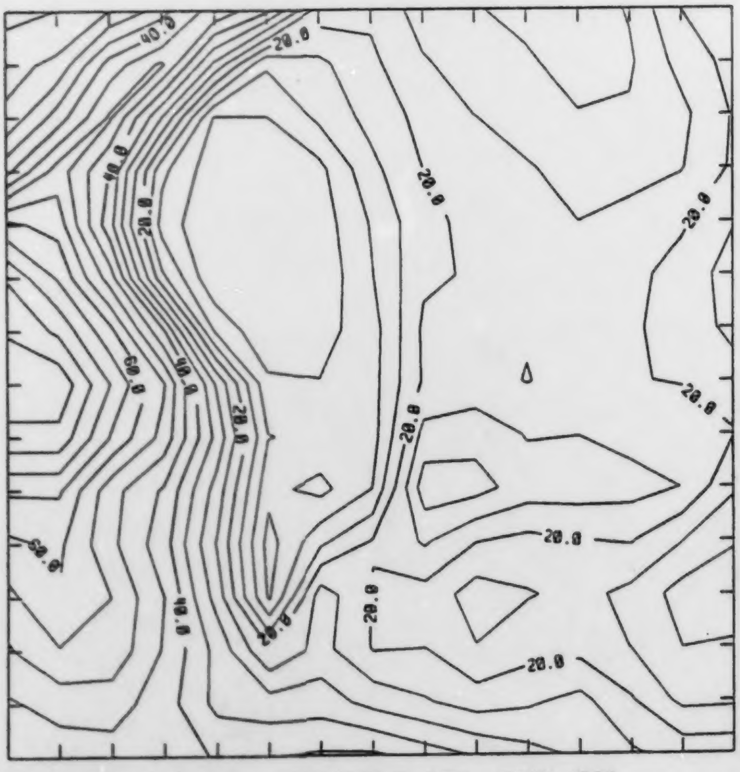

Figure 29

03 conc. (ppb)

02/08/88 2:00 a.m.

LEVEL = 4 03

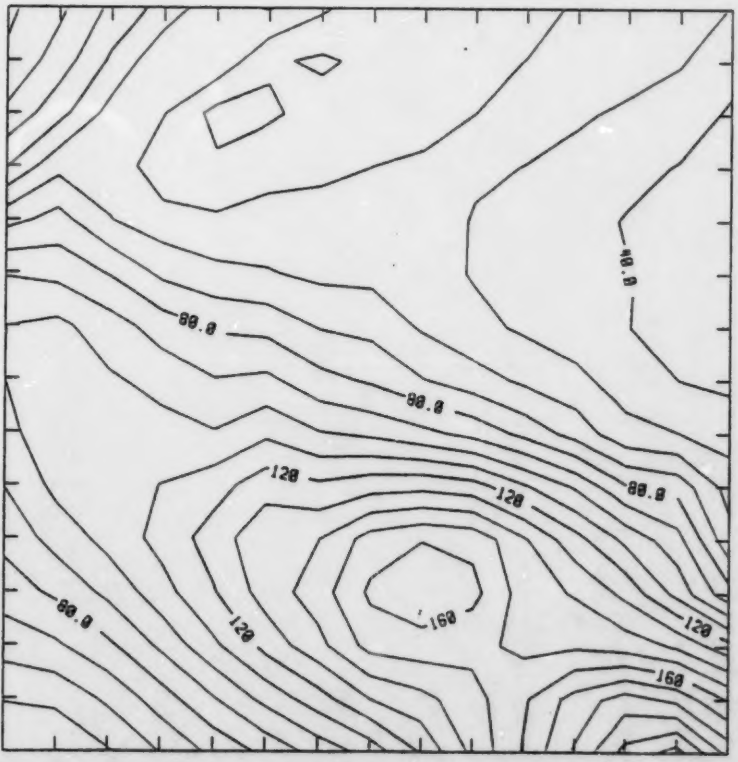

CONTOUR FROM 0.20000E-03 TO 210.00 CONTOUR INTERVAL OF 10.000 PT(3,3)= 70.271

Figure 30

03 conc. (ppb)

02/08/88 2:00 a.m.

LEVEL = 7 03

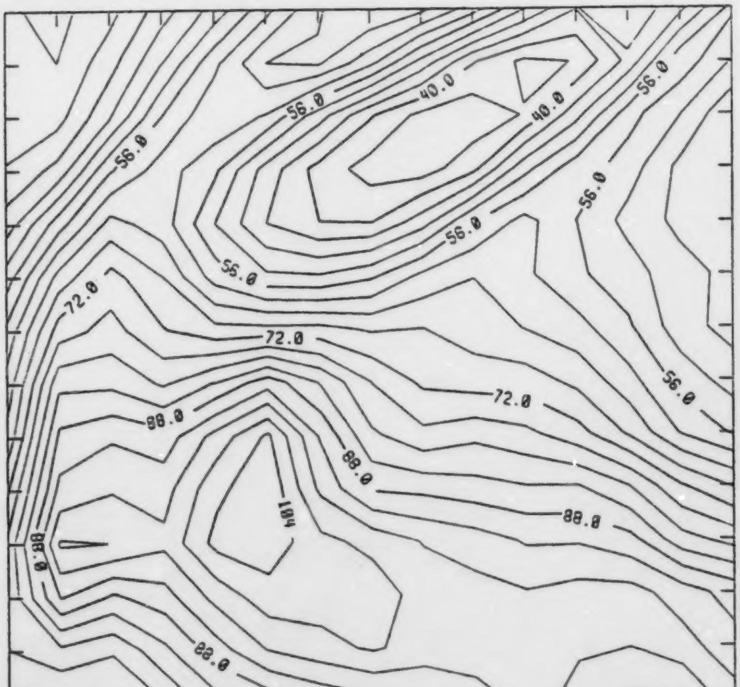

CONTOUR FROM 20.000 TO 104.29 CONTOUR INTERVAL OF 4.2222 PT(3,3)= 76.463

Figure 31

O3 conc. (ppb)

02/08/88 8:00 a.m.

LEVEL = 1 O3

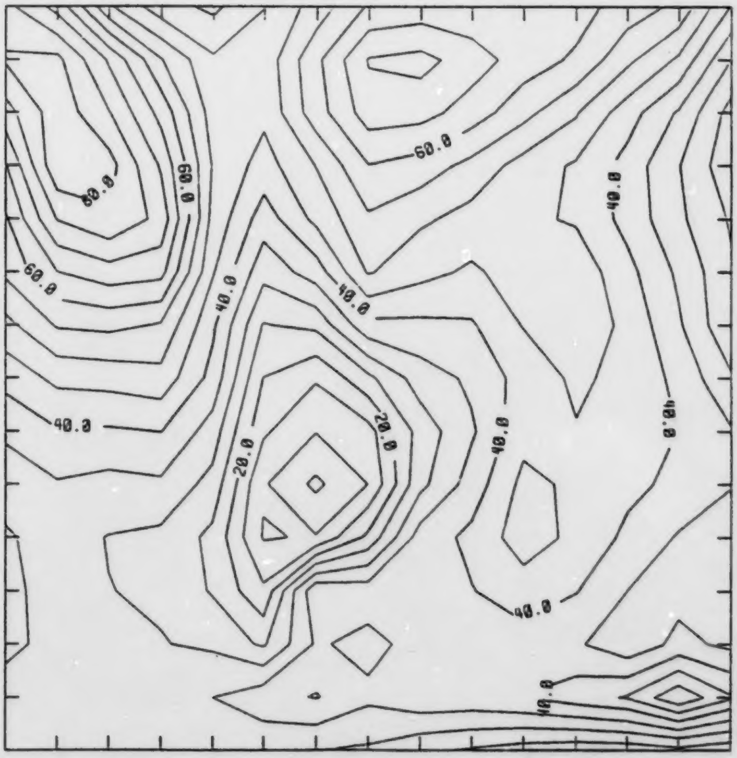
60.0
60.0
60.0
60.0
40.0
40.0
40.0
40.0
20.0
20.0
40.0
40.0
40.0
40.0
CONTOUR FROM 0.00000E+00 TO 90.000 CONTOUR INTERVAL OF 5.0000 PT(3,3)= 38.947

Figure 32

O3 conc. (ppb)
02/08/88 8:00 a.m.

LEVEL = 4 O3

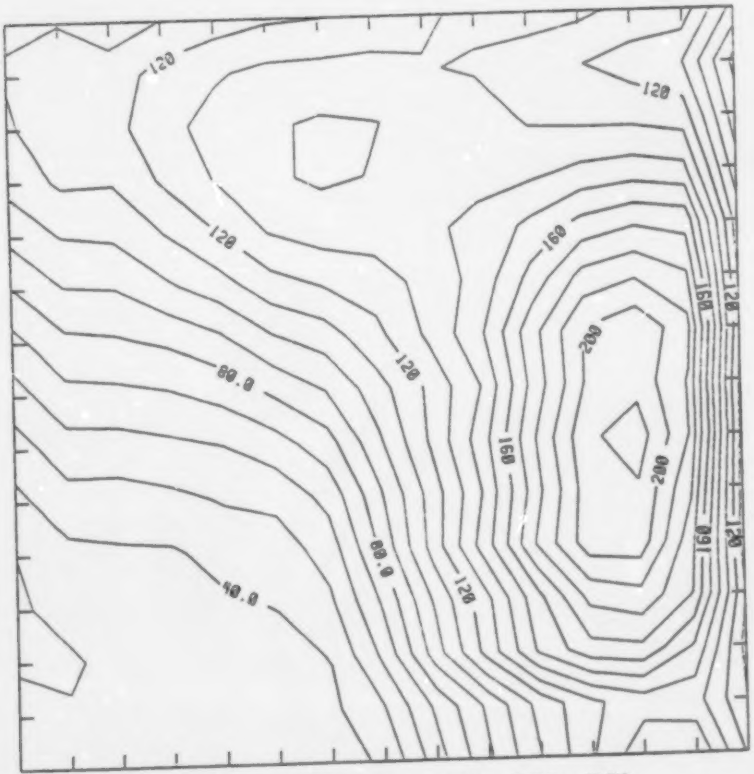

CONTOUR FROM 20.000 TO 210.00 CONTOUR INTERVAL OF 10.000 PT(3,3)= 32.513

Figure 33

O3 conc. (ppb)

02/08/88 2:00 p.m.

LEVEL = 1 O3

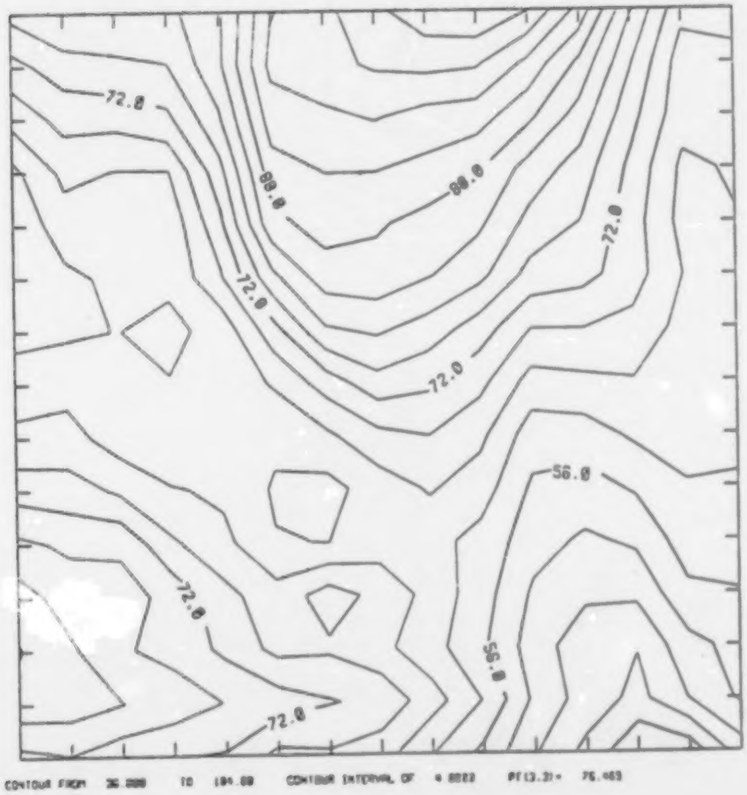

Figure 34

O3 conc. (ppb)

02/08/88 2:00 p.m.

LEVEL = 4 O3

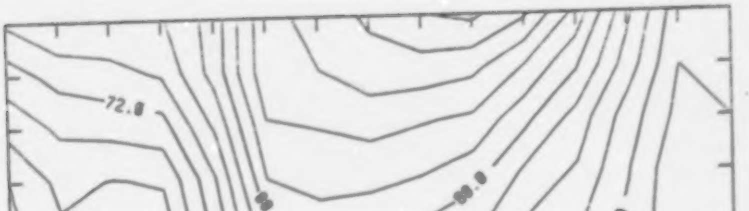
72.0
80.0
80.0
72.0
72.0
72.0
56.0
72.0
56.0
72.0
CONTOUR FROM 56.000 TO 132.00 CONTOUR INTERVAL OF 4.0000 PT(3,3)= 77.600

Figure 35

O3 conc. (ppb)

02/08/88 2:00 p.m.

LEVEL = 7 O3

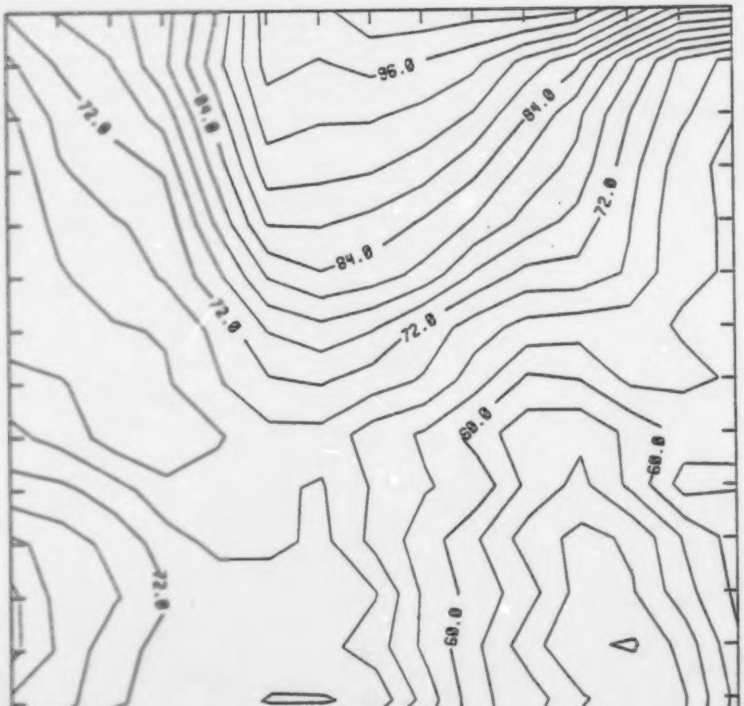
96.0
84.0
84.0
72.0
84.0
72.0
72.0
72.0
60.0
60.0
72.0
60.0
CONTOUR FROM 45.000 TO 99.000 CONTOUR INTERVAL OF 3.0000 PT(3,3)= 72.852

Figure 36

O3 conc. (ppb)

02/08/88 8:00 p.m.

LEVEL = 1 O3

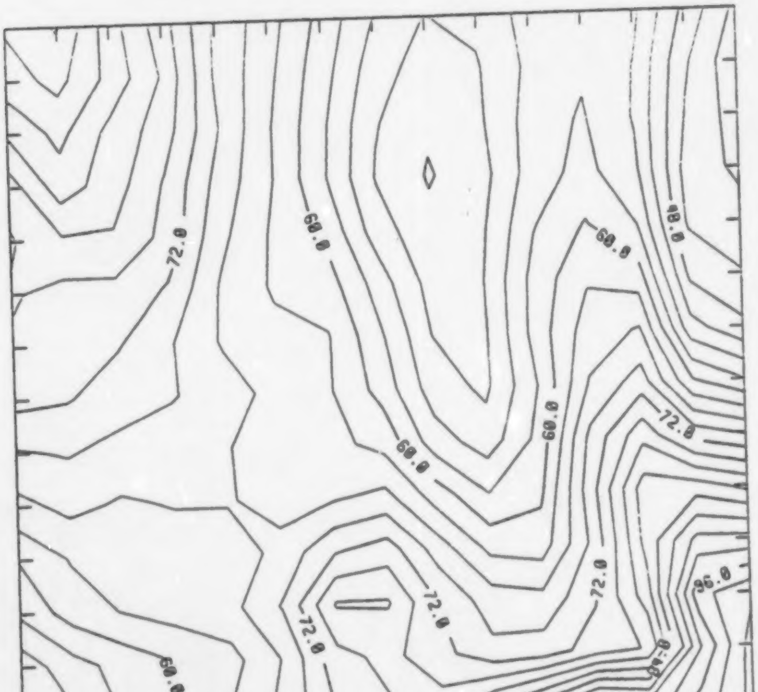

CONTOUR FROM 39.000 TO 102.00 CONTOUR INTERVAL OF 3.0000 PT(3,3)= 58.221

Figure 37

O3 conc. (ppb) .

02/08/88 8:00 p.m.

LEVEL = 4 O3

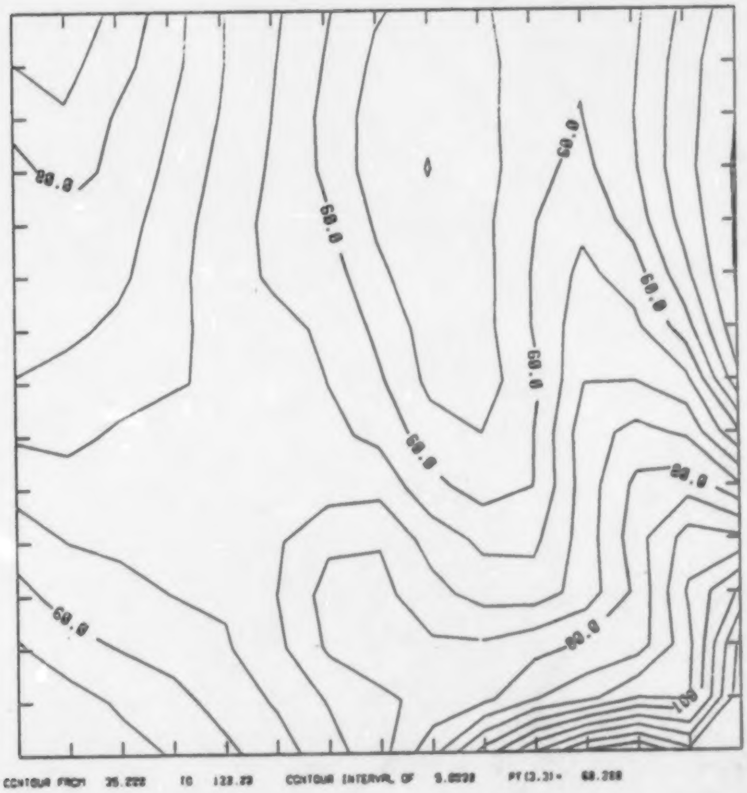

Figure 38

O3 conc. (ppb)

03/08/88 2:00 a.m.

LEVEL = 1 O3

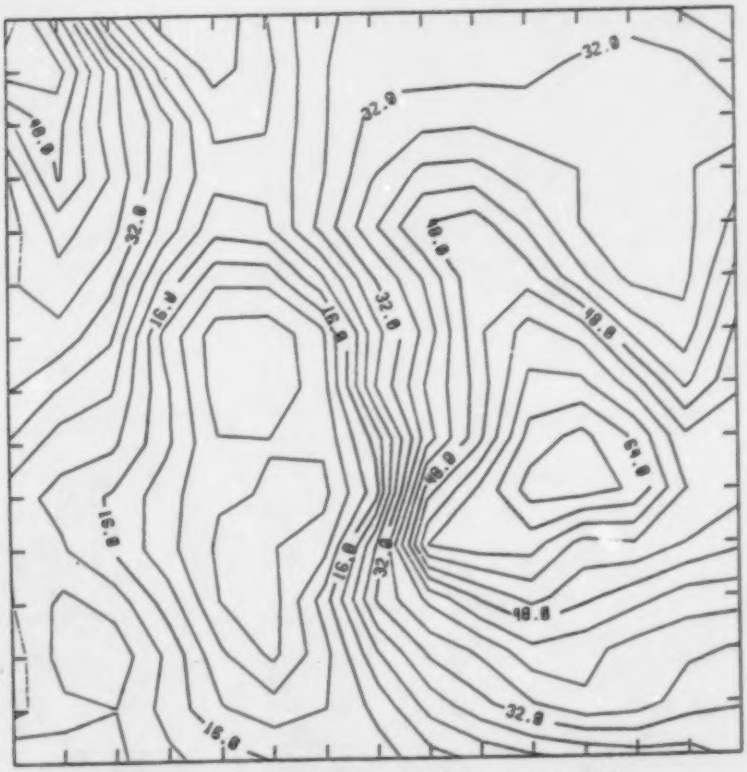

Figure 39

O3 conc. (ppb)

03/08/88 2:00 a.m.

LEVEL = 4 O3

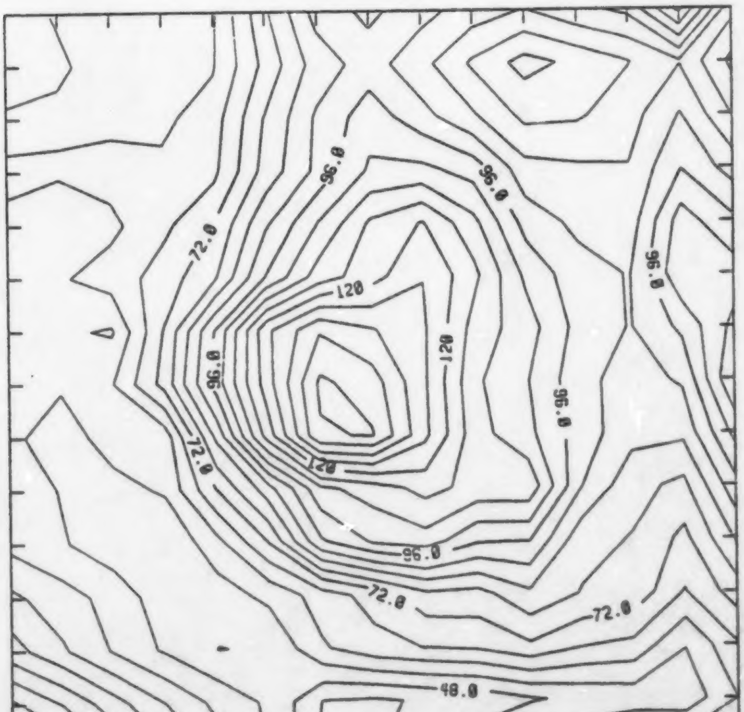

Figure 40

O3 conc. (ppb)

03/08/88 2:00 a.m.

LEVEL = 7 O3

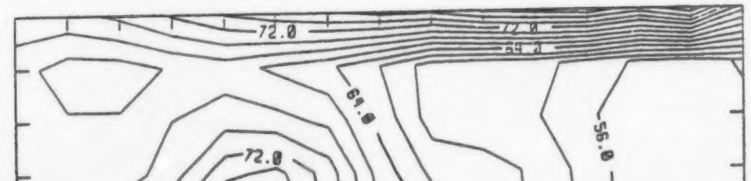

Figure 41

O3 conc. (ppb)
03/08/88 8:00 a.m.

LEVEL = 1 O3

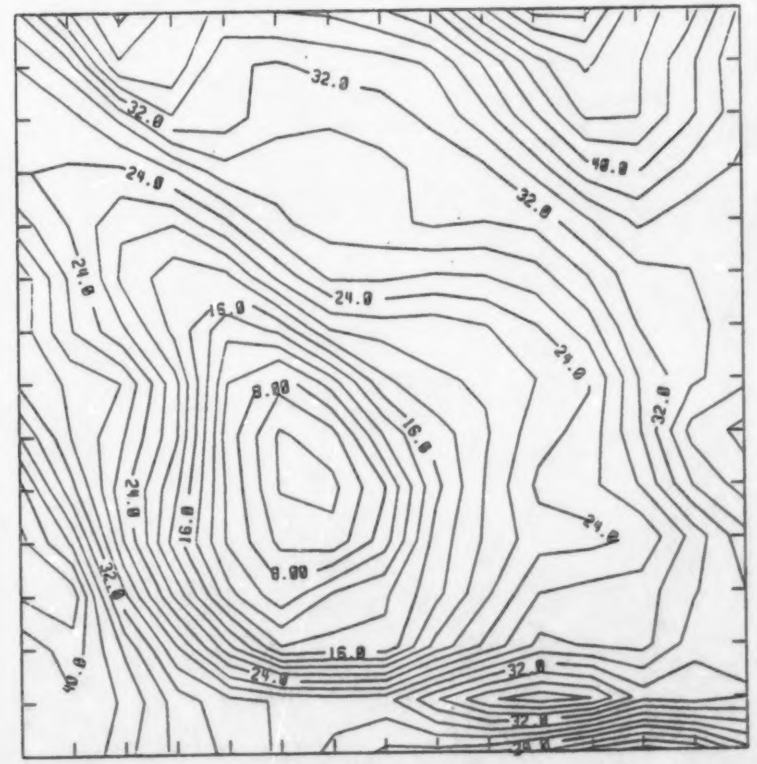

Figure 42

O3 conc. (ppb)

03/08/88 8:00 a.m.

LEVEL = 4 O3

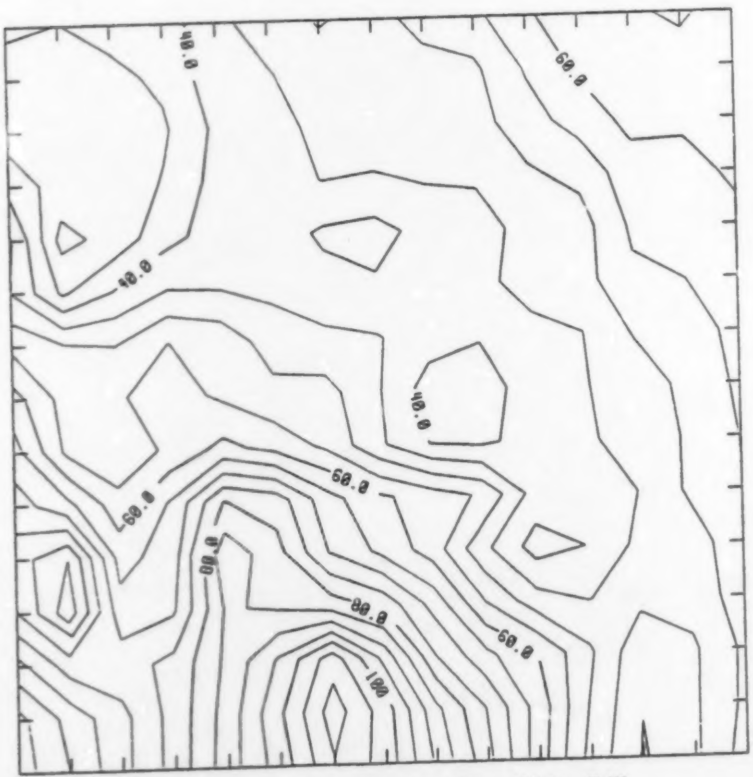

Figure 43

O3 conc. (ppb)

03/08/88 8:00 a.m.

LEVEL = 7 O3

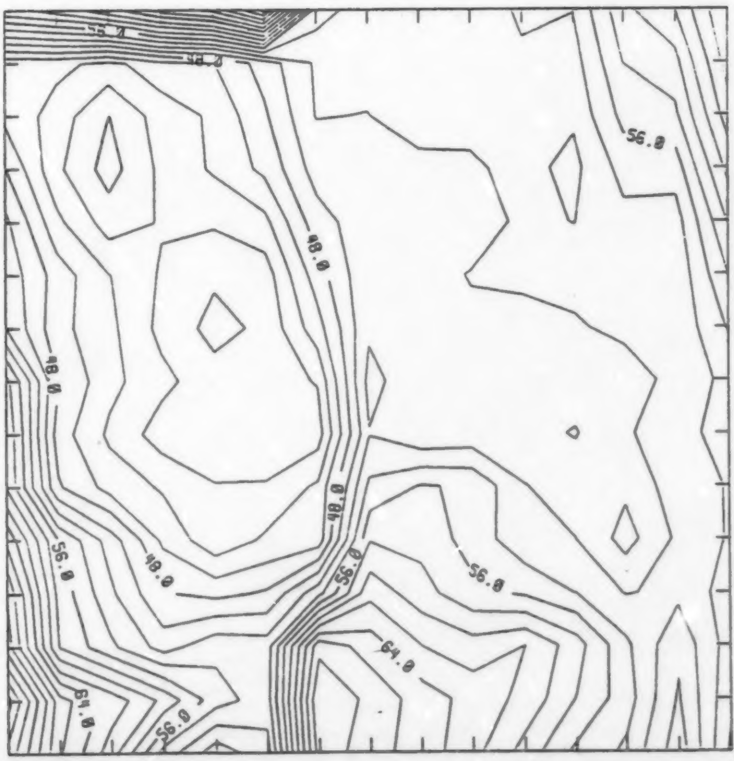

Figure 44

O3 conc. (ppb)
03/08/88 2:00 p.m.

LEVEL = 1 O3

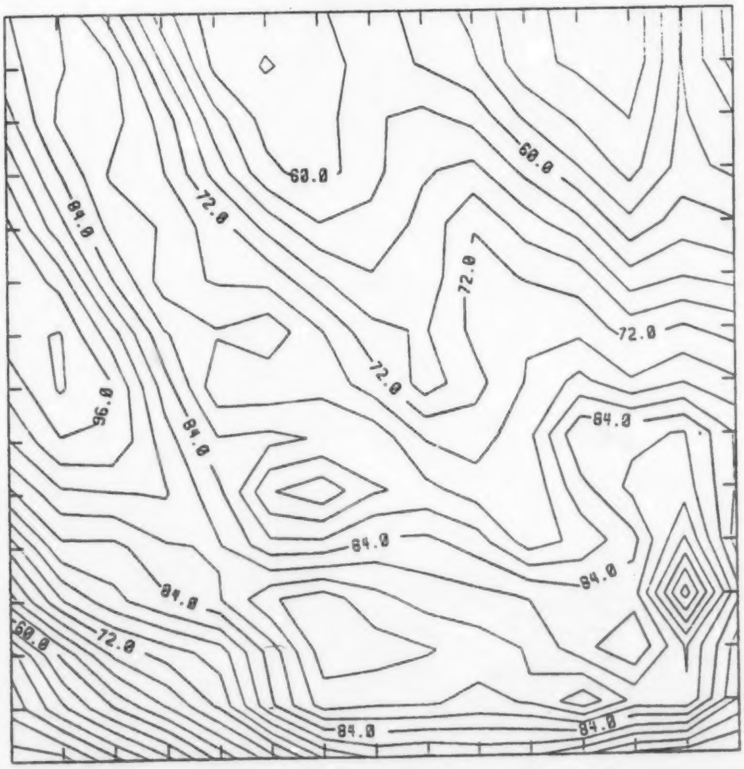

CONTOUR FROM 38.222 TO 122.22 CONTOUR INTERVAL OF 3.2223 PT(3,3)= 69.842

Figure 45

O3 conc. (ppb)

03/08/88 2:00 p.m.

LEVEL = 4 O3

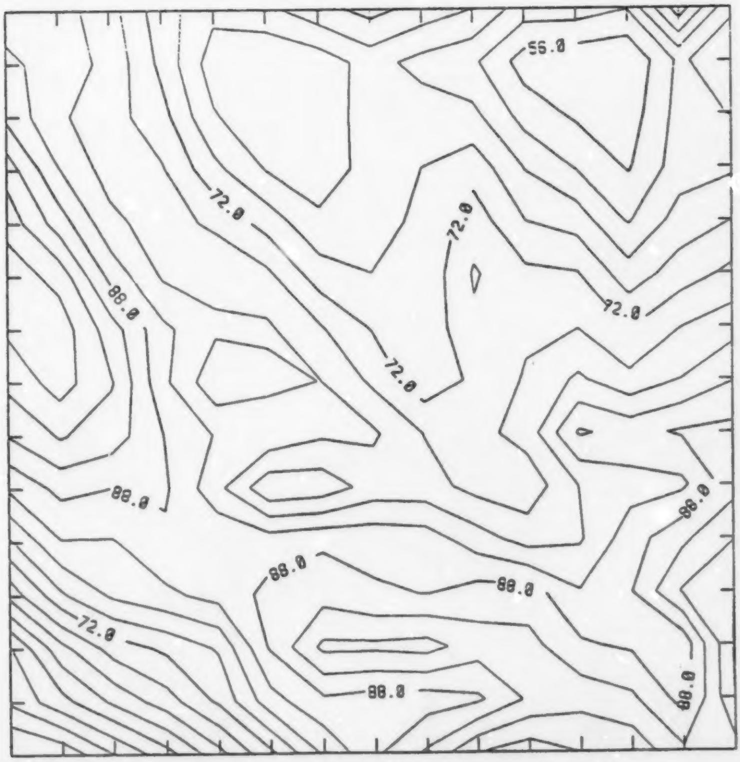

Figure 46

O3 conc. (ppb)
03/08/88 2:00 p.m.

LEVEL = 7 O3

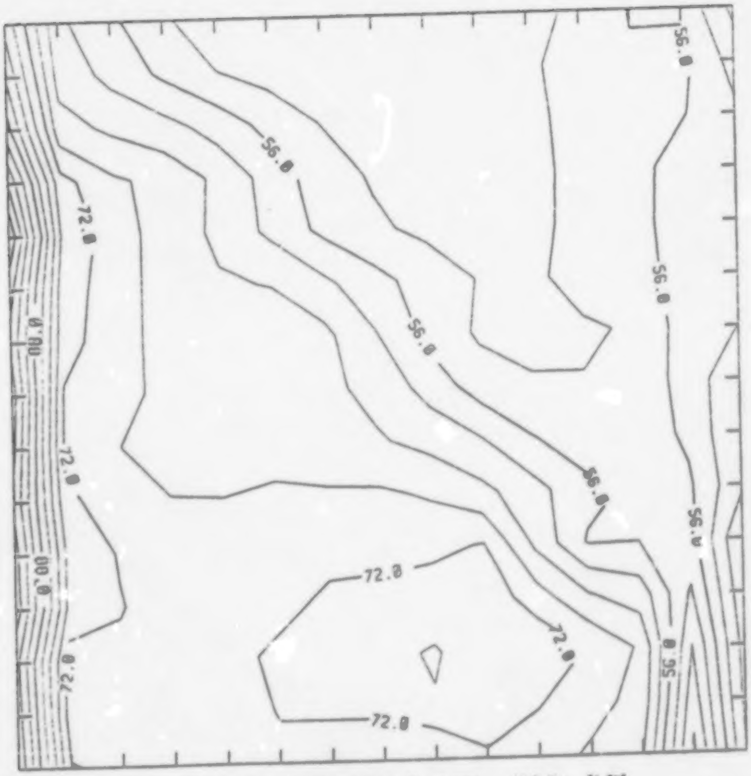

Figure 47

O3 conc. (ppb)

03/08/88 8:00 p.m.

LEVEL = 1 O3

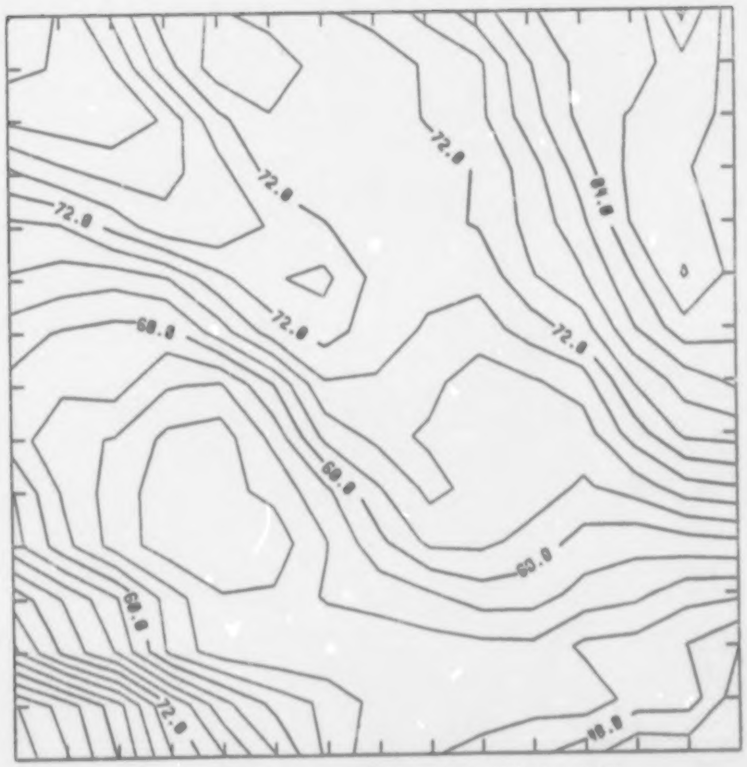
72.0
72.0
84.0
72.0
72.0
72.0
60.0
60.0
60.0
60.0
72.0
48.0
CONTOUR FROM 42.000 TO 93.000 CONTOUR INTERVAL OF 3.0000 PT(3,3)= 63.627

Figure 48

O3 conc. (ppb)

03/08/88 8:00 p.m.

LEVEL = 4 O3

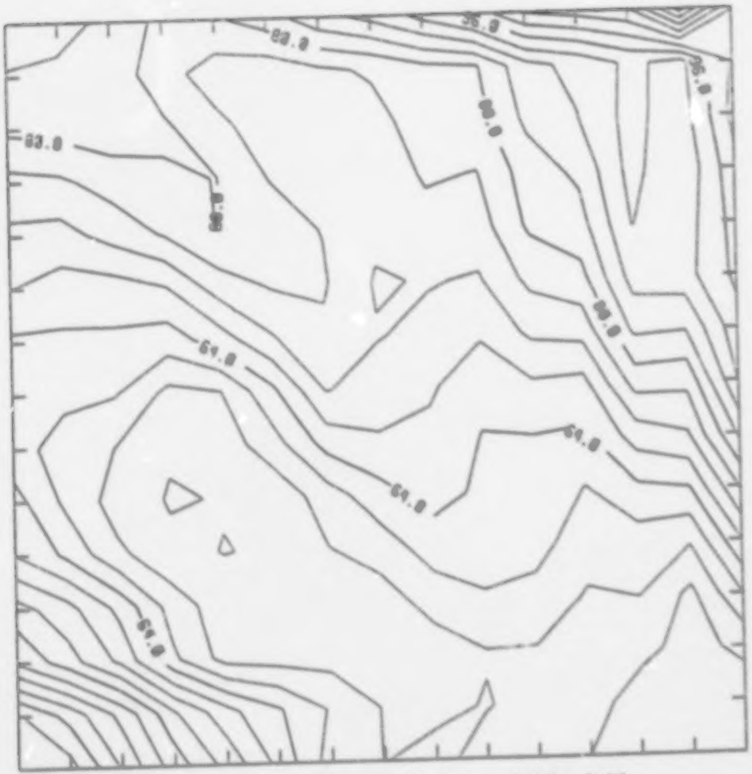
60.0
60.0
60.0
64.0
68.0
64.0
64.0
64.0
64.0
CONTOUR FROM 48.000 TO 120.00 CONTOUR INTERVAL OF 4.0000 PT(3,3)= 71.246

Figure 49

O3 conc. (ppb)

03/08/88 8:00 p.m.

LEVEL = 7 O3

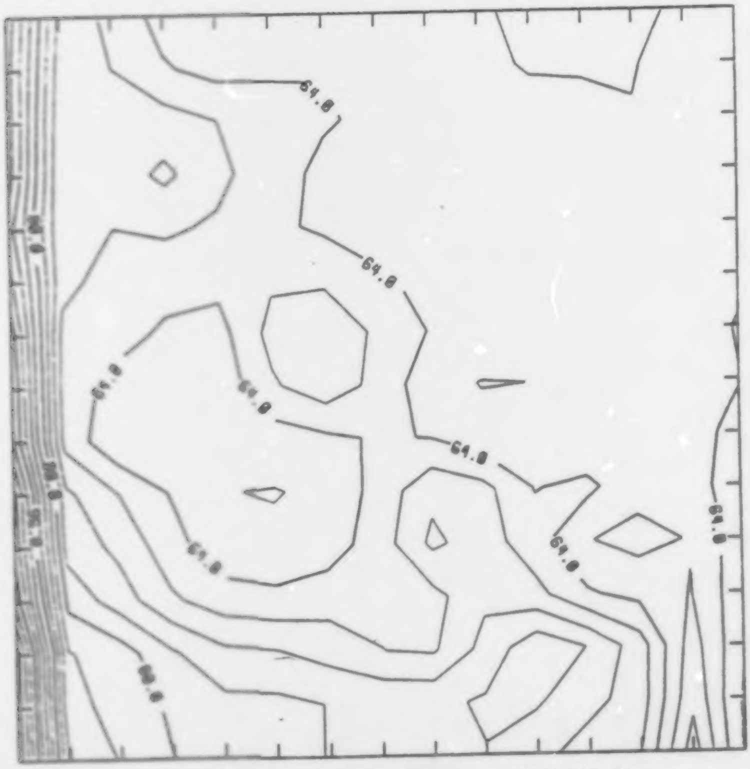

Figure 50

O3 conc. (ppb)

04/08/88 2:00 a.m.

LEVEL = 1 O3

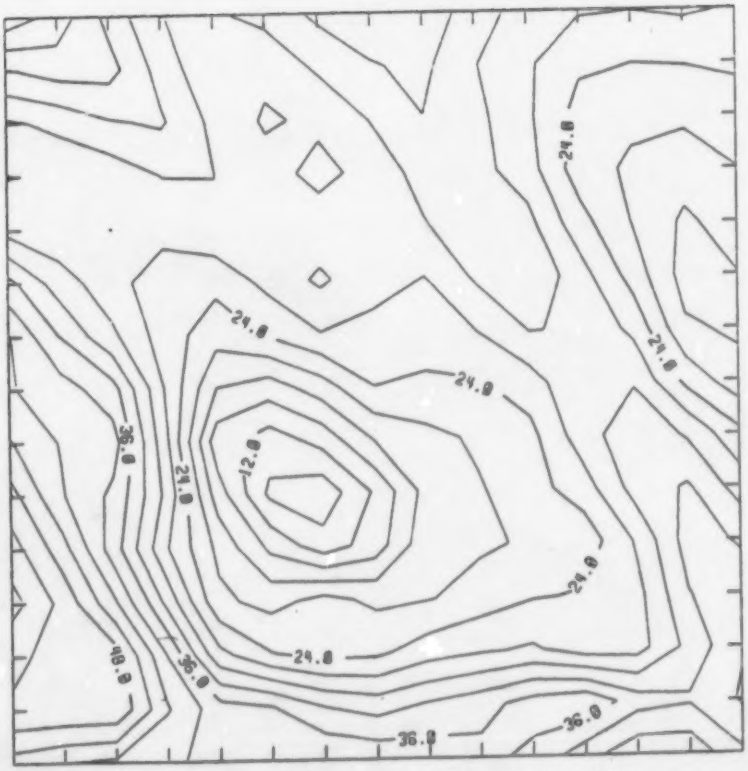

CONTOUR FROM 6.0000 TO 54.000 CONTOUR INTERVAL OF 3.0000 PT(3,3)= 40.311

Figure 51

O3 conc. (ppb)

04/08/88 2:00 a.m.

LEVEL = 4 O3

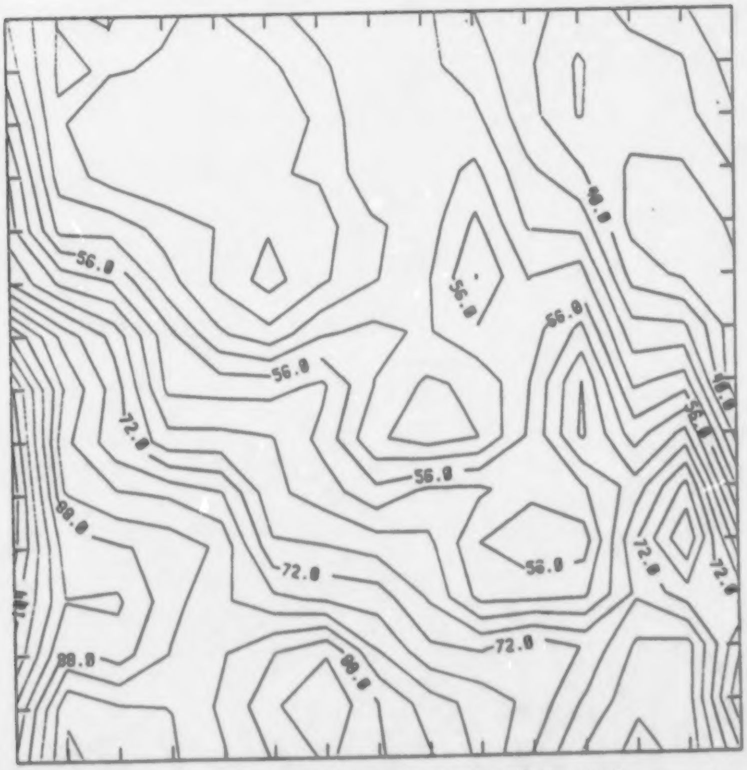

CONTOUR FROM 20.000 TO 108.00 CONTOUR INTERVAL OF 4.0000 PT(3,3)= 88.718

Figure 52

O3 conc. (ppb)

04/08/88 2:00 a.m.

LEVEL = 7 O3

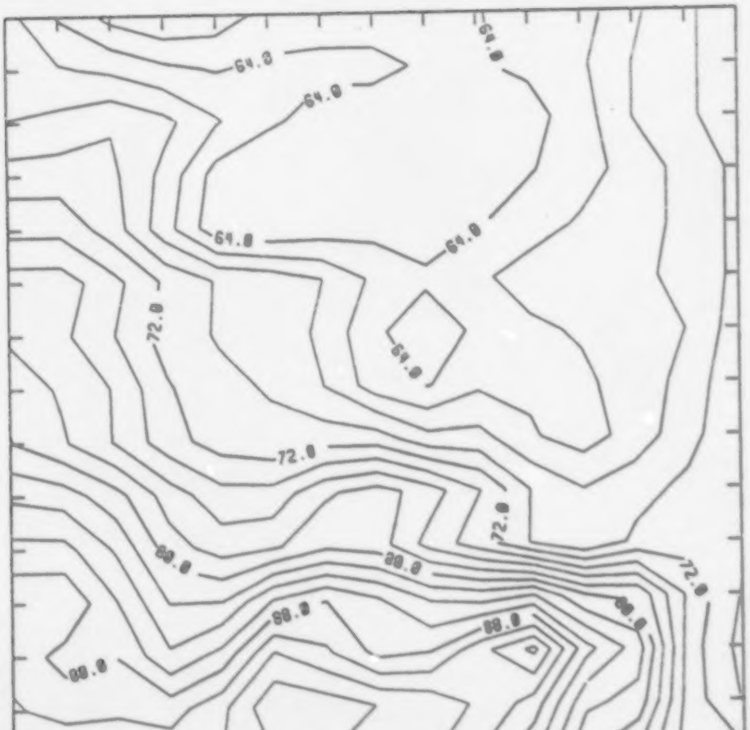
64.0
64.0
64.0
64.0
64.0
64.0
72.0
72.0
72.0
72.0
80.0
80.0
80.0
88.0
88.0
88.0
80.0
D
CONTOUR FROM 62.000 TO 94.000 CONTOUR INTERVAL OF 2.0000 PT(3,3)= 87.584

Figure 53

O3 conc. (ppb)

04/08/88 8:00 a.m.

LEVEL = 1 O3

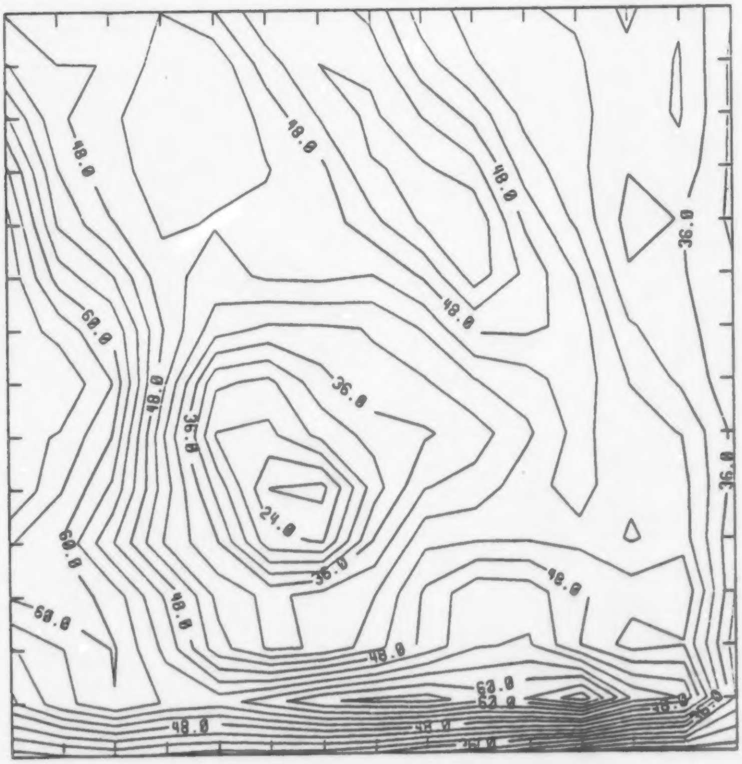

CONTOUR FROM 18.000 TO 69.000 CONTOUR INTERVAL OF 3.0000 PT(3,3)= 62.200

Figure 54

O3 conc. (ppb)

04/08/88 8:00 a.m.

LEVEL = 4 O3

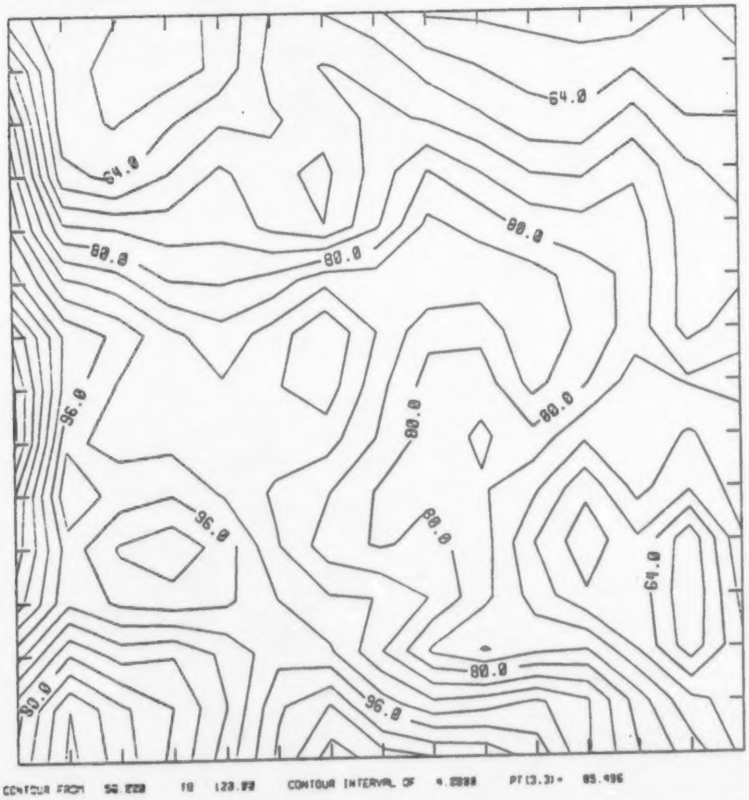

CONTOUR FROM 56.000 TO 128.00 CONTOUR INTERVAL OF 4.0000 PT(3,3)= 85.496

Figure 55

O3 conc. (ppb)

04/08/88 8:00 a.m.

LEVEL = 7 O3

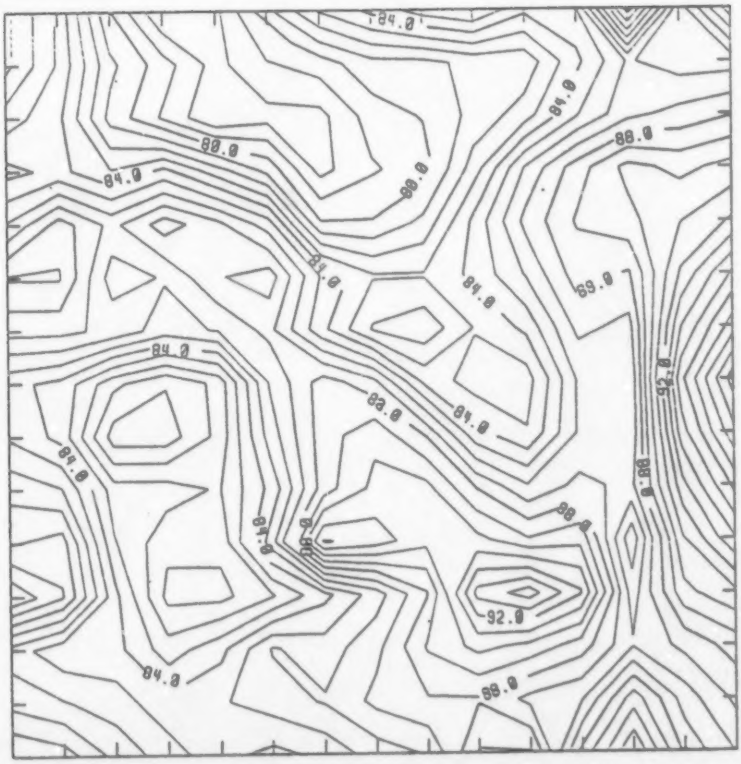

CONTOUR FROM 77.000 TO 100.00 CONTOUR INTERVAL OF 1.0000 PT(3,3)= 84.292

Figure 56

O3 conc. (ppb)
04/08/88 2:00 p.m.

LEVEL = 1 O3

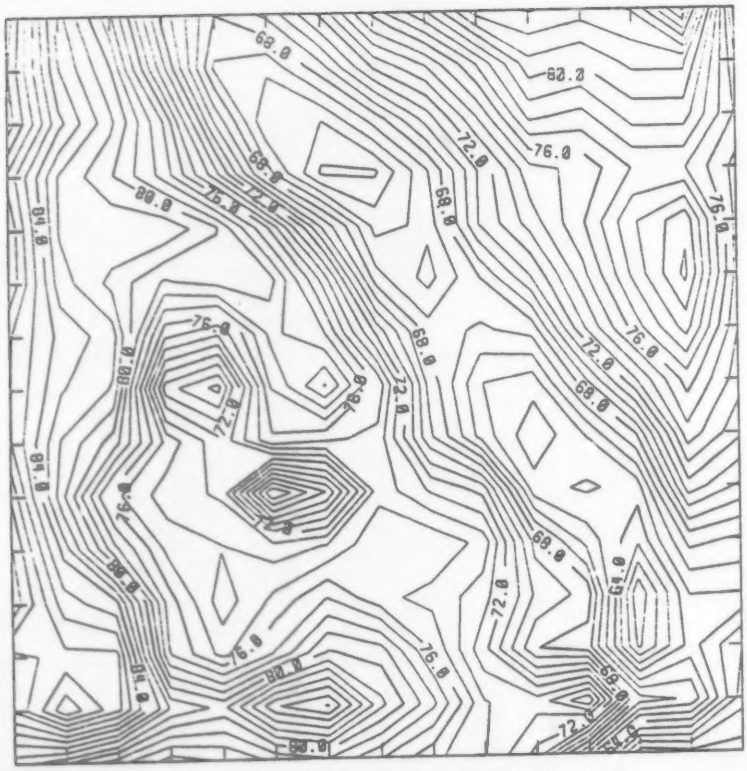

Figure 57

O3 conc. (ppb)

04/08/88 2:00 p.m.

LEVEL = 4 O3

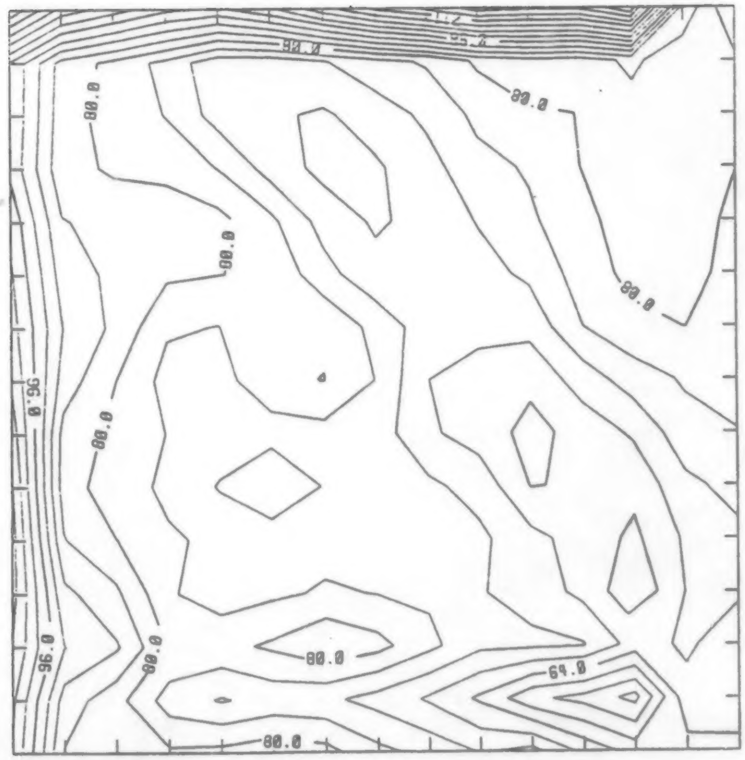

Figure 58

O3 conc. (ppb)

04/08/88 2:00 p.m.

LEVEL = 7 O3

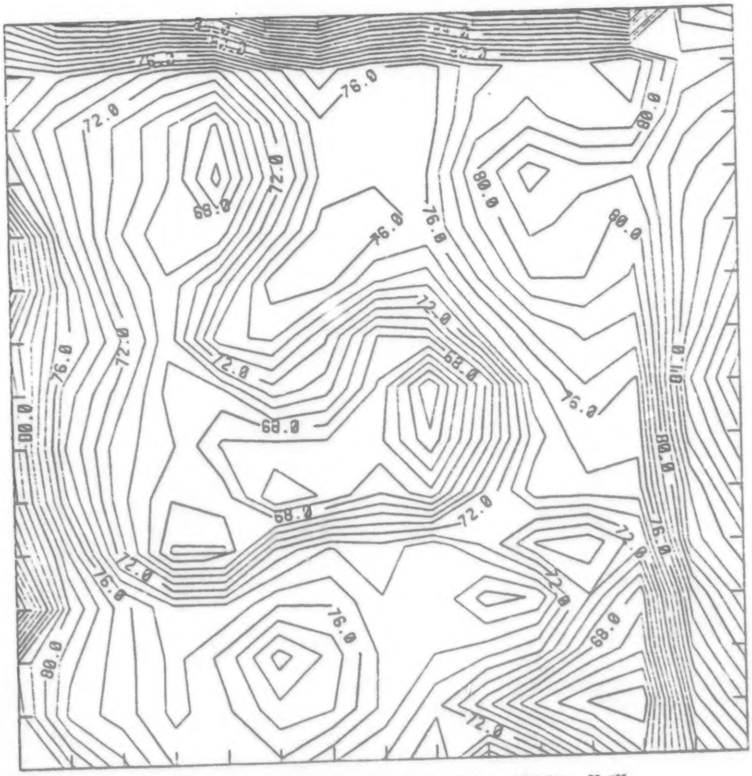

CONTOUR FROM 62.000 TO 91.000 CONTOUR INTERVAL OF 1.0000 PT(3,3)= 76.465

Figure 59

O3 conc. (ppb)

04/08/88 8:00 p.m.

LEVEL = 1 O3

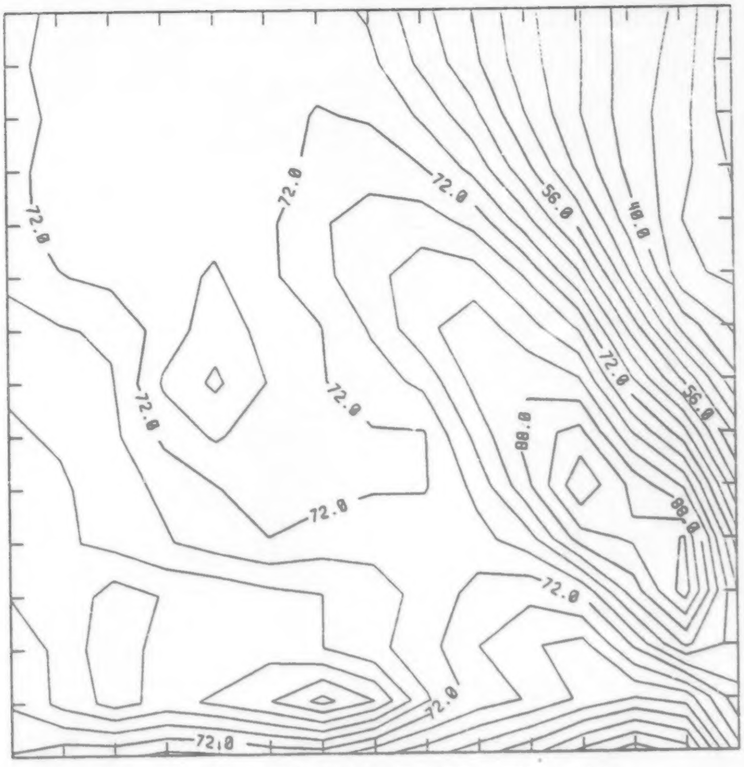

CONTOUR FROM 24.000 TO 96.000 CONTOUR INTERVAL OF 4.0000 PT(3,3)= 87.382

Figure 60

O3 conc. (ppb)

04/08/88 8:00 p.m.

LEVEL = 4 O3

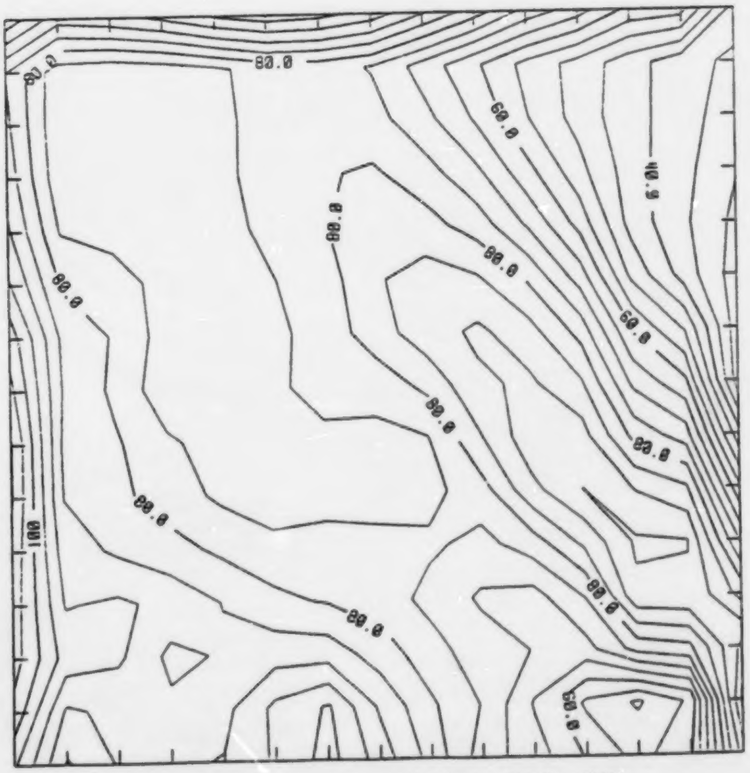

CONTOUR FROM 25.000 TO 110.00 CONTOUR INTERVAL OF 5.0000 PT(3,3)= 98.915

Figure 61

O3 conc. (ppb)
24/08/88 8:00 p.m.

LEVEL = 7 O3

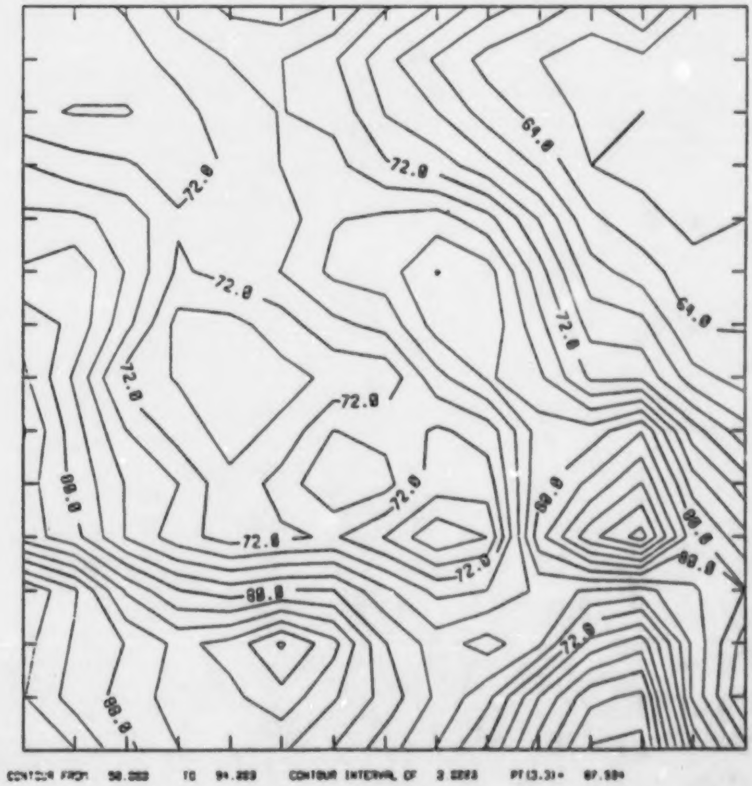

Figure 62

NO conc. (u/m**3)

01/08/88 2:00 a.m.

LEVEL = 1 NO

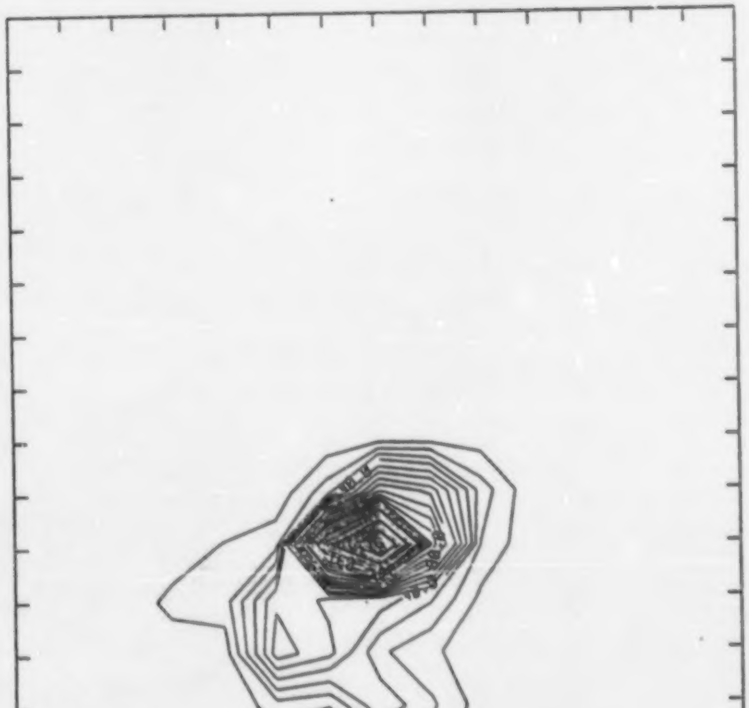

Figure 63

NO conc. (u/m**3)
01/08/88 2:00 a.m.

LEVEL = 4 NO

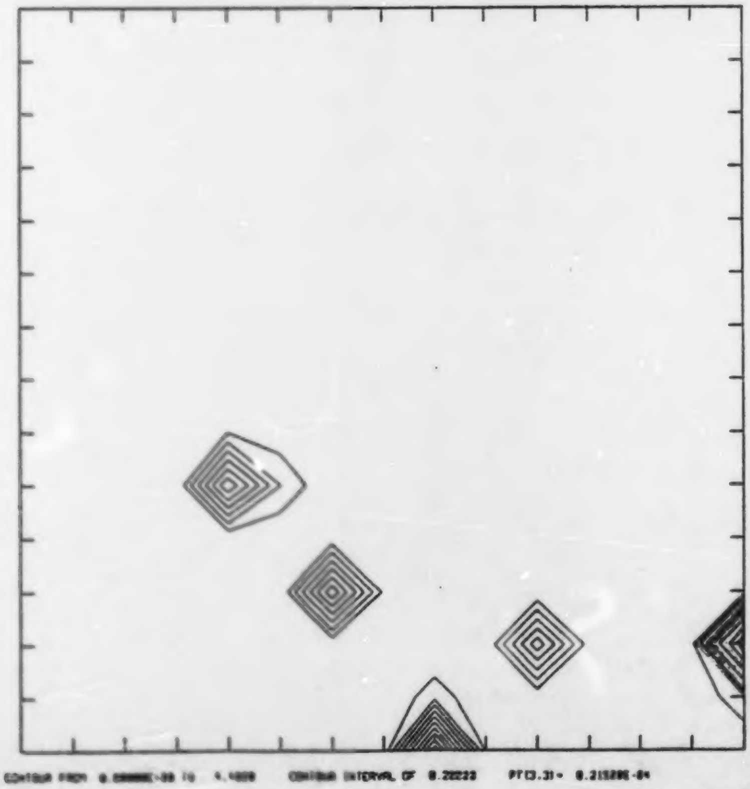

Figure 64

NO conc. (u/m**3)

01/08/88 2:00 p.m.

LEVEL = 1 NO

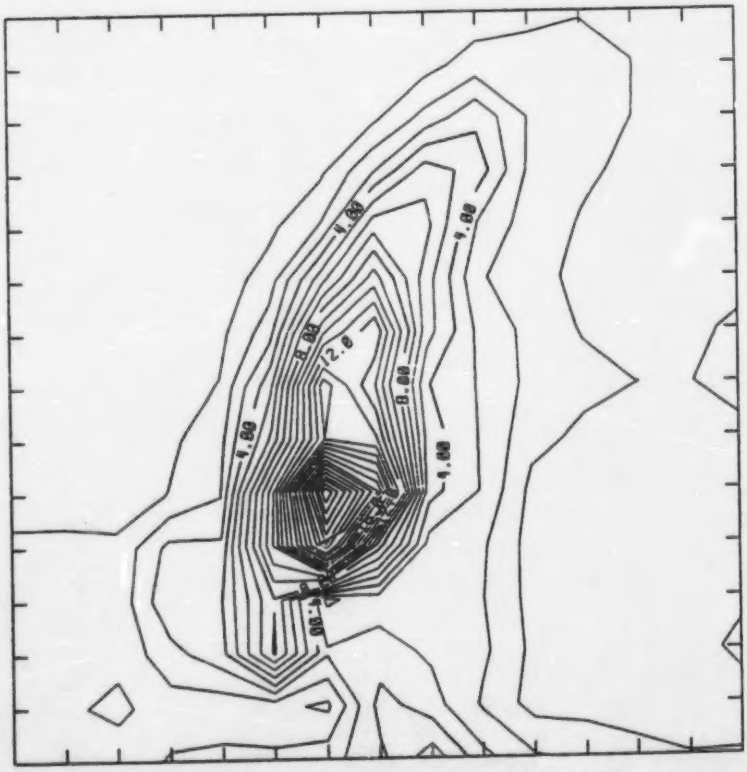

CONTOUR FROM 0.00000E+00 TO 27.000 CONTOUR INTERVAL OF 1.0000 PT(3,3)= 1.2333

Figure 65

NO conc. (u/m**3)

01/08/88 2:00 p.m.

LEVEL = 4 NO

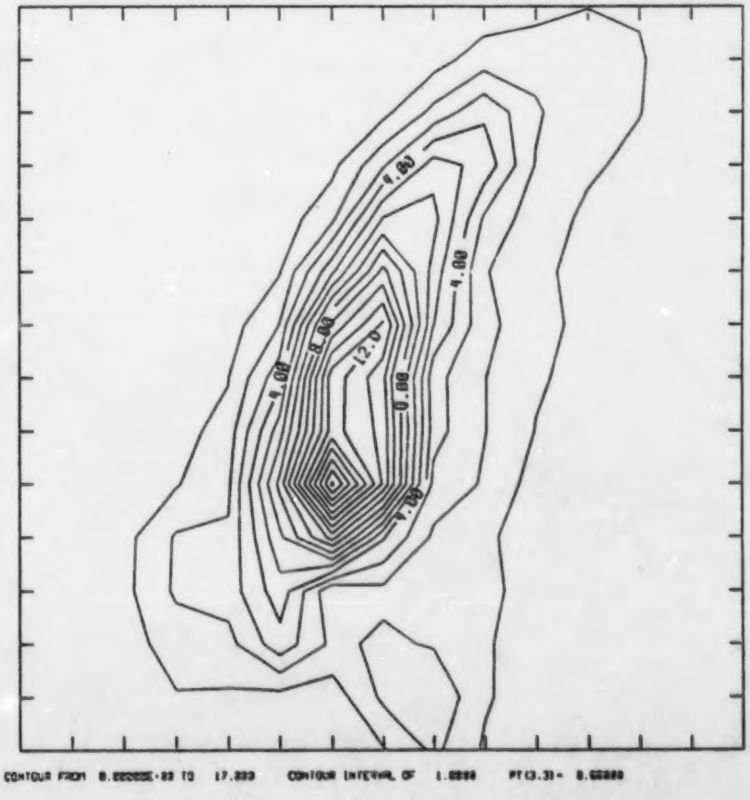

Figure 66

NO conc. (u/m**3)
02/08/88 2:00 a.m.

LEVEL = 1 NO

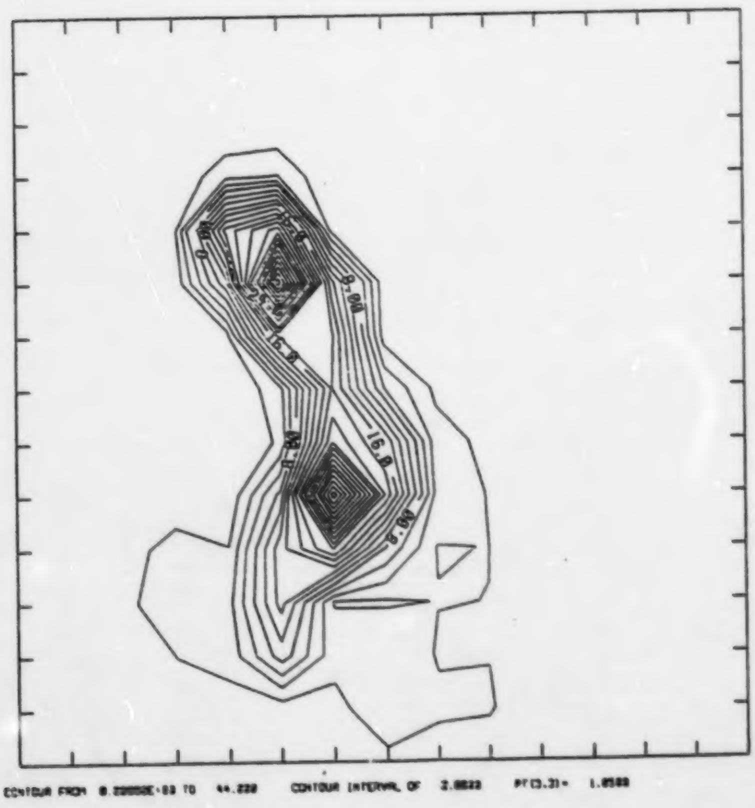

Figure 67

NO conc. (u/m**3)

02/08/88 2:00 a.m.

LEVEL = 4. NO

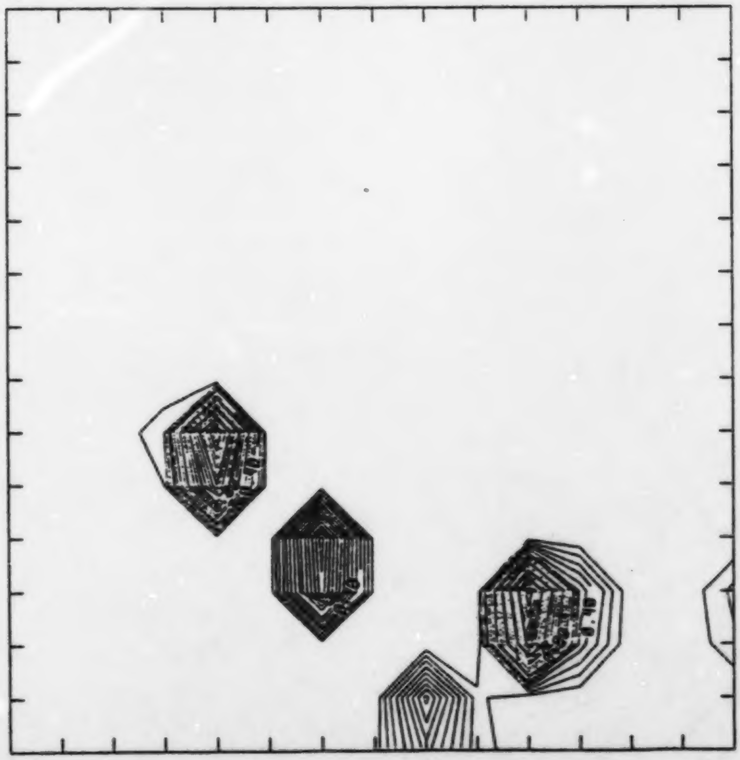

Figure 68

NO conc. (u/m**3)

02/08/88 2:00 p.m.

LEVEL = 1 NO

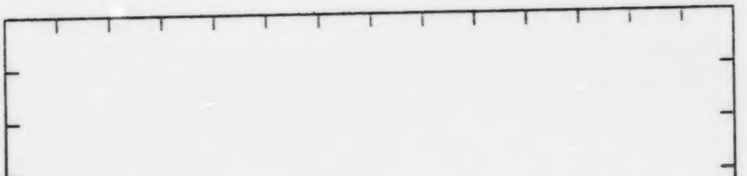

Figure 69

NO conc. (u/m**3)

02/08/88 2:00 p.m.

LEVEL = 4 NO

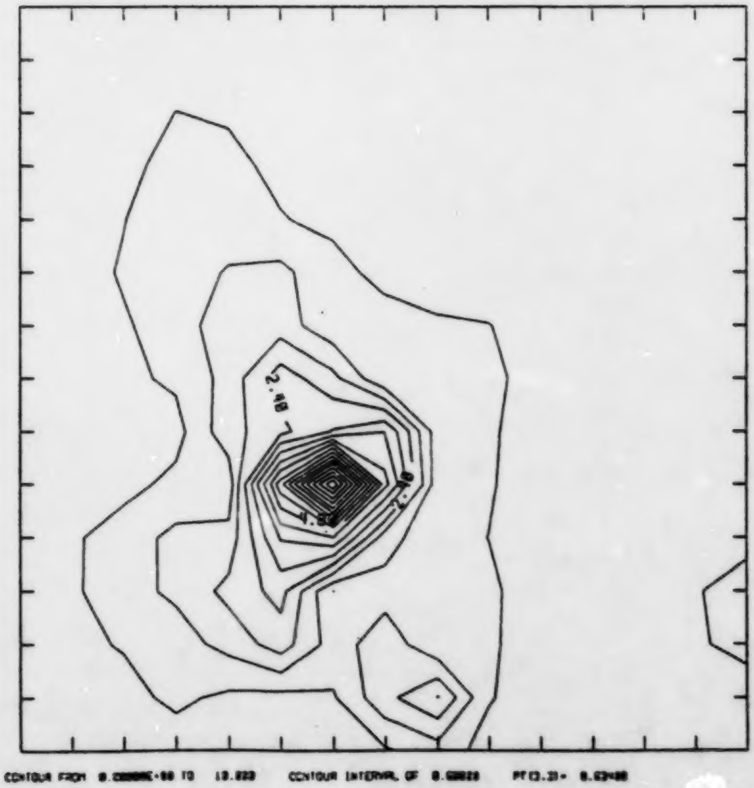

Figure 70

NO conc. (u/m**3)

03/08/88 2:00 a.m.

LEVEL = 1 NO

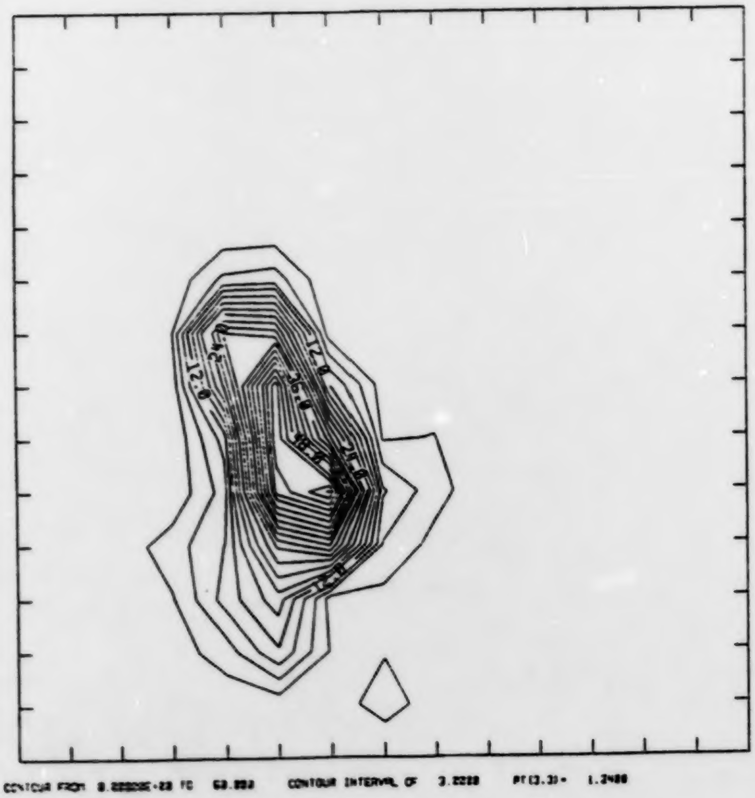

Figure 71

NO conc. (u/m**3)

03/08/88 2:00 a.m.

LEVEL = 4 NO

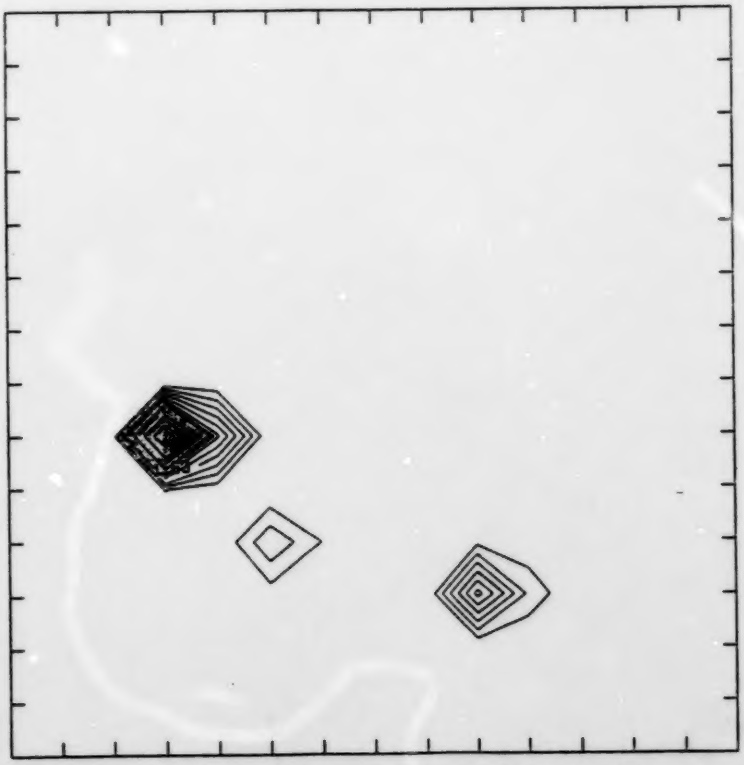

CONTOUR FROM 0.00000E+00 TO 7.6300 CONTOUR INTERVAL OF 0.40000 PT(3,3)= 0.36532E-05

Figure 72

NO conc. (u/m**3)

03/08/88 2:00 p.m.

LEVEL = 1 NO

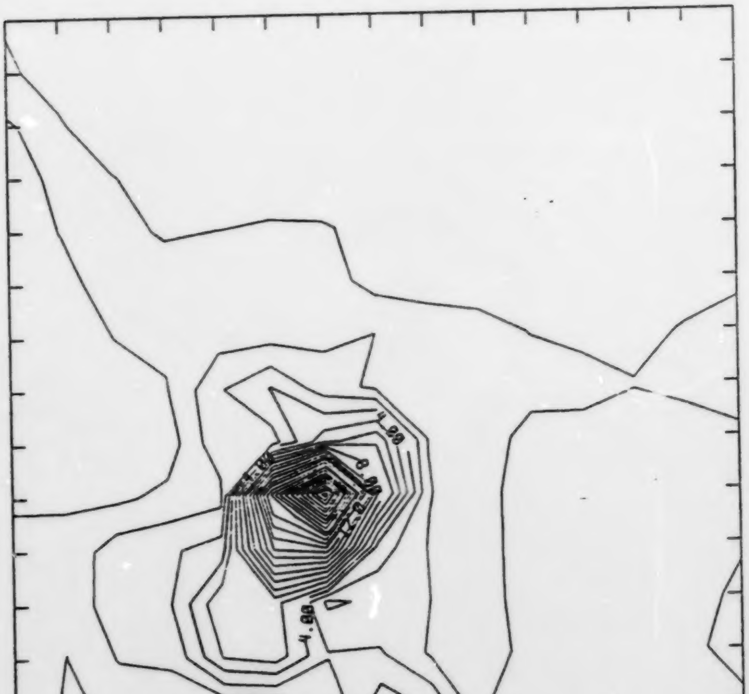

CONTOUR FROM 0.00000E+00 TO 20.000 CONTOUR INTERVAL OF 1.0000 PT(3,3)= 0.0000

Figure 73

NO conc. (u/m**3)

03/08/88 2:00 p.m.

LEVEL = 4 NO

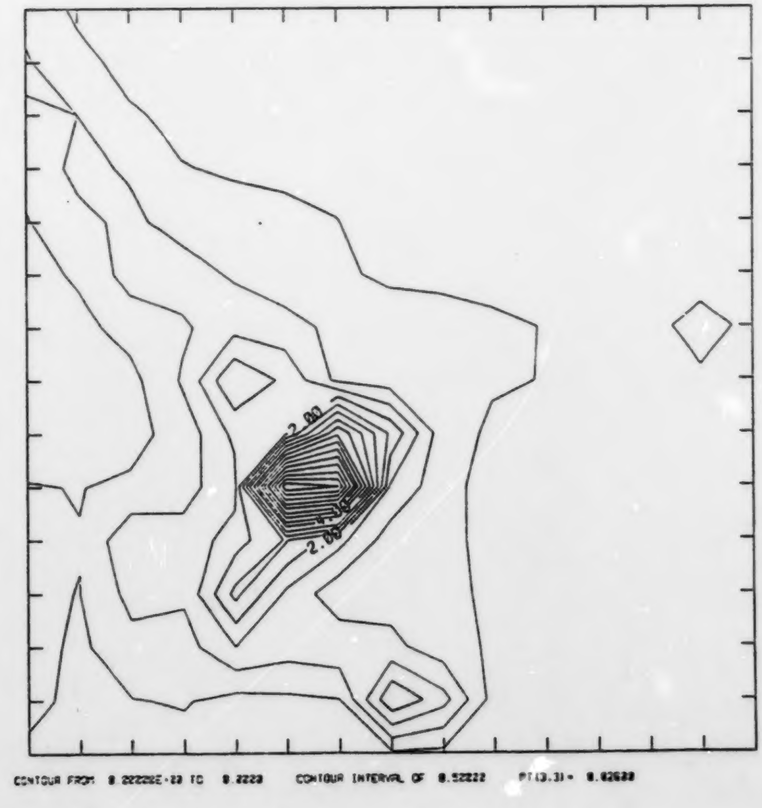

Figure 74

NO conc. (u/m**3)

04/08/88 2:00 a.m.

LEVEL = 1 NO

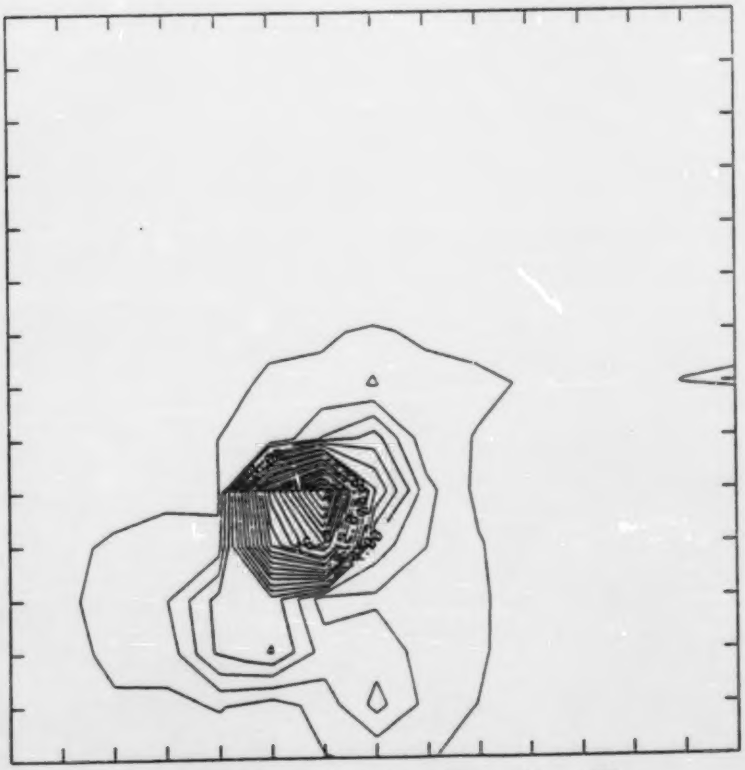

CONTOUR FROM 0.22000E-23 TO 25.000 CONTOUR INTERVAL OF 1.0000 PT(3,3)= 1.3200

Figure 75

NO conc. (u/m**3)

04/08/88 2:00 a.m.

LEVEL = 4 NO

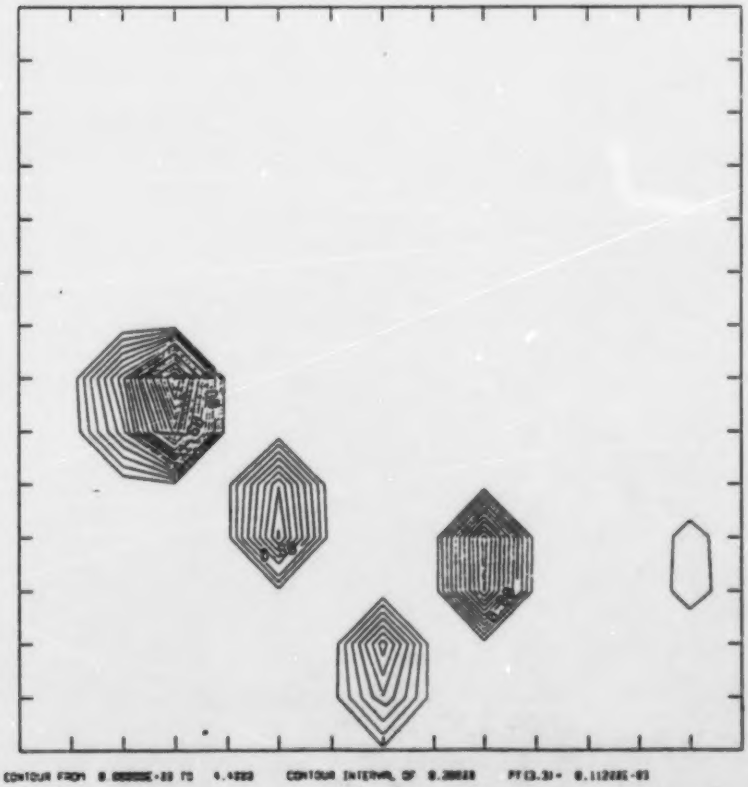

Figure 76

NO2 conc. (u/m**3)

01/08/88 2:00 a.m.

LEVEL = 1 NO2

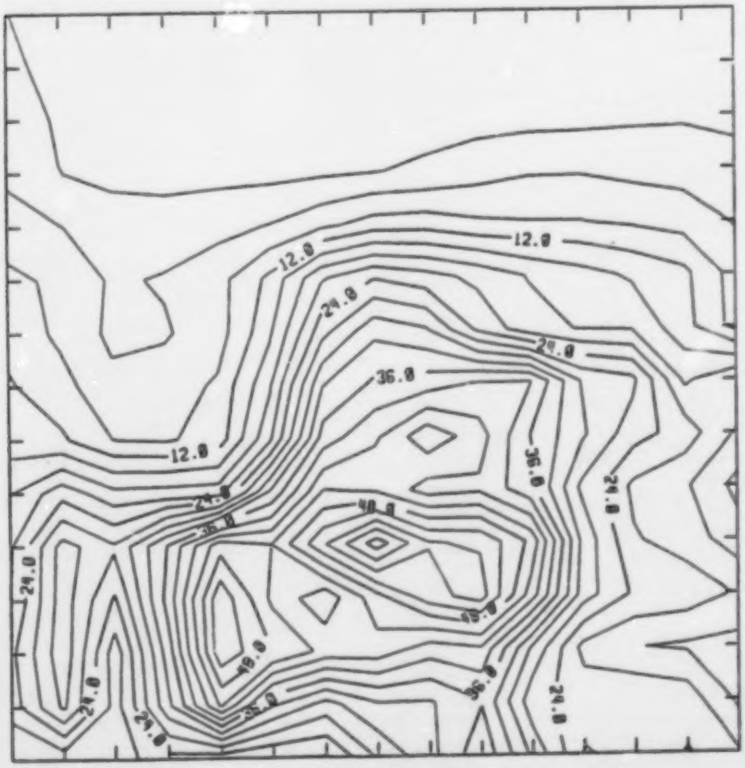

Figure 77

NO2 conc. (u/m**3)

01/08/88 2:00 a.m.

LEVEL = 4 NO2

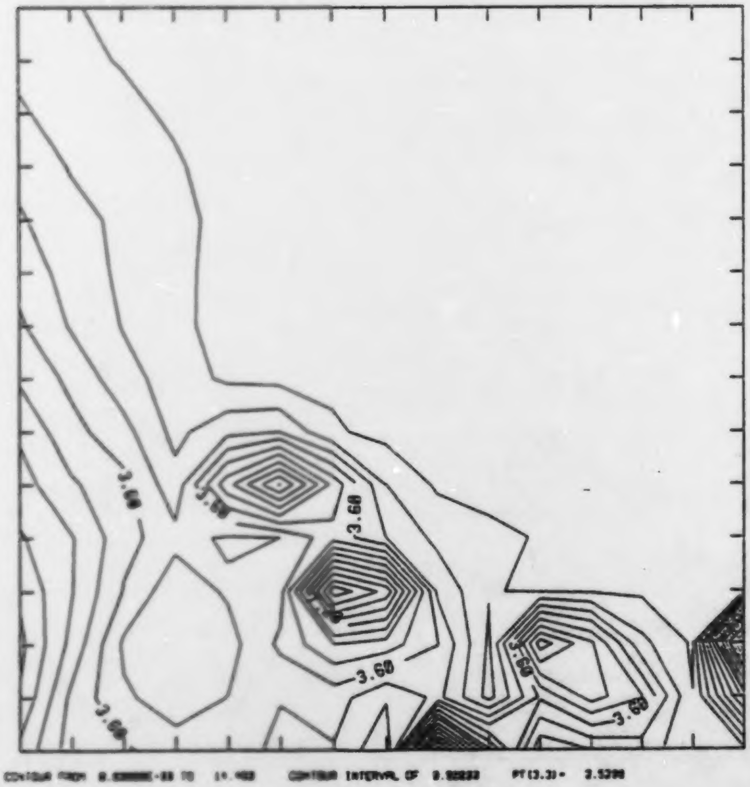

Figure 78

NO2 conc. (u/m**3)

01/08/88 2:00 p.m.

LEVEL = 1 NO2

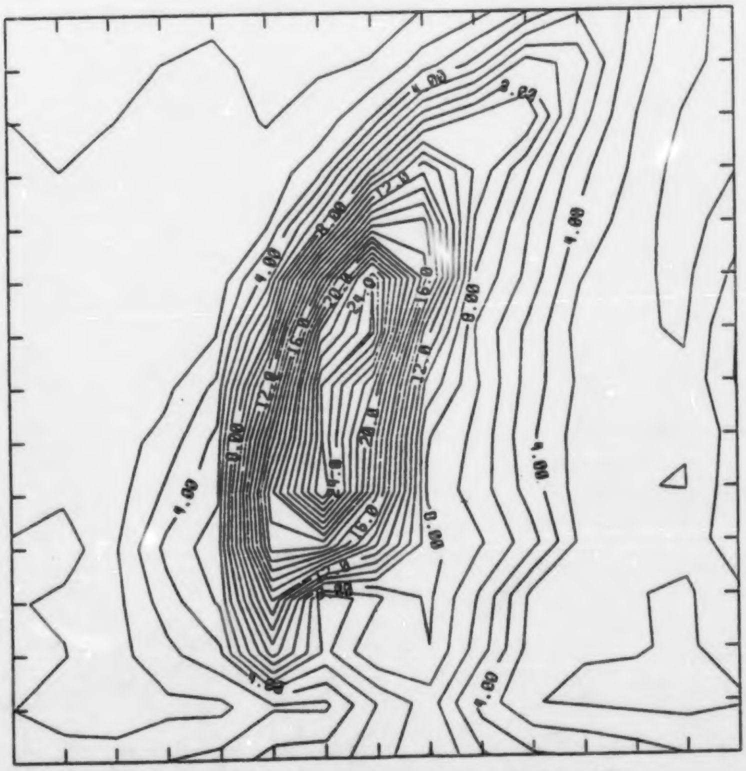

CONTOUR FROM 0.00000E+00 TO 27.000 CONTOUR INTERVAL OF 1.0000 PT(3,3)= 1.6400

Figure 79

NO2 conc. (u/m**3)

01/08/88 2:00 p.m.

LEVEL = 4 NO2

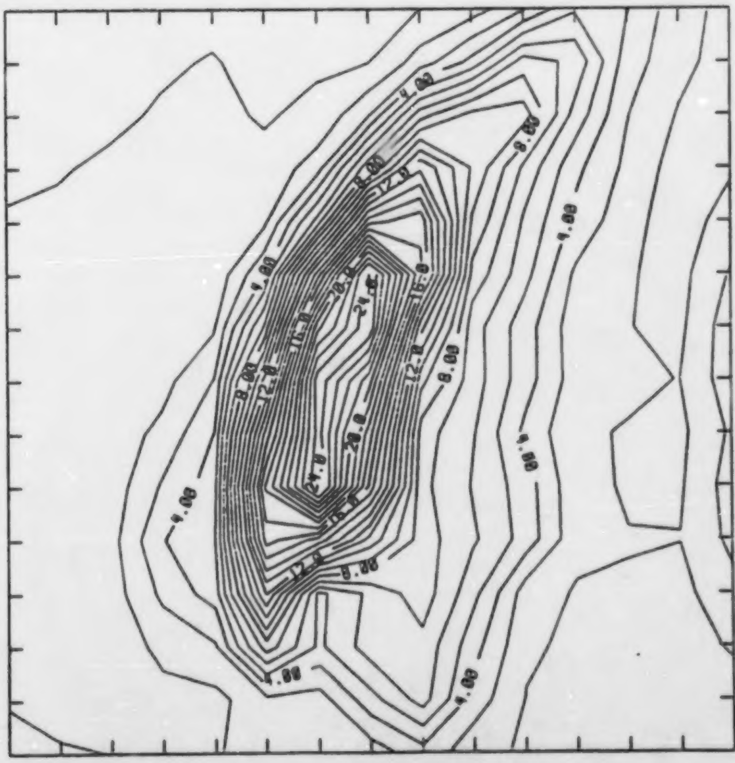

CONTOUR FROM 0.00000E+00 TO 25.200 CONTOUR INTERVAL OF 1.0000 PT(3,3)= 1.4300

Figure 80

NO2 conc. (u/m**3)

02/08/88 2:00 a.m.

LEVEL = 1 NO2

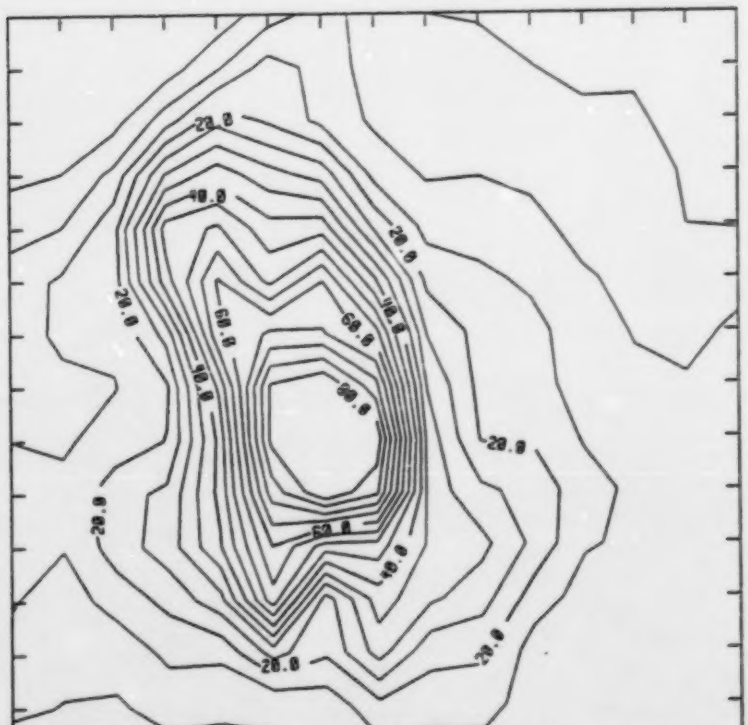

Figure 81

NO2 conc. (u/m**3)

02/08/88 2:00 a.m.

LEVEL = 4 NO2

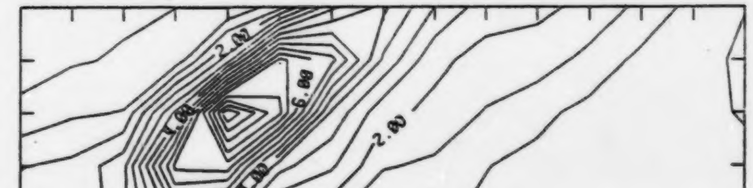

Figure 82

NO2 conc. (u/m**3)

02/08/88 2:00 p.m.

LEVEL = 1 NO2

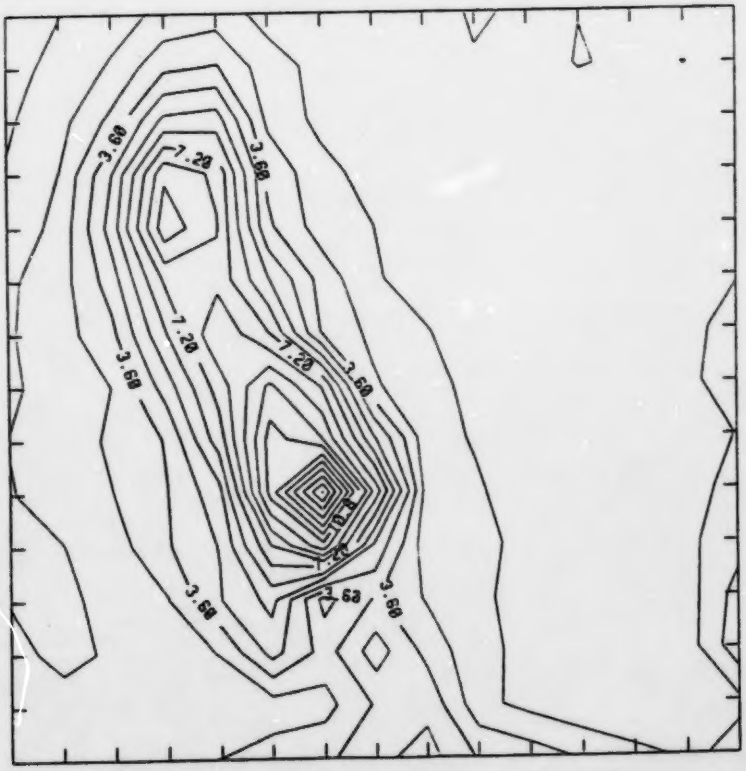

CONTOUR FROM 0.22222E-23 TO 16.220 CONTOUR INTERVAL OF 0.92222 PT(3,3)= 1.9182

Figure 83

NO2 conc. (u/m**3)

02/08/88 2:00 p.m.

LEVEL = 4 NO2

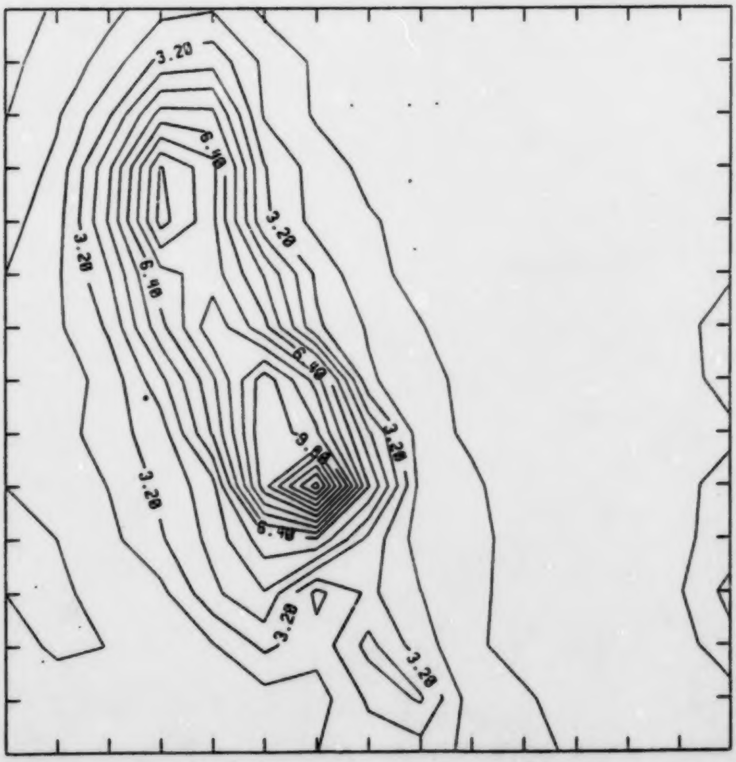

Figure 84

NO2 conc. (u/m**3)

03/08/88 2:00 a.m.

LEVEL = 1 NO2

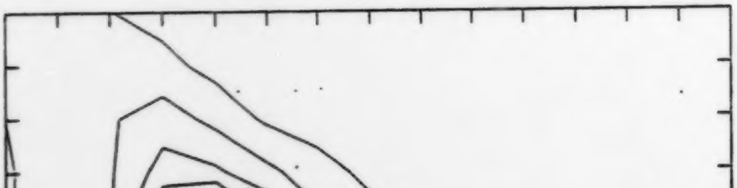

Figure 85

NO2 conc. (u/m**3)

03/08/88 2:00 a.m.

LEVEL = 4 NO2

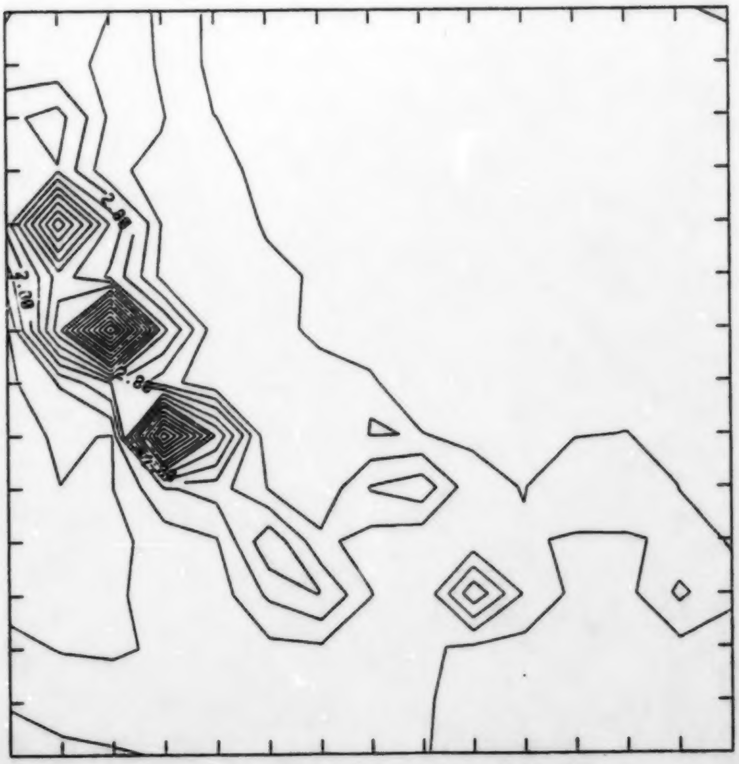

CONTOUR FROM 0.00000E+00 TO 11.022 CONTOUR INTERVAL OF 0.72228 PT(3,3)= 0.63338

Figure 86

NO2 conc. (u/m**3)

03/08/88 2:00 p.m.

LEVEL = 1 NO2

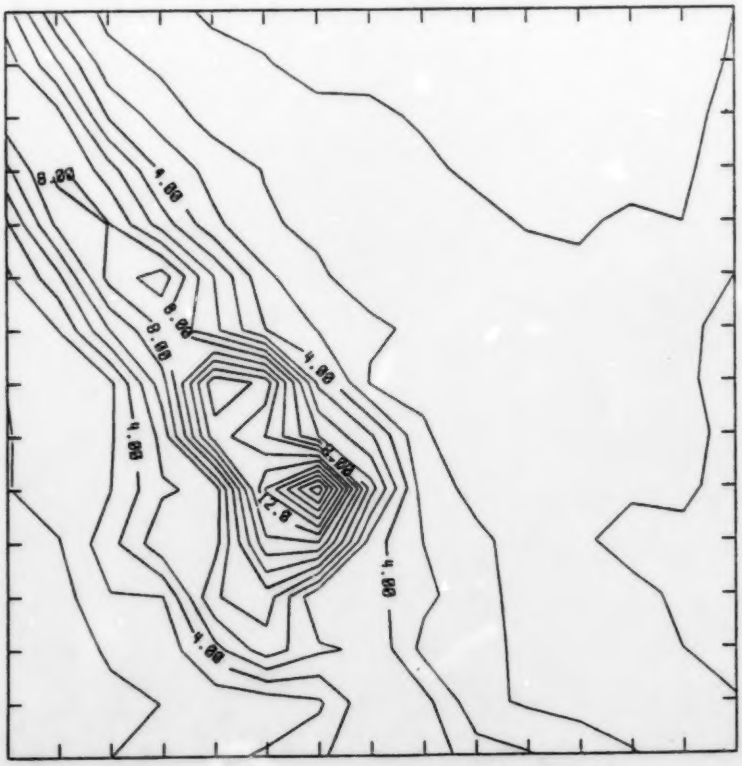

CONTOUR FROM 0.00000E+00 TO 17.000 CONTOUR INTERVAL OF 1.0000 PT(3,3)= 2.1480

Figure 87

NO2 conc. (u/m**3)

03/08/88 2:00 p.m.

LEVEL = 4 NO2

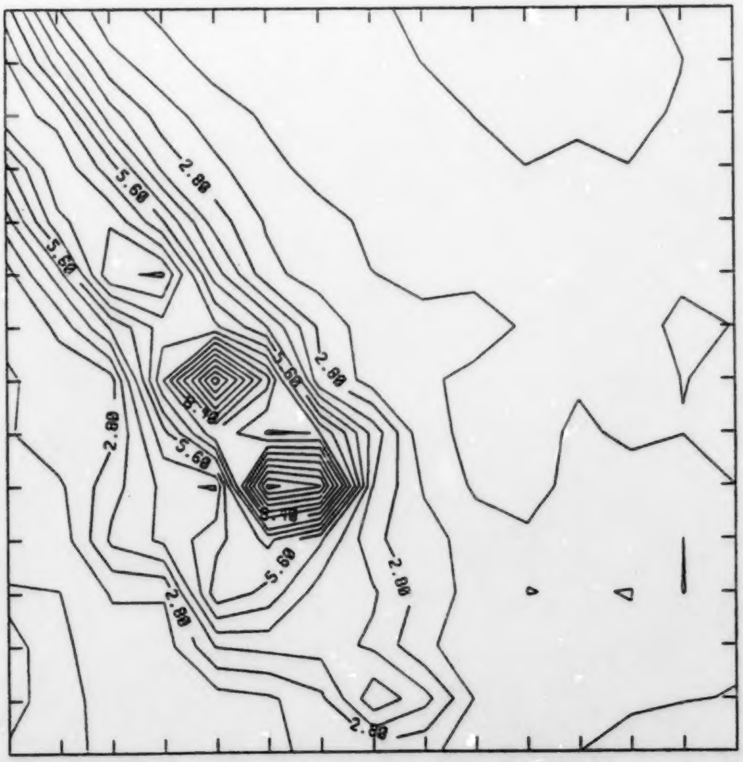

CONTOUR FROM 0.20000E-02 TO 12.600 CONTOUR INTERVAL OF 0.70000 PT(3,3)= 1.0233

Figure 88

NO2 conc. (u/m**3)

04/08/88 2:00 a.m.

LEVEL = 4 NO2

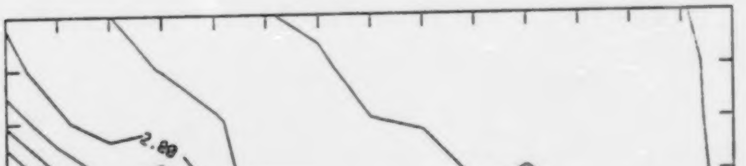

Figure 89

NO2 conc. (u/m**3)

04/08/88 2:00 a.m.

LEVEL = 1 NO2

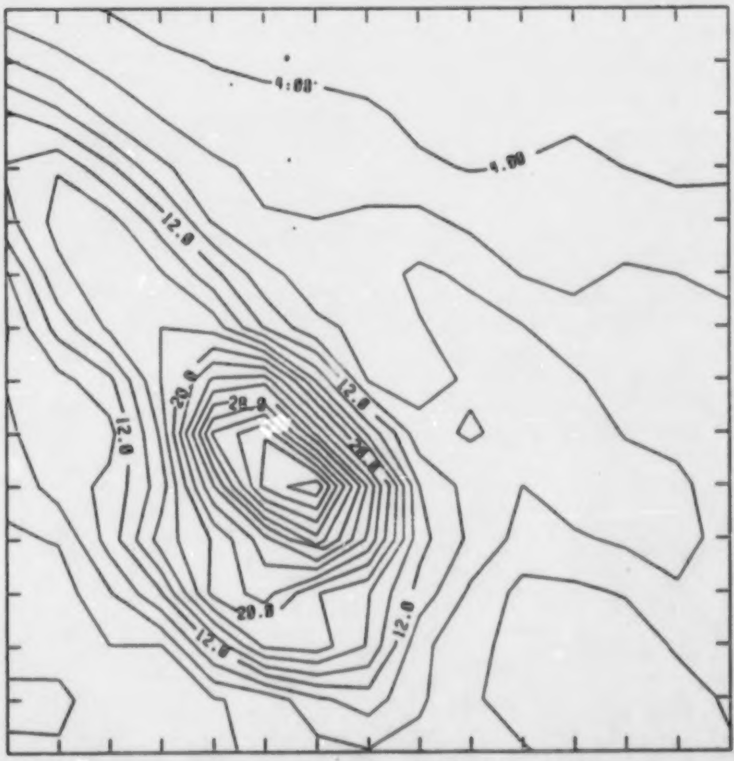

Figure 90

NO2 conc. (u/m**3)

04/08/88   2:00 p.m.

LEVEL = 1   NO2

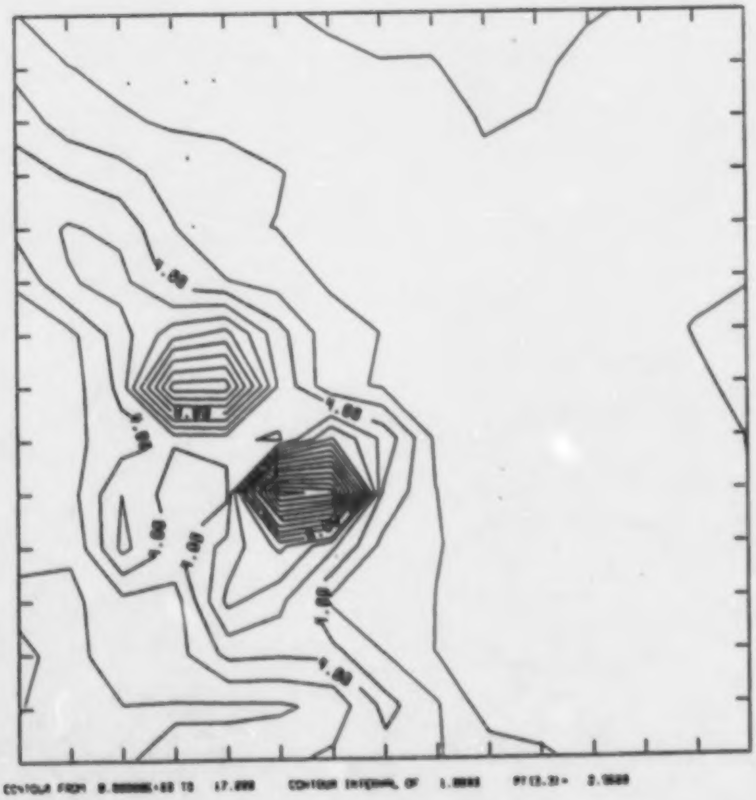

Figure 91

NO2 conc. (u/m**3)
04/08/88 2:00 p.m.

LEVEL = 4 NO2

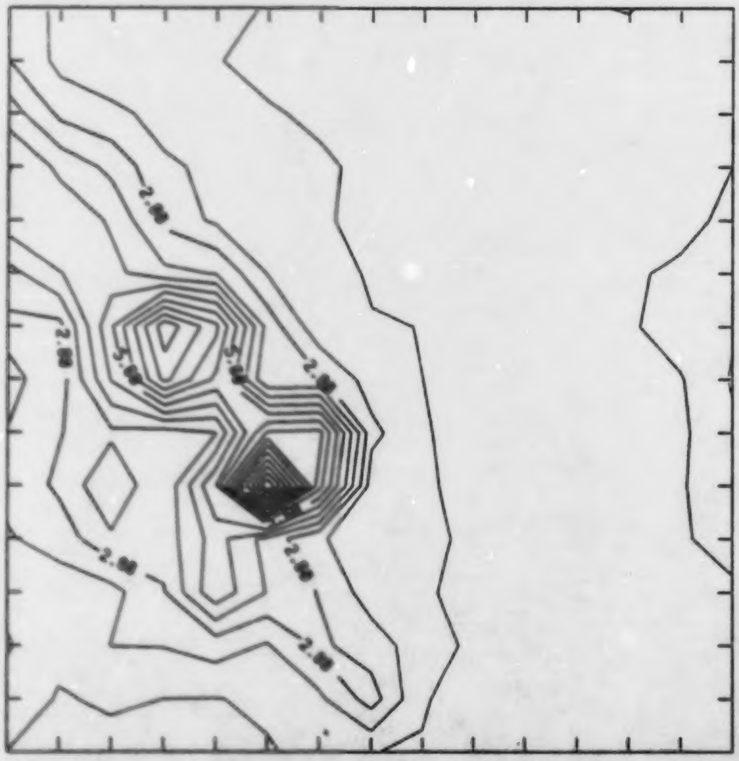

Figure 92

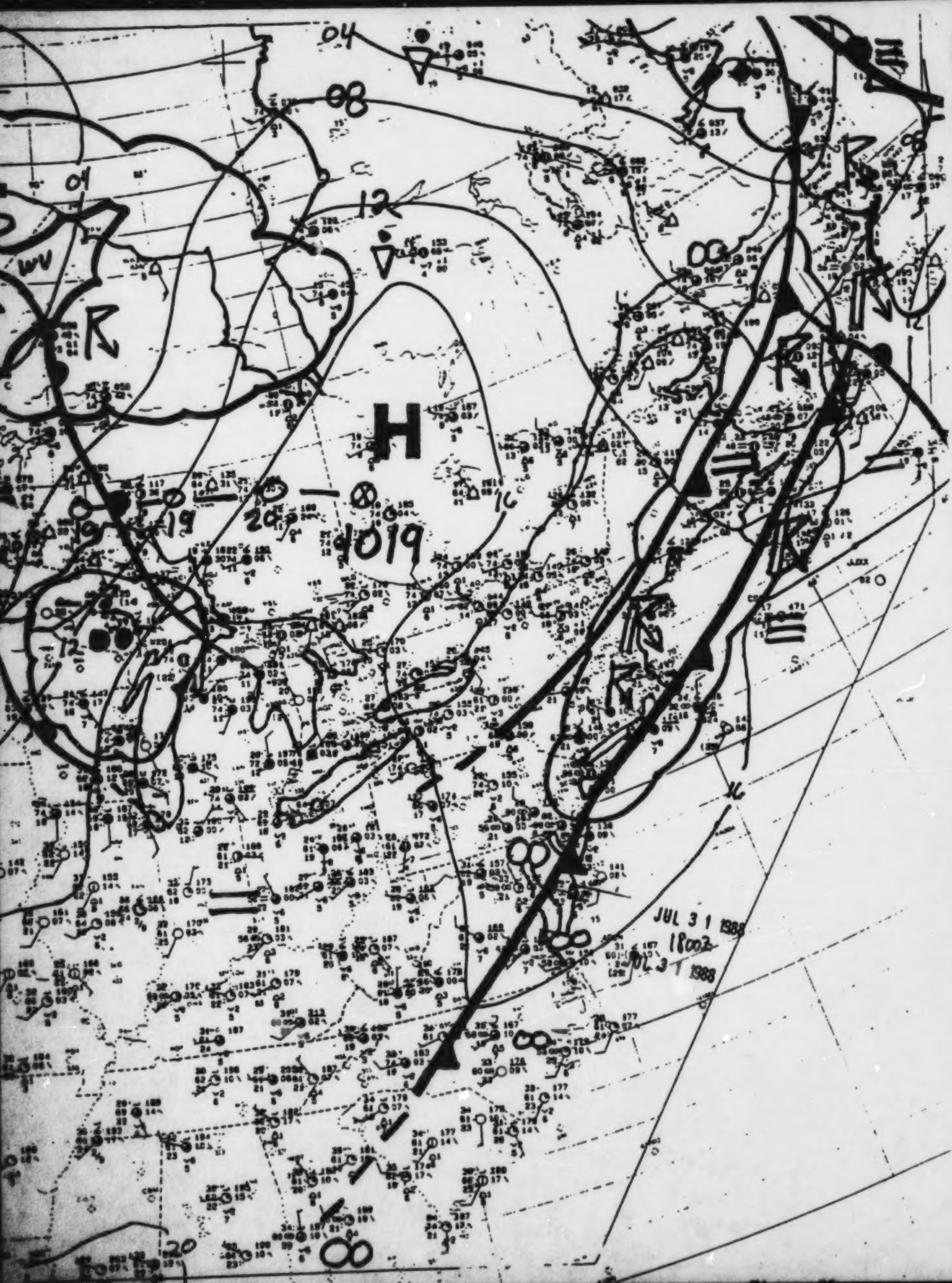

JUL 3 1 1988
1800Z
JUL 3 1 1988

04
08
04
12
WV
R
H
1019
16
19
19
20
12
00
08
12
16
20
00

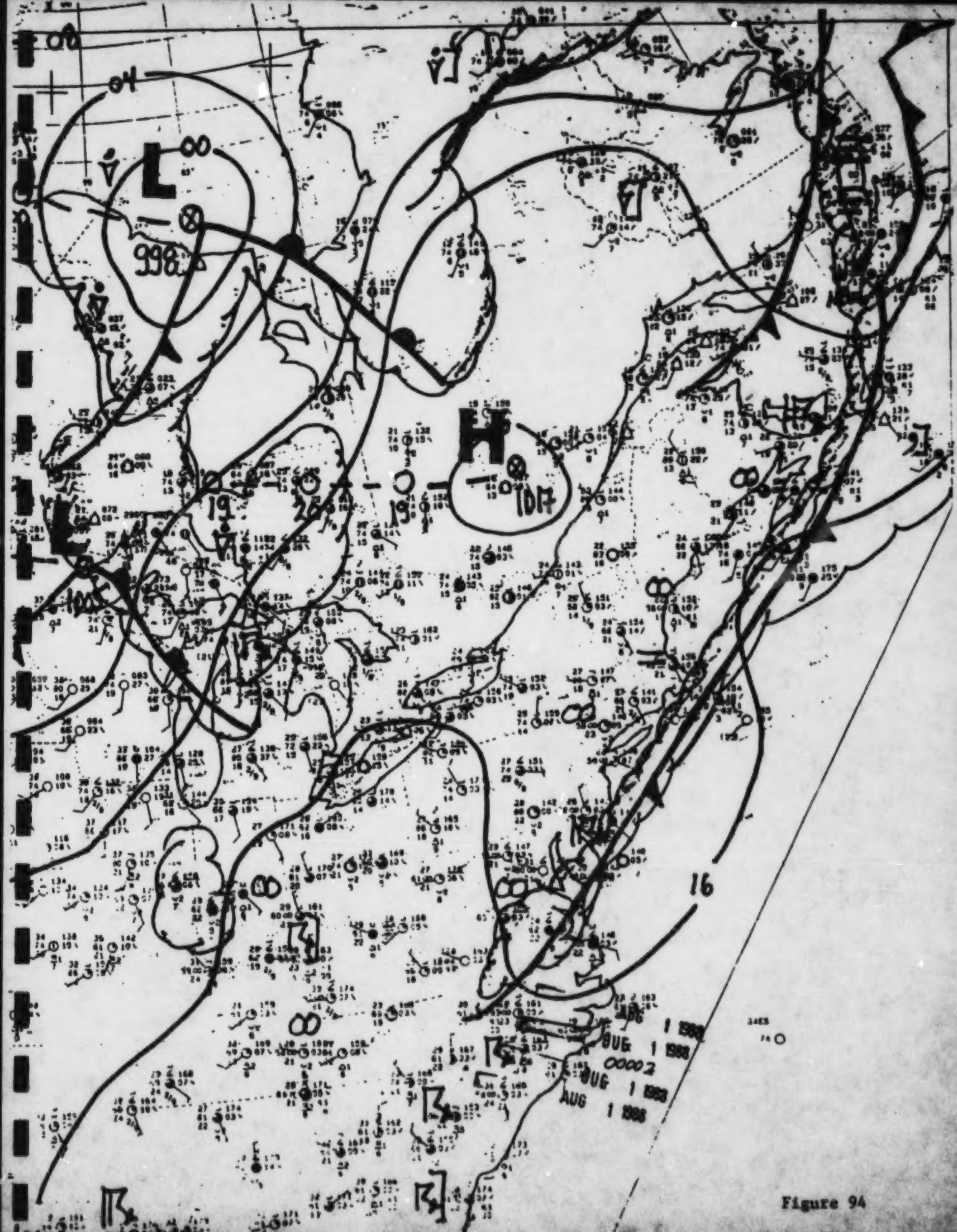

L
998
H
1017
L
1008
19
20
19
16
AUG 1 1988
AUG 1 1988
00002
AUG 1 1988
AUG 1 1988

Figure 94

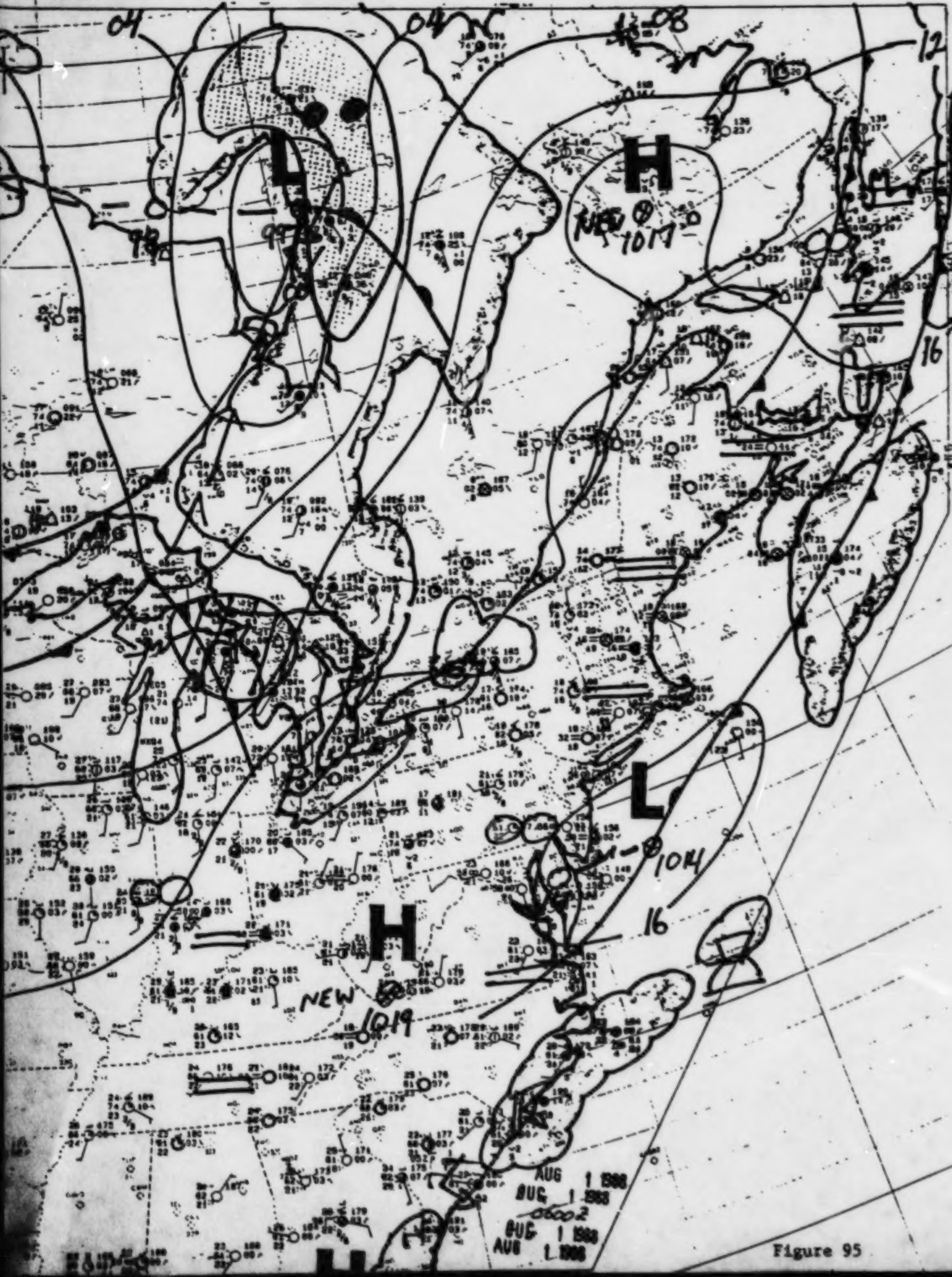
04
04
08
12
L
99
H
NEW
1017
16
L
1014
16
H
NEW
1019
AUG 1 1988
AUG 1 1988
0600Z
AUG 1 1988
AUG 1 1988

Figure 95

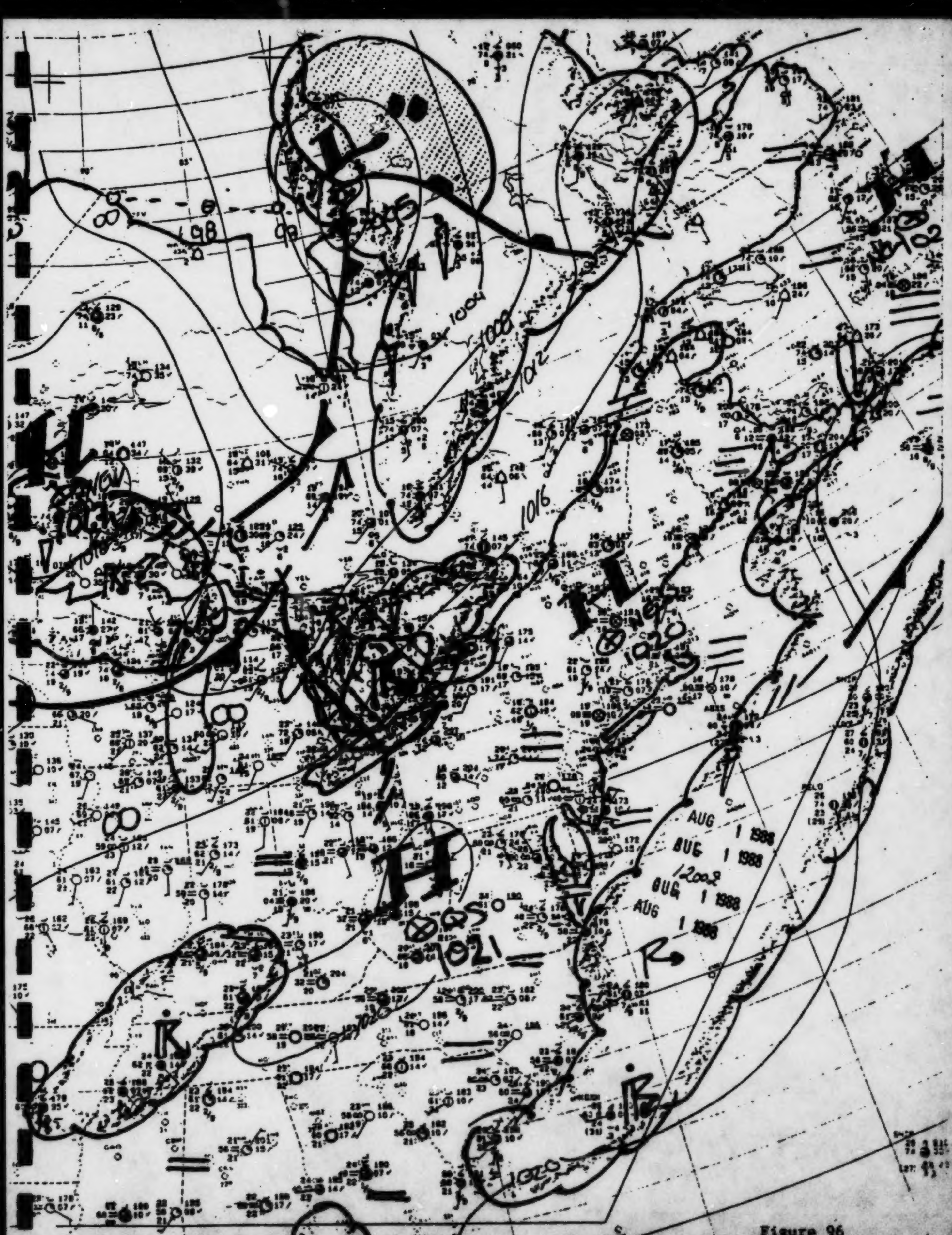
L
H
1004
1008
1012
1016
1020
1021
1020
1020
R
K
AUG 1 1988
AUG 1 1988
1200Z
AUG 1 1988
AUG 1 1988

Figure 96

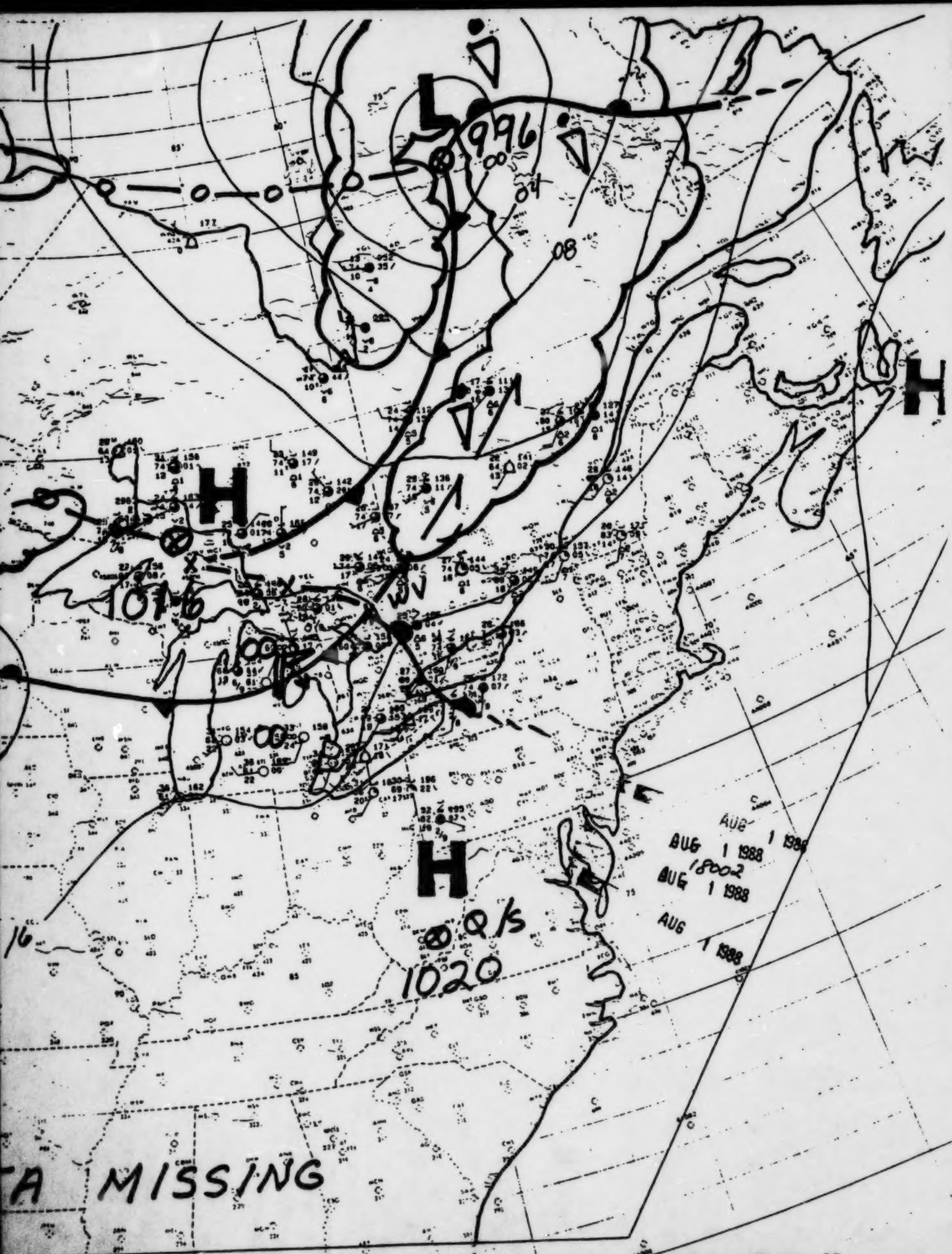
L
996
00
04
08
H
H
1016
WV
H
Q/S
1020
16
TA MISSING
AUG 1 1988
AUG 1 1988
1800Z
AUG 1 1988
AUG 1 1988

Figure 97

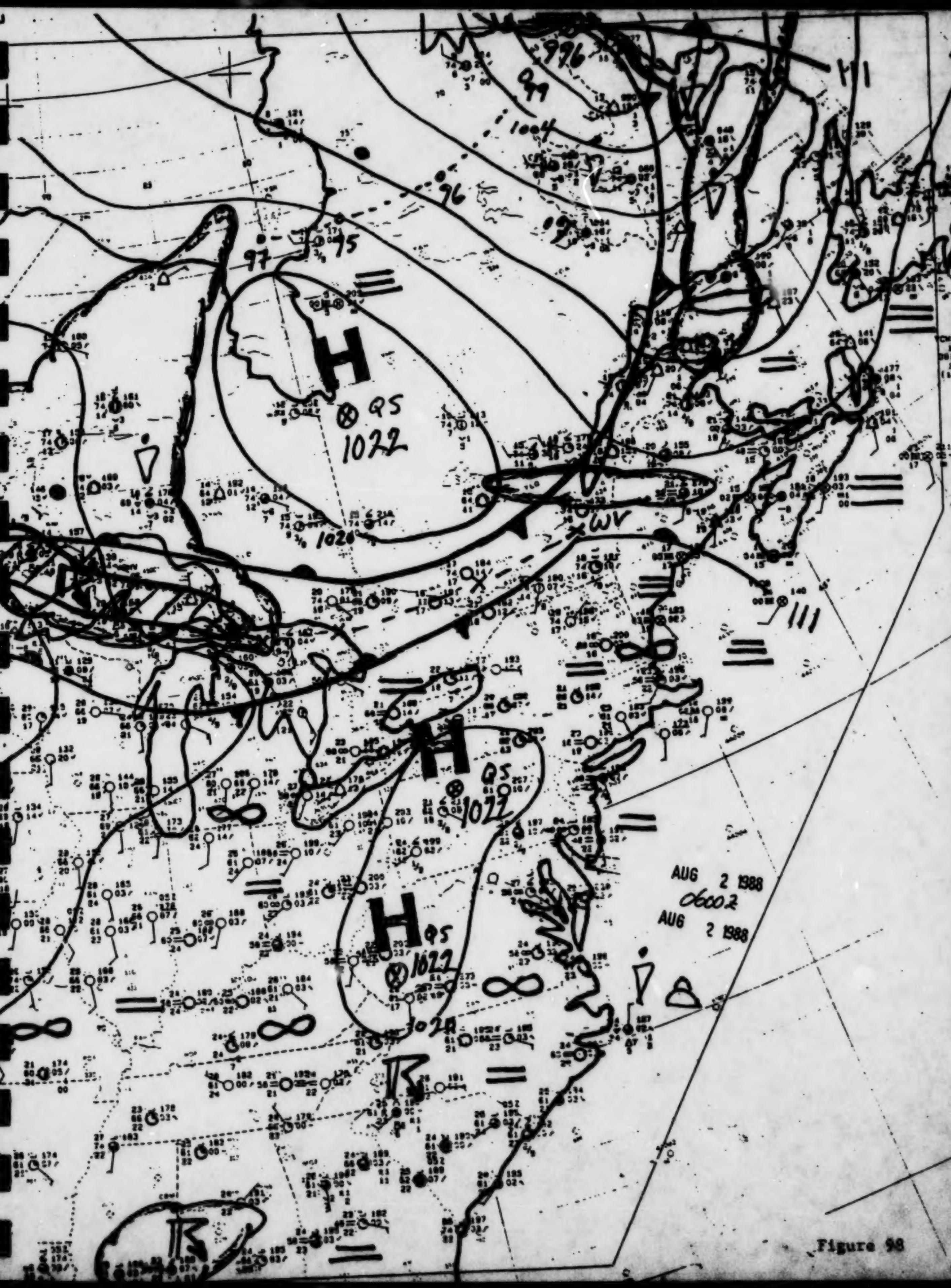
996
999
1004
96
97
75
H
QS
1022
1020
WV
H
QS
1022
H
QS
1022
1020
R
R

AUG 2 1988
0600Z
AUG 2 1988

Figure 98

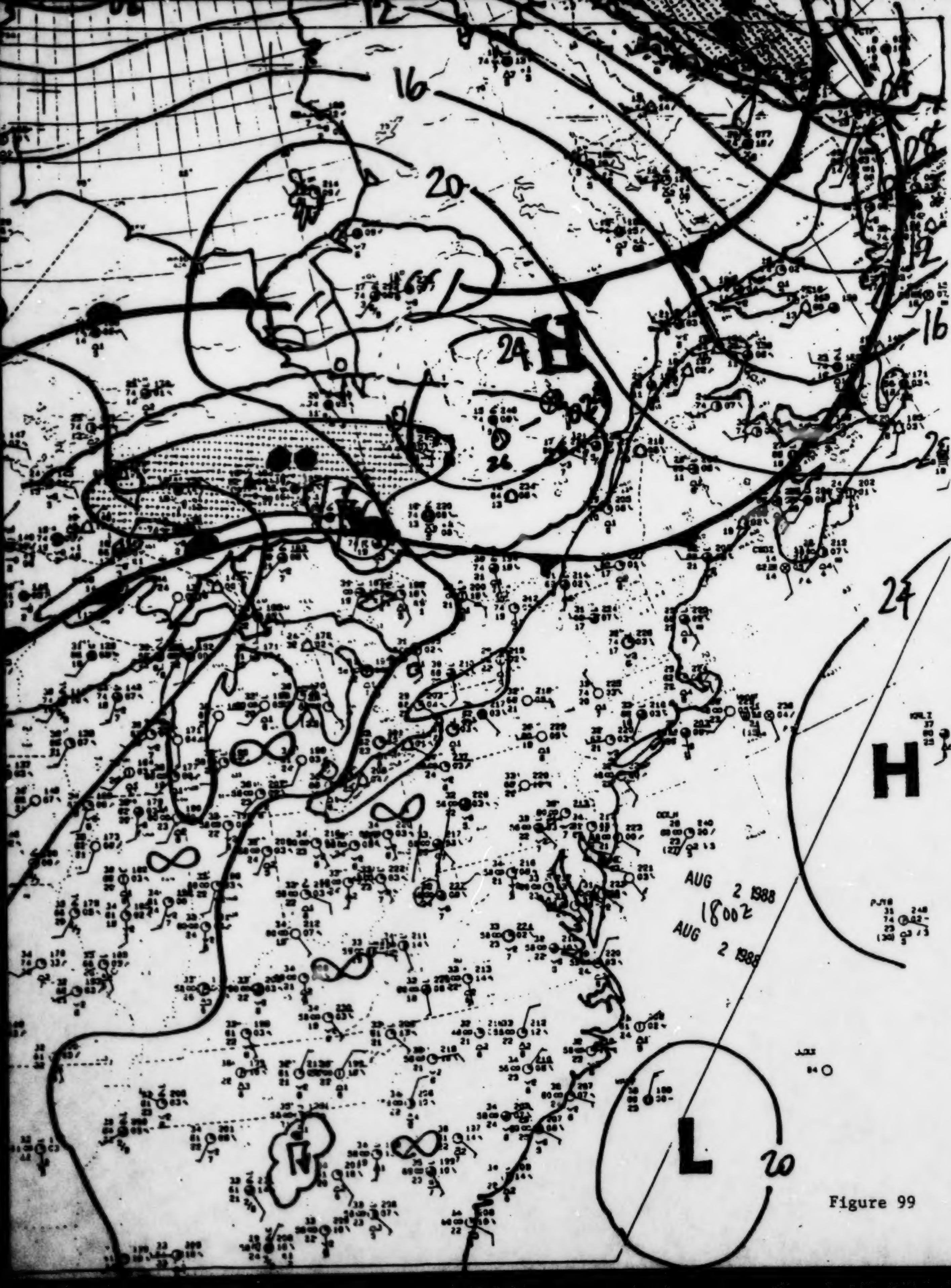

16
20
24
H
12
08
04
16
26
24
H
AUG 2 1988
1800Z
AUG 2 1988
L
20

Figure 99

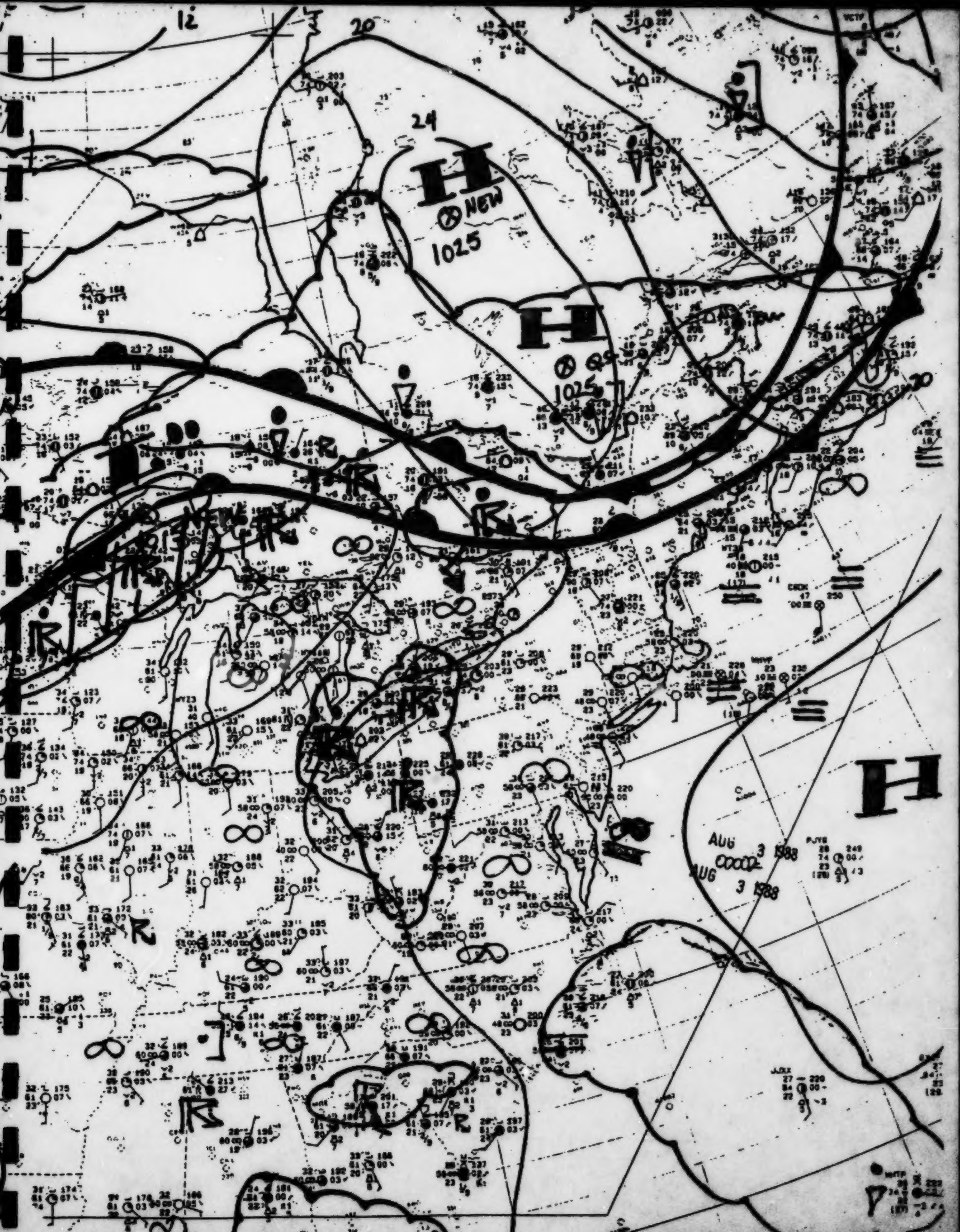
12
20
24
H
NEW
1025
H
1025
30
H
AUG 3 1988
AUG 3 1988

Figure 100

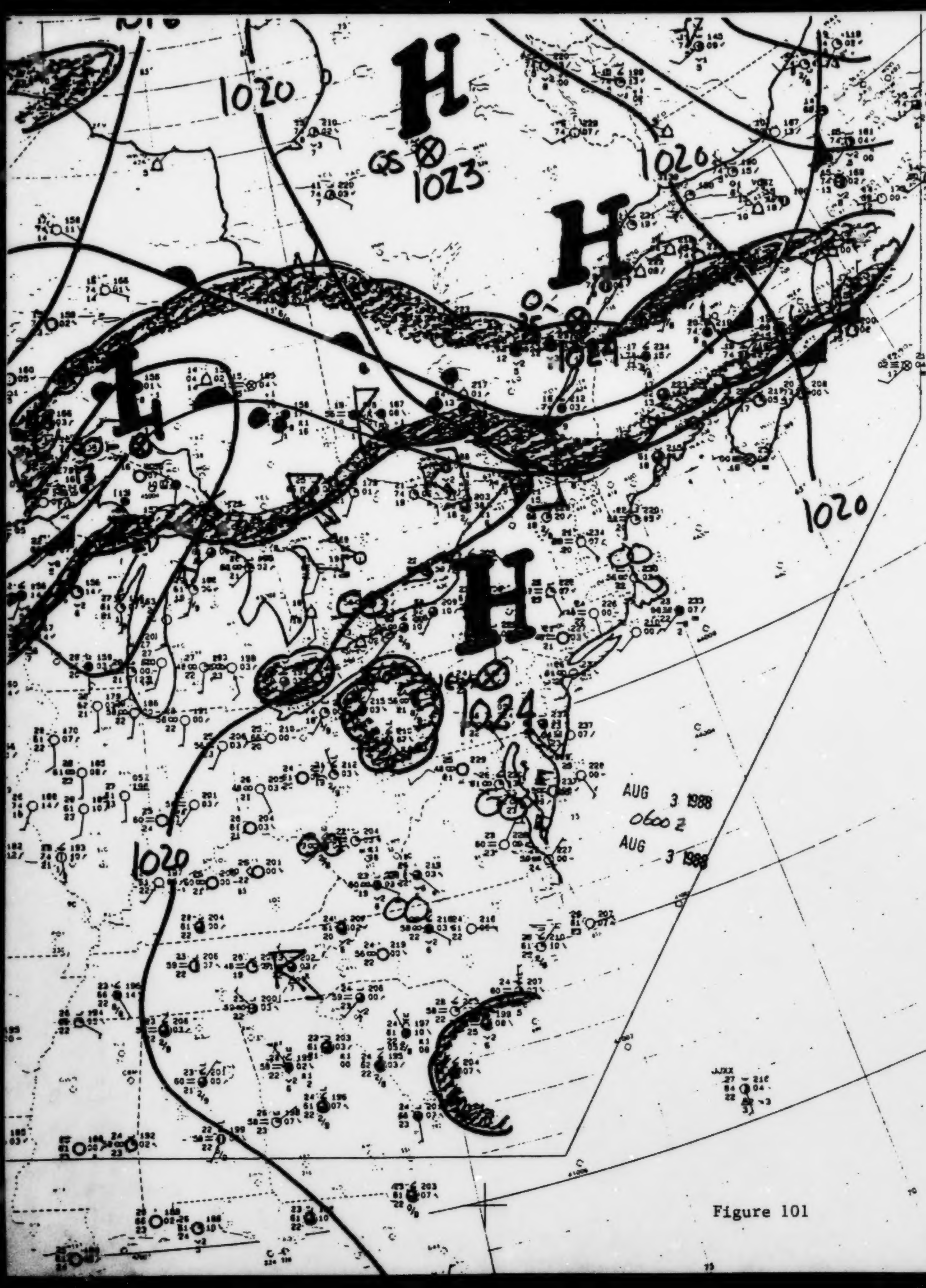
1020
H
QS
1023
1020
H
1024
L
H
1024
1020
1020
1020
AUG 3 1988
0600 Z
AUG 3 1988

Figure 101

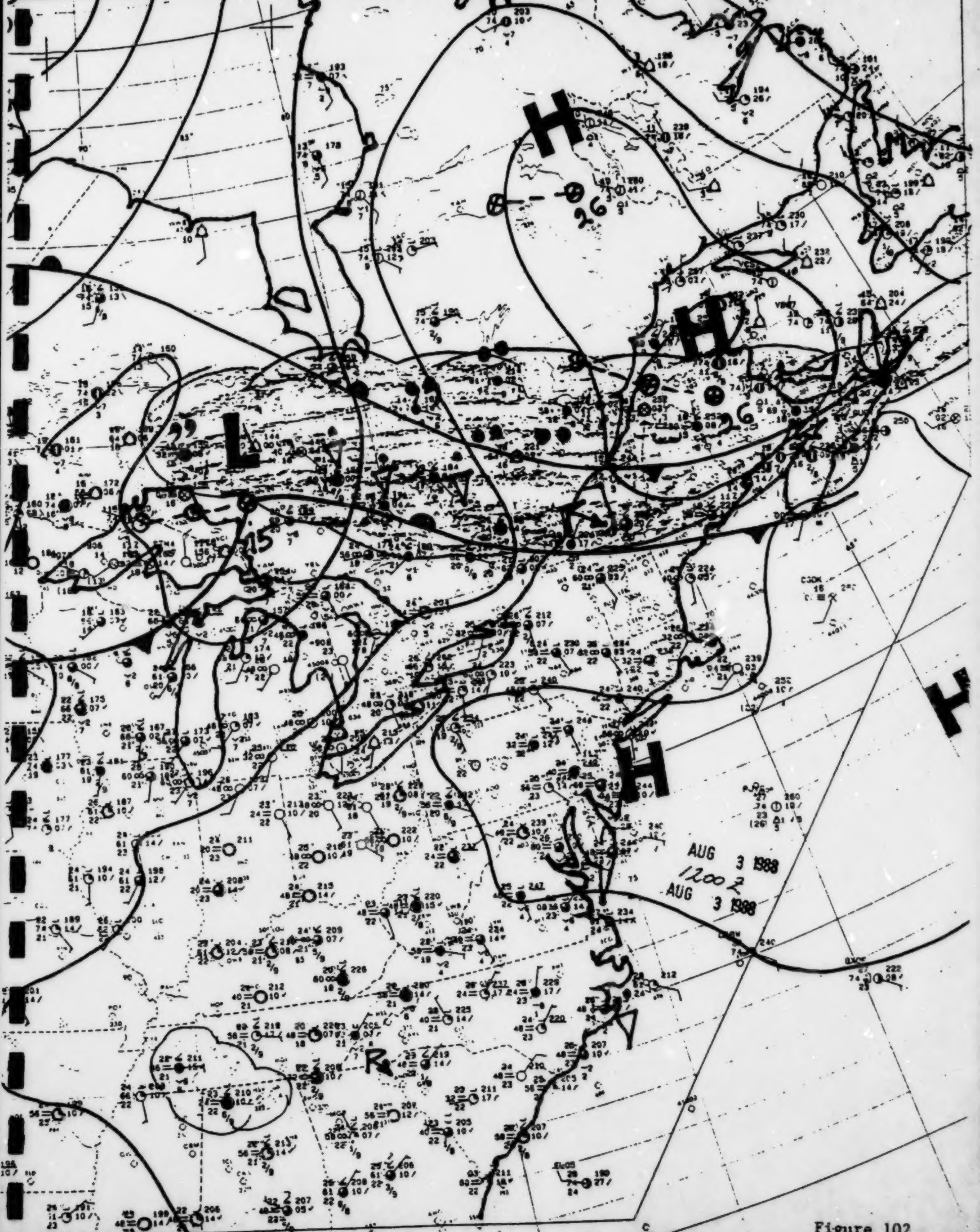
H
26
H
26
L
15
H
R
AUG 3 1988
1200Z
AUG 3 1988

Figure 102

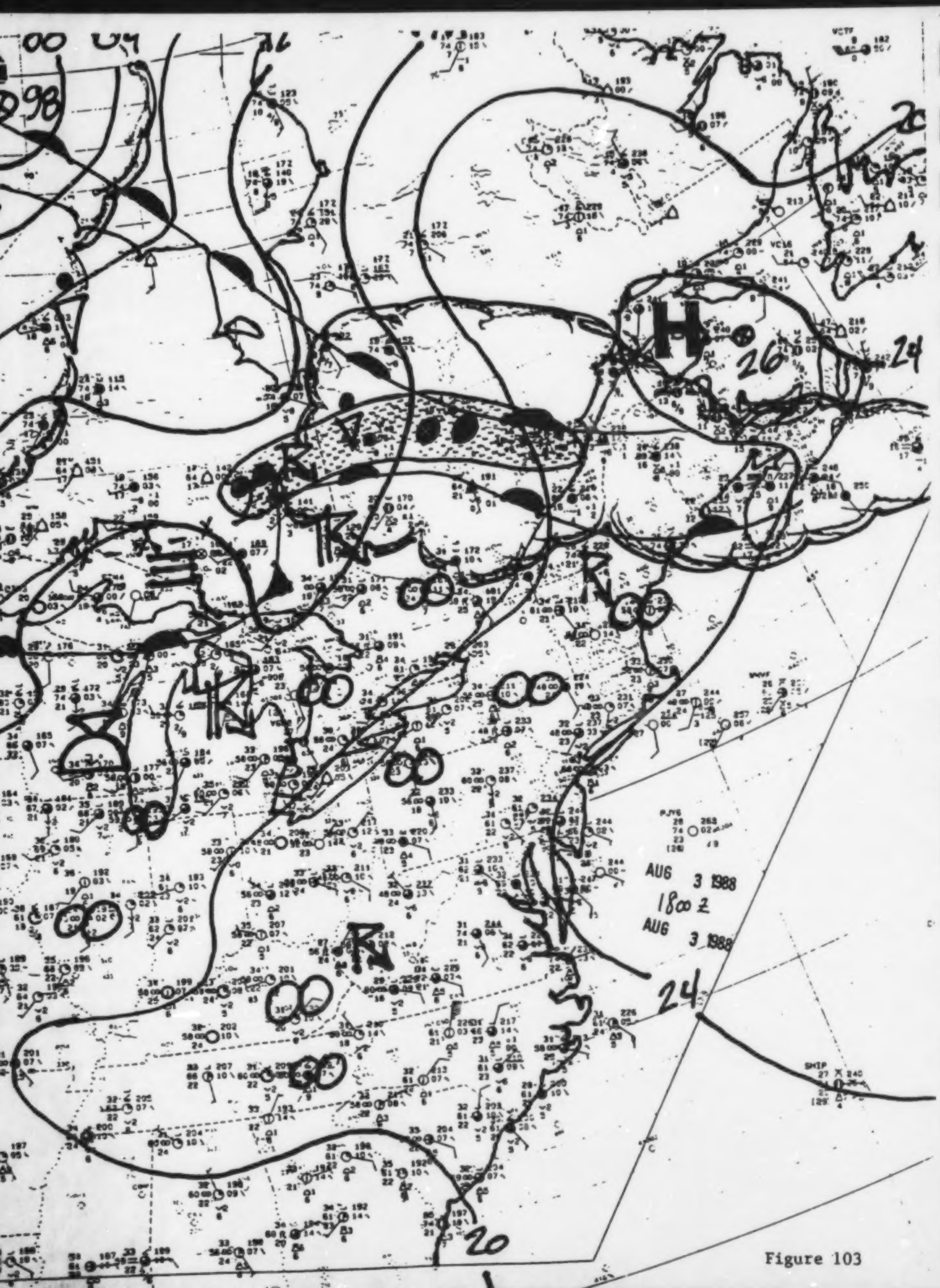
00
04
998
16
20
H
26
24
AUG 3 1988
1800 Z
AUG 3 1988
24
20

Figure 103

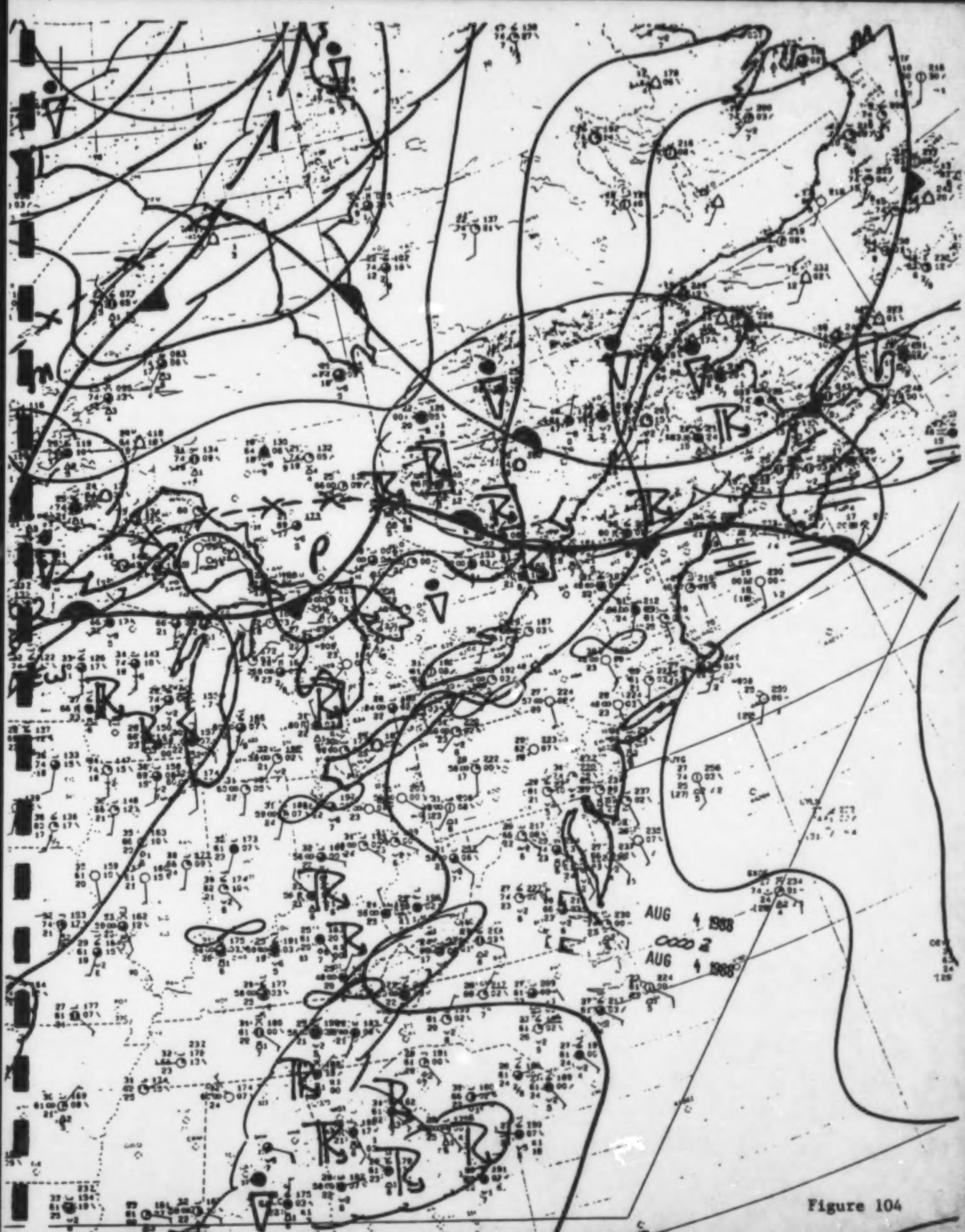
AUG 4 1988
0000 Z
AUG 4 1988

Figure 104

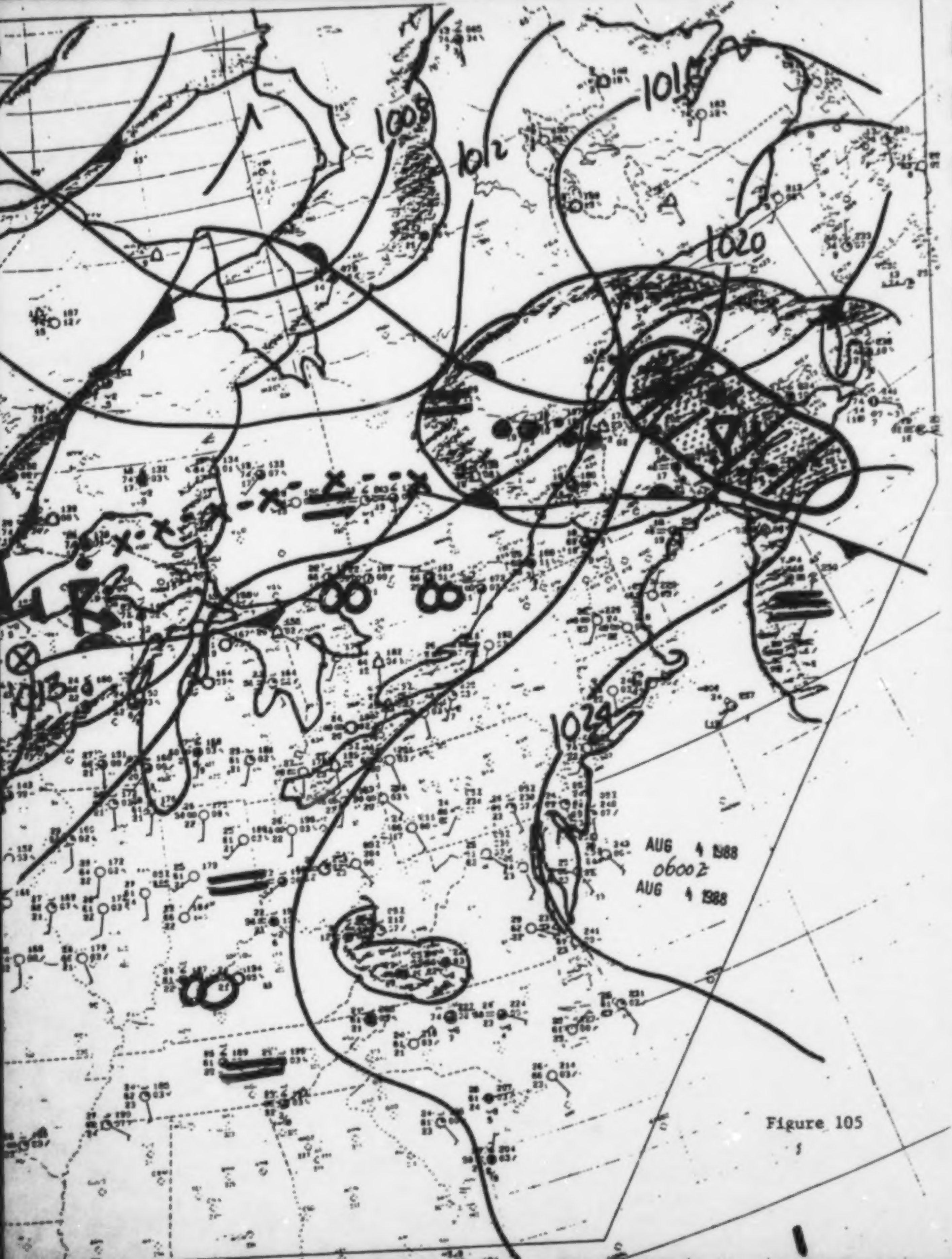
1008
1012
1016
1020
1024
1013
AUG 4 1988
0600Z
AUG 4 1988

Figure 105

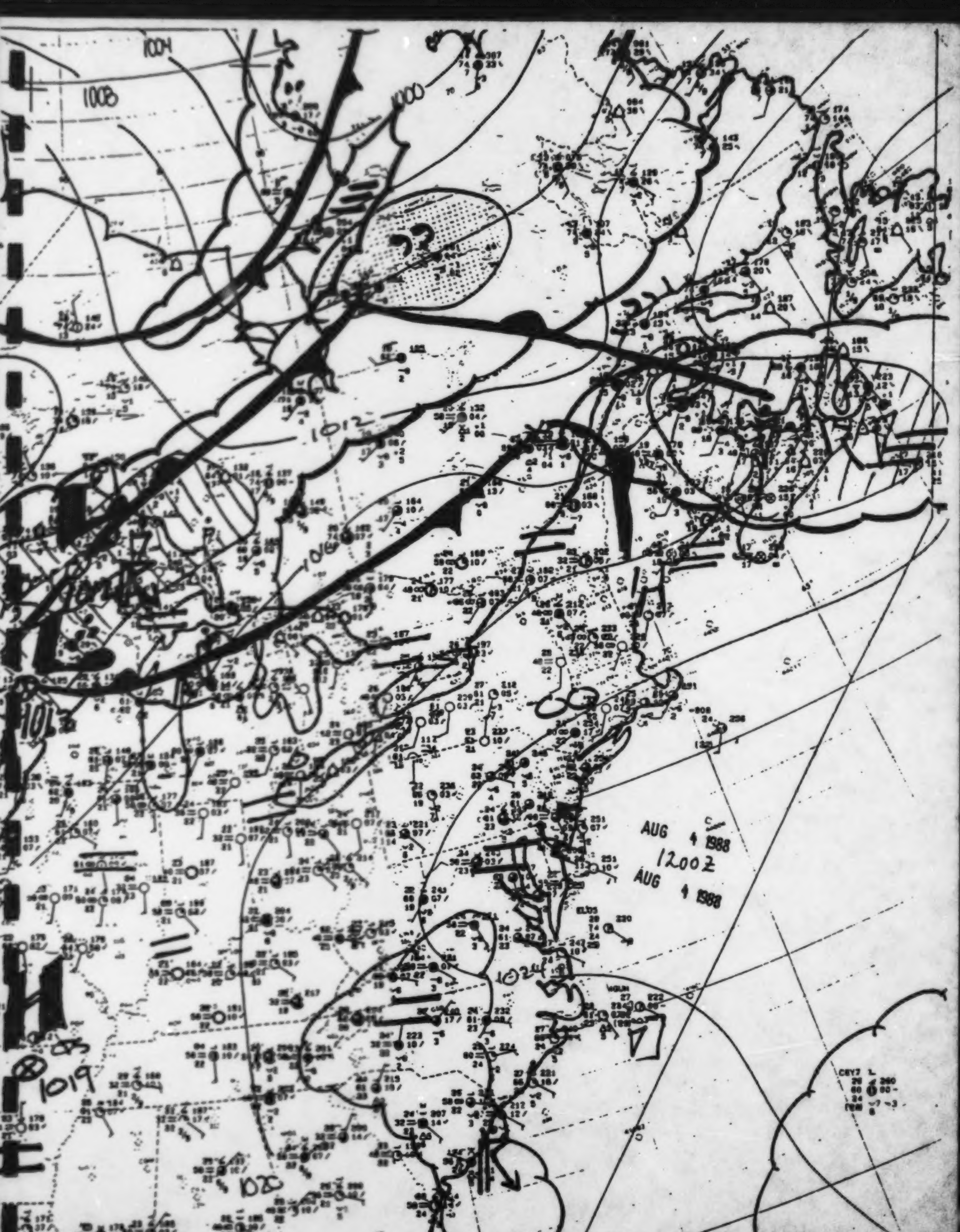
1004
1008
1000
1012
1016
AUG 4 1988
1200Z
AUG 4 1988
1024
101
1019
1020

Figure 106

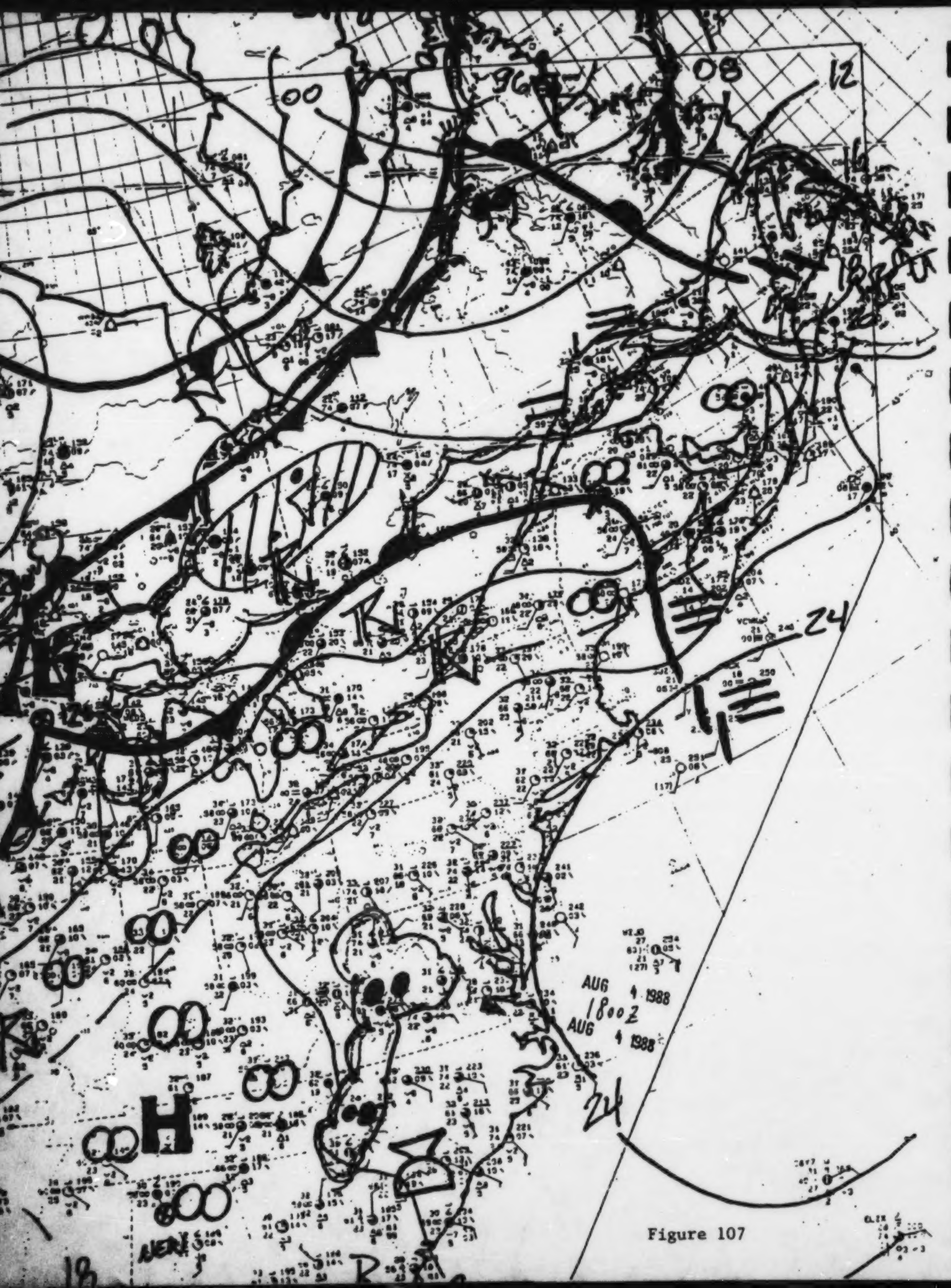
00
96
08
12
16
24
24
18
H
AUG 4 1988
1800Z
AUG 4 1988

Figure 107

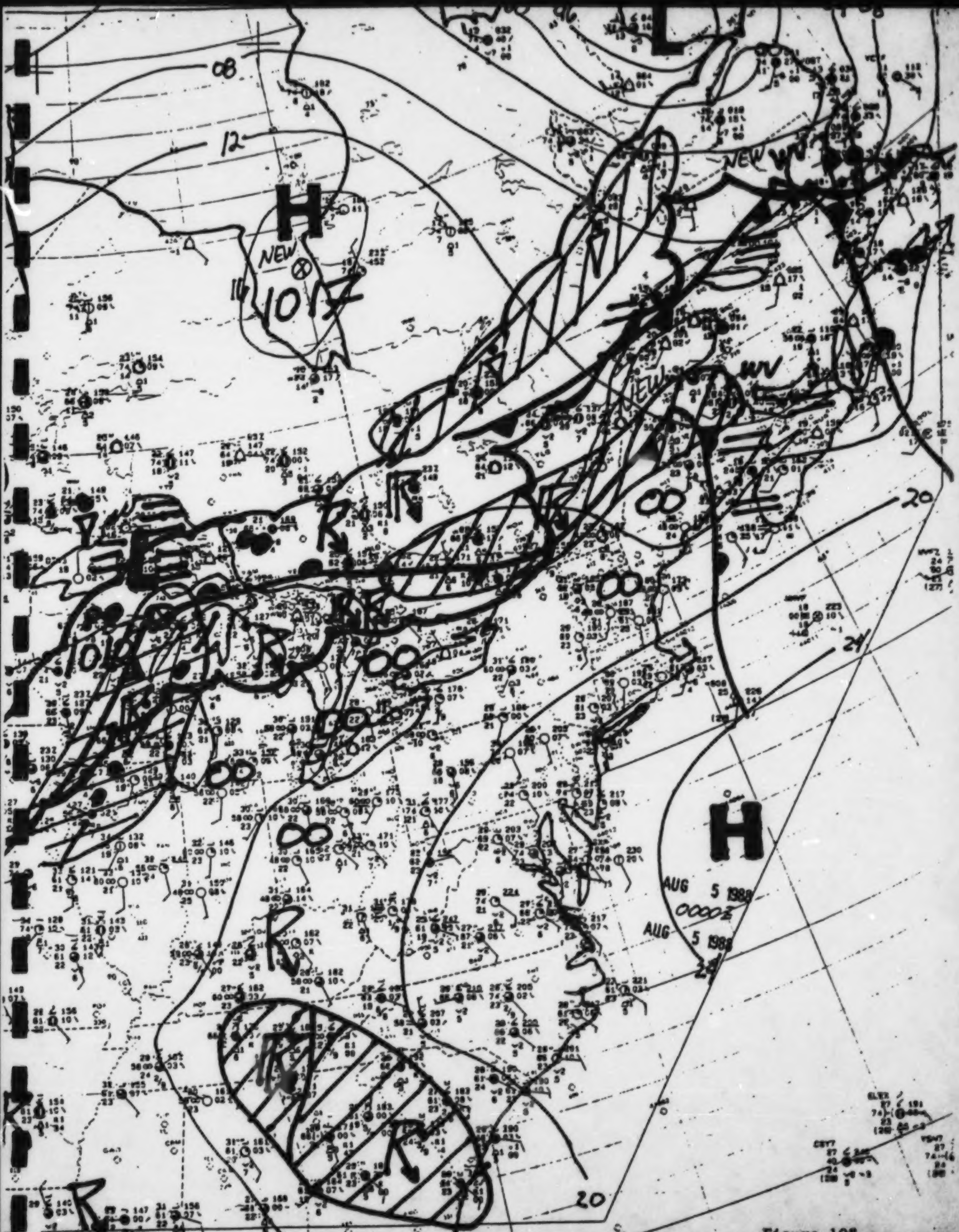
L
08
12
H
NEW
1017
16
NEW
WV
NEW
WV
R
1012
20
24
H
AUG 5 1988
0000Z
AUG 5 1988
24
20

Figure 108

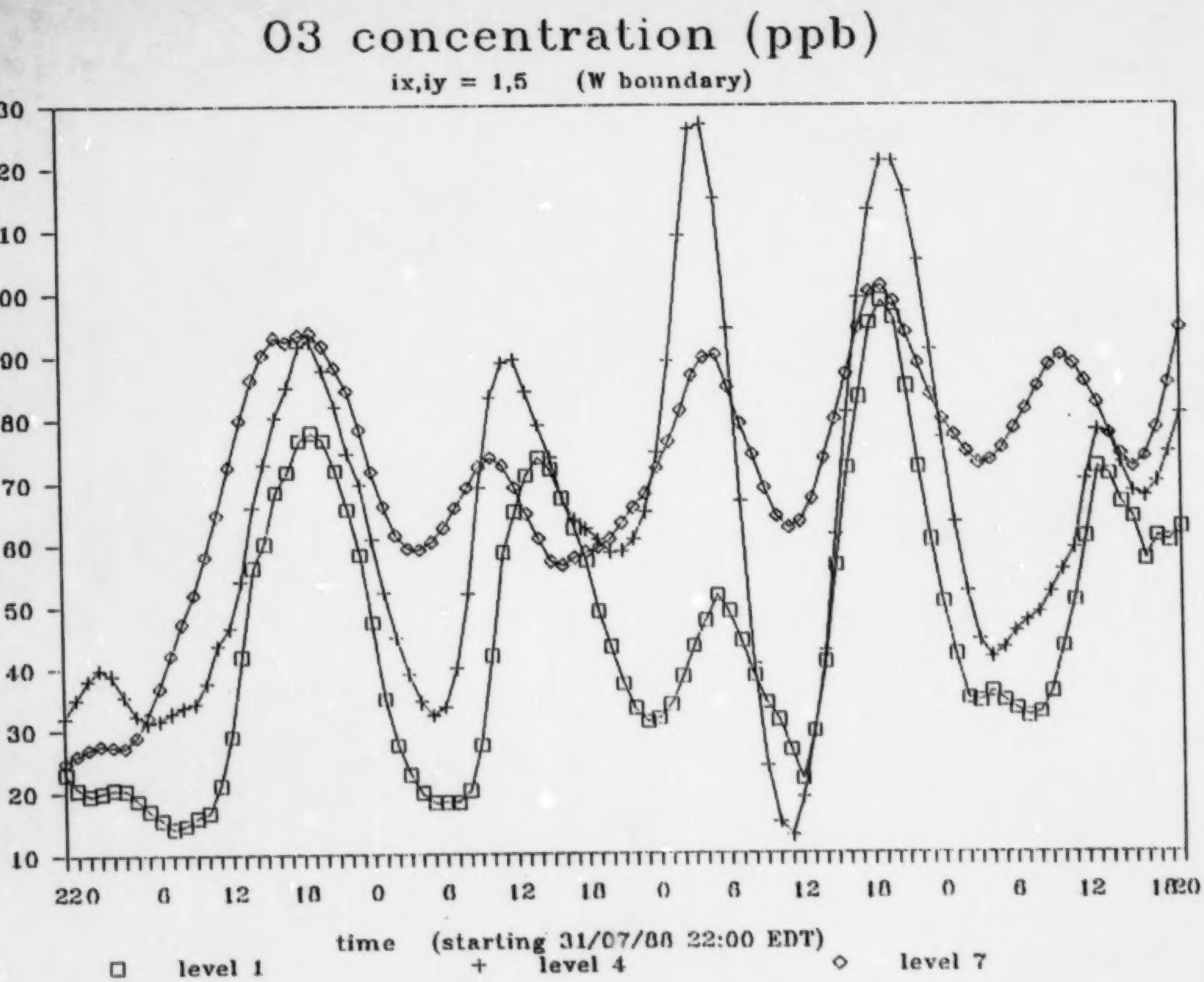
O3 concentration (ppb)
ix,iy = 1,5 (W boundary)
130
120
110
100
90
80
70
60
50
40
30
20
10
22 0
6
12
18
0
6
12
18
0
6
12
18
0
6
12
18 20
time (starting 31/07/88 22:00 EDT)
□ level 1
+ level 4
◇ level 7

Figure 109

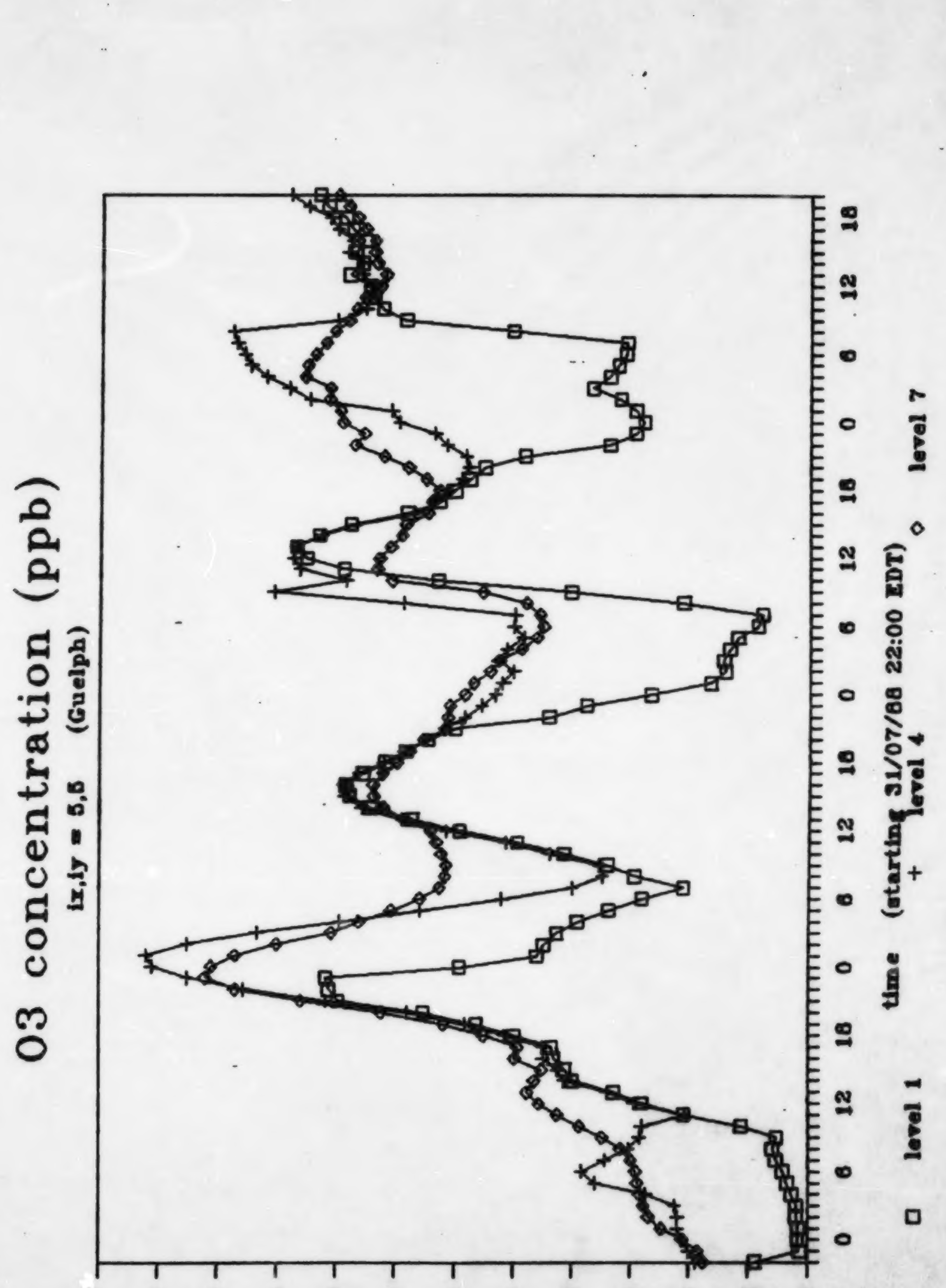
O3 concentration (ppb)
ix,iy = 5,5 (Guelph)
0
10
20
30
40
50
60
70
80
90
100
110
120
0
6
12
18
0
6
12
18
0
6
12
18
0
6
12
18
time (starting 31/07/88 22:00 EDT)
□ level 1
+ level 4
◇ level 7

Figure 110

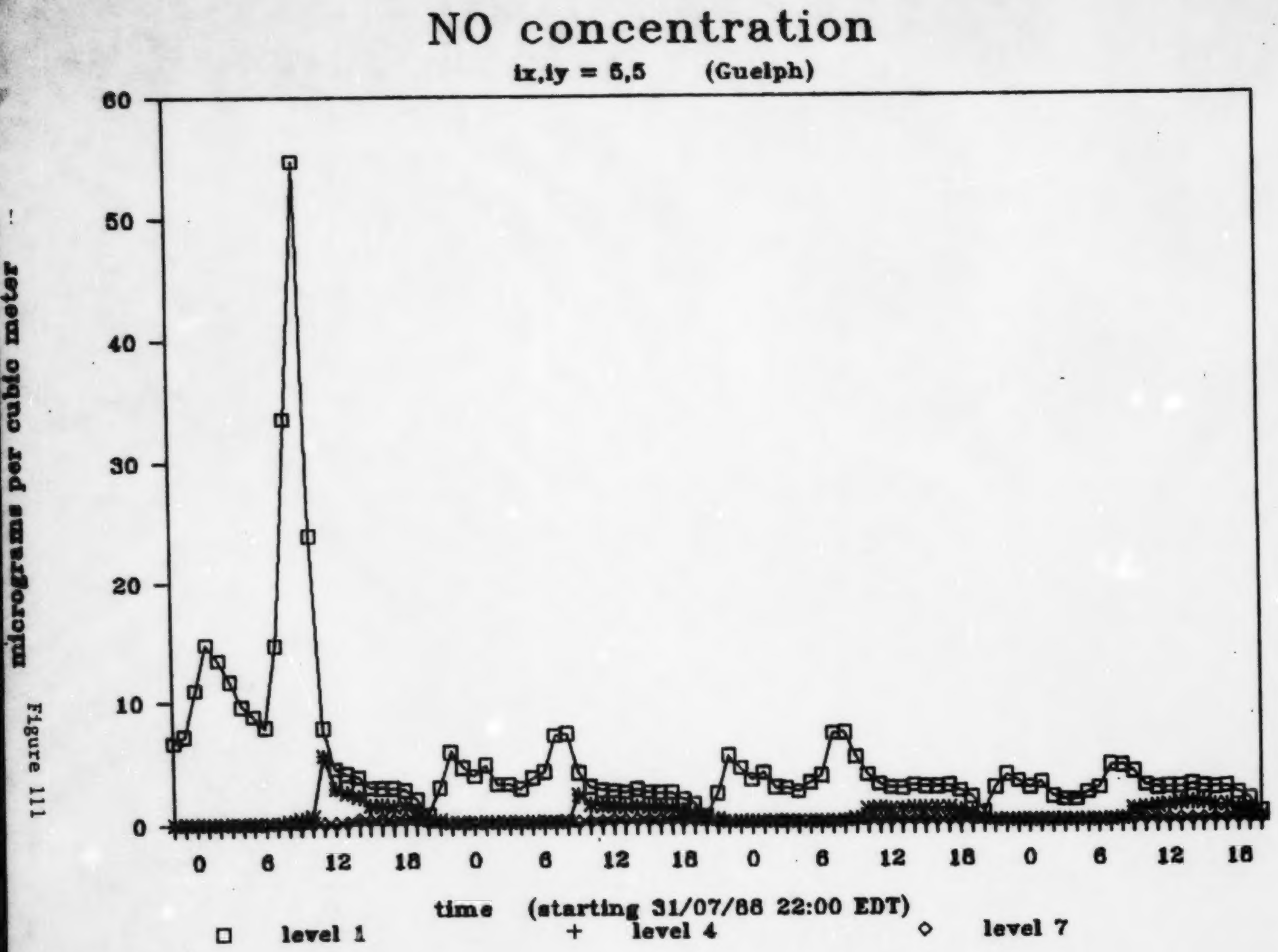
NO concentration
ix,iy = 5,5 (Guelph)
micrograms per cubic meter
0
10
20
30
40
50
60
0
6
12
18
0
6
12
18
0
6
12
18
0
6
12
18
time (starting 31/07/88 22:00 EDT)
□ level 1
+ level 4
◇ level 7

Figure 111

NO2 concentration

ix,iy = 5,5 (Guelph)

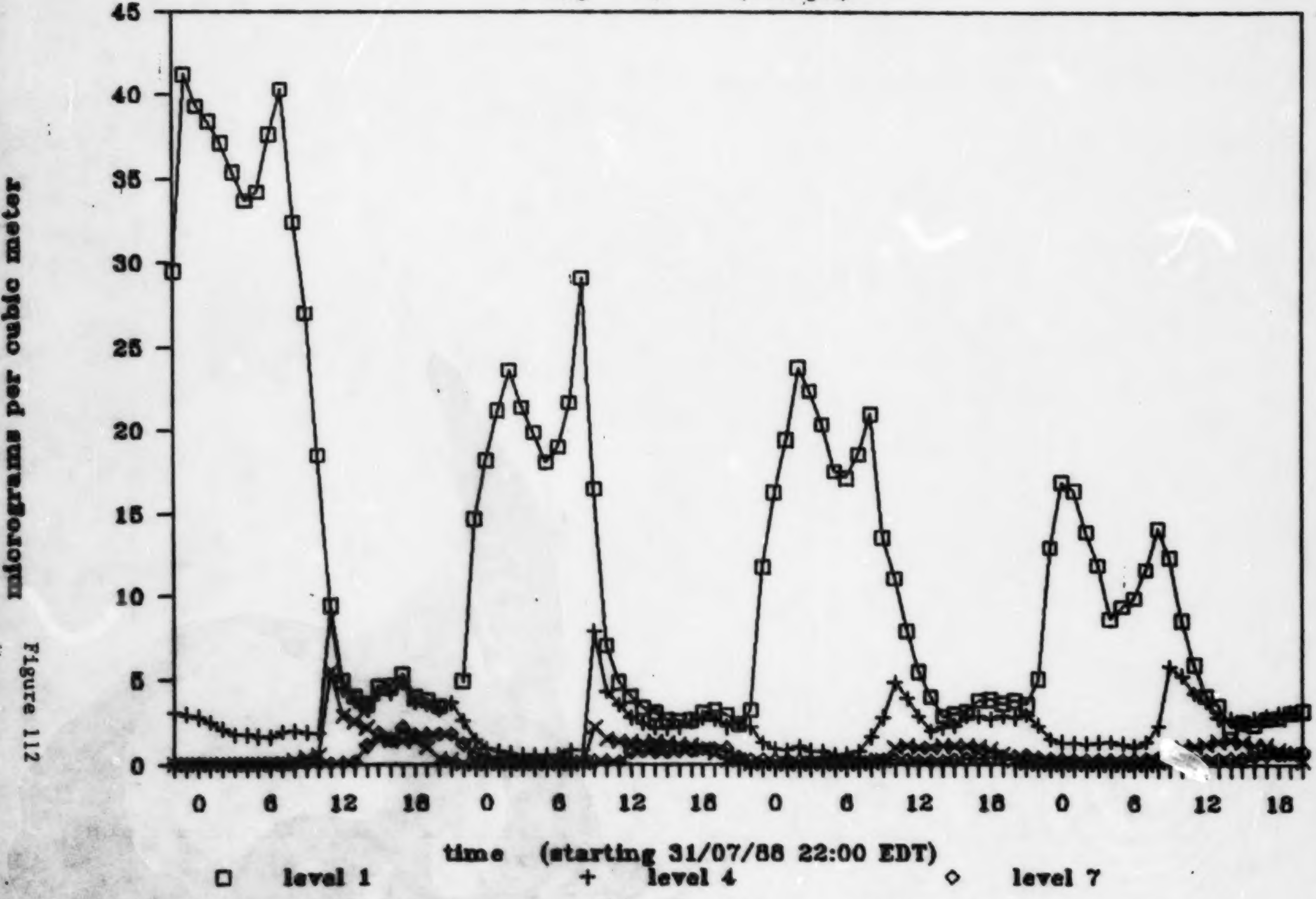

Figure 112

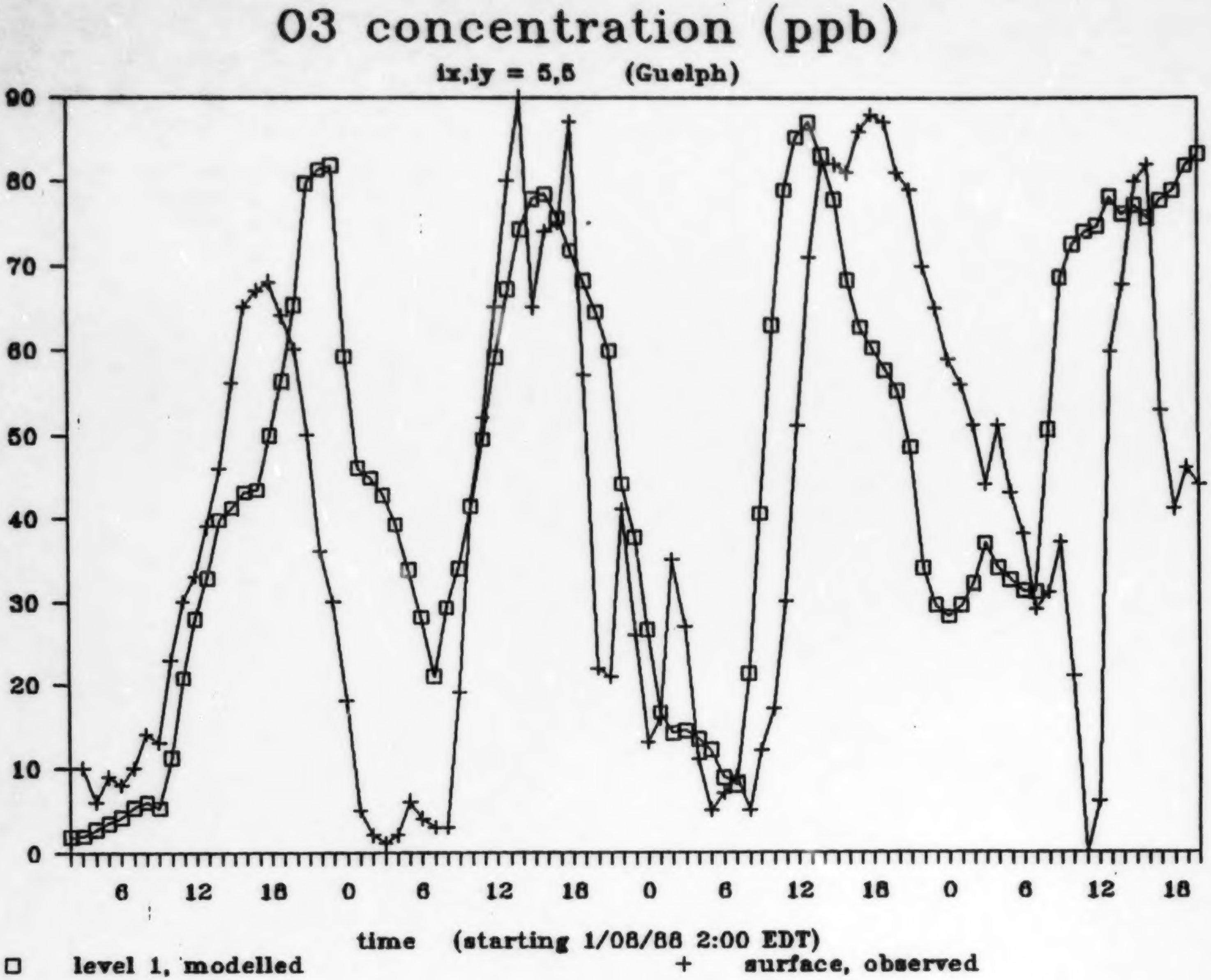
O3 concentration (ppb)
ix,iy = 5,5 (Guelph)
90
80
70
60
50
40
30
20
10
0
6
12
18
0
6
12
18
0
6
12
18
0
6
12
18
time (starting 1/08/88 2:00 EDT)
□ level 1, modelled
+ surface, observed

Figure 113

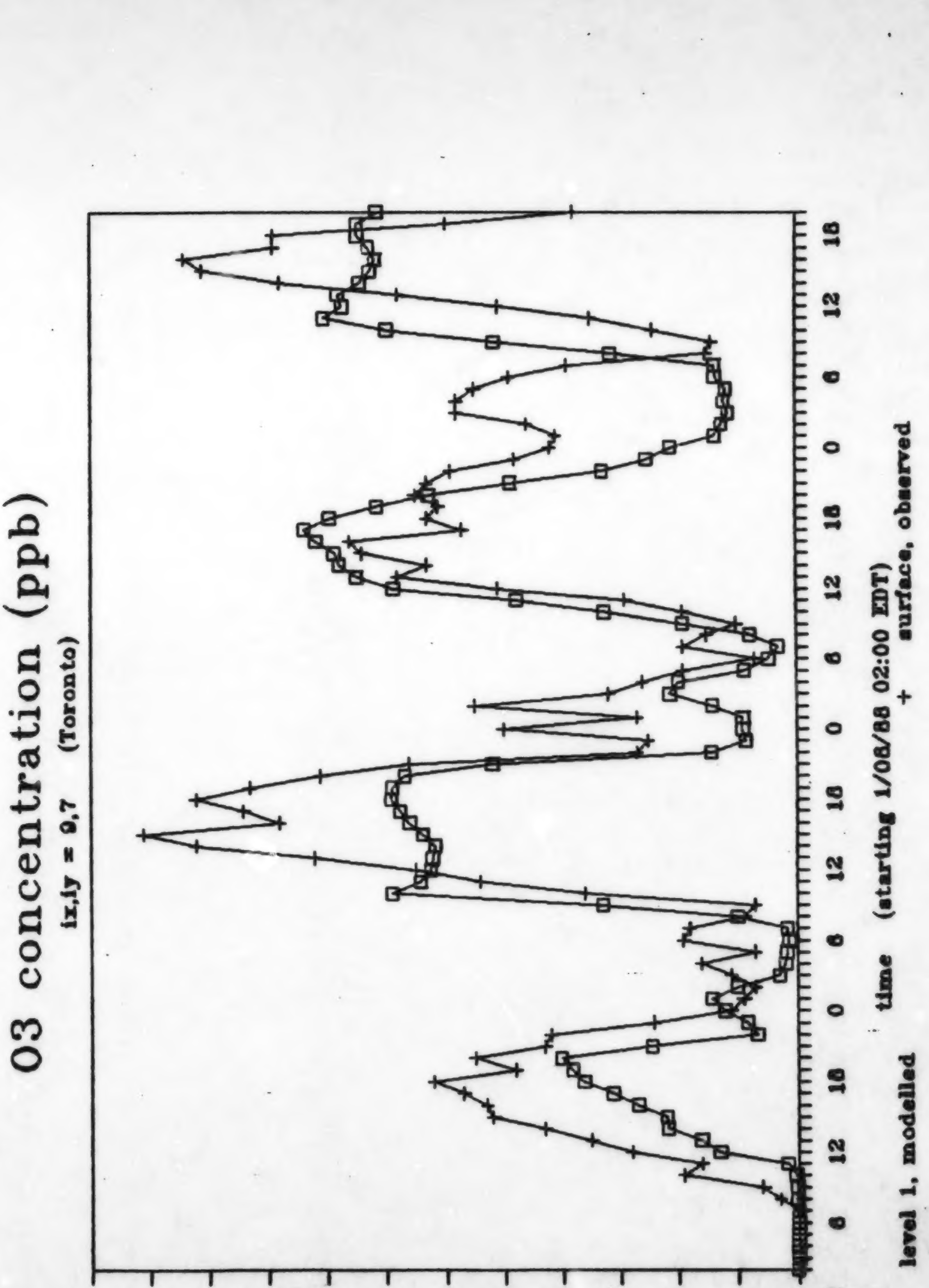
O3 concentration (ppb)
ix,iy = 9,7 (Toronto)
0
10
20
30
40
50
60
70
80
90
100
110
120
6
12
18
0
6
12
18
0
6
12
18
0
6
12
18
time (starting 1/08/88 02:00 EDT)
□ level 1, modelled
+ surface, observed

Figure 114

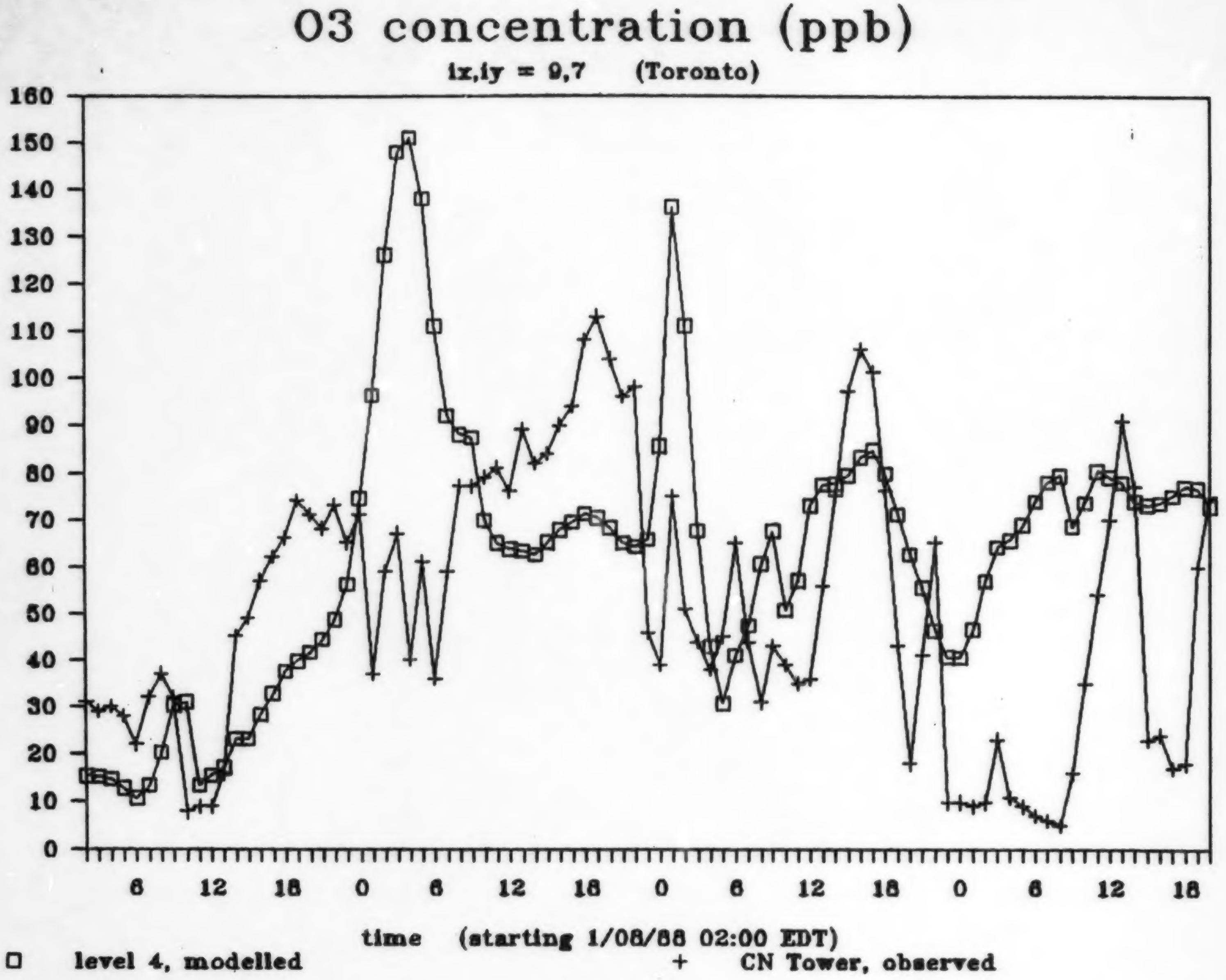
O3 concentration (ppb)
ix,iy = 9,7 (Toronto)
160
150
140
130
120
110
100
90
80
70
60
50
40
30
20
10
0
6
12
18
0
6
12
18
0
6
12
18
0
6
12
18
time (starting 1/08/88 02:00 EDT)
□ level 4, modelled
+ CN Tower, observed

Figure 115

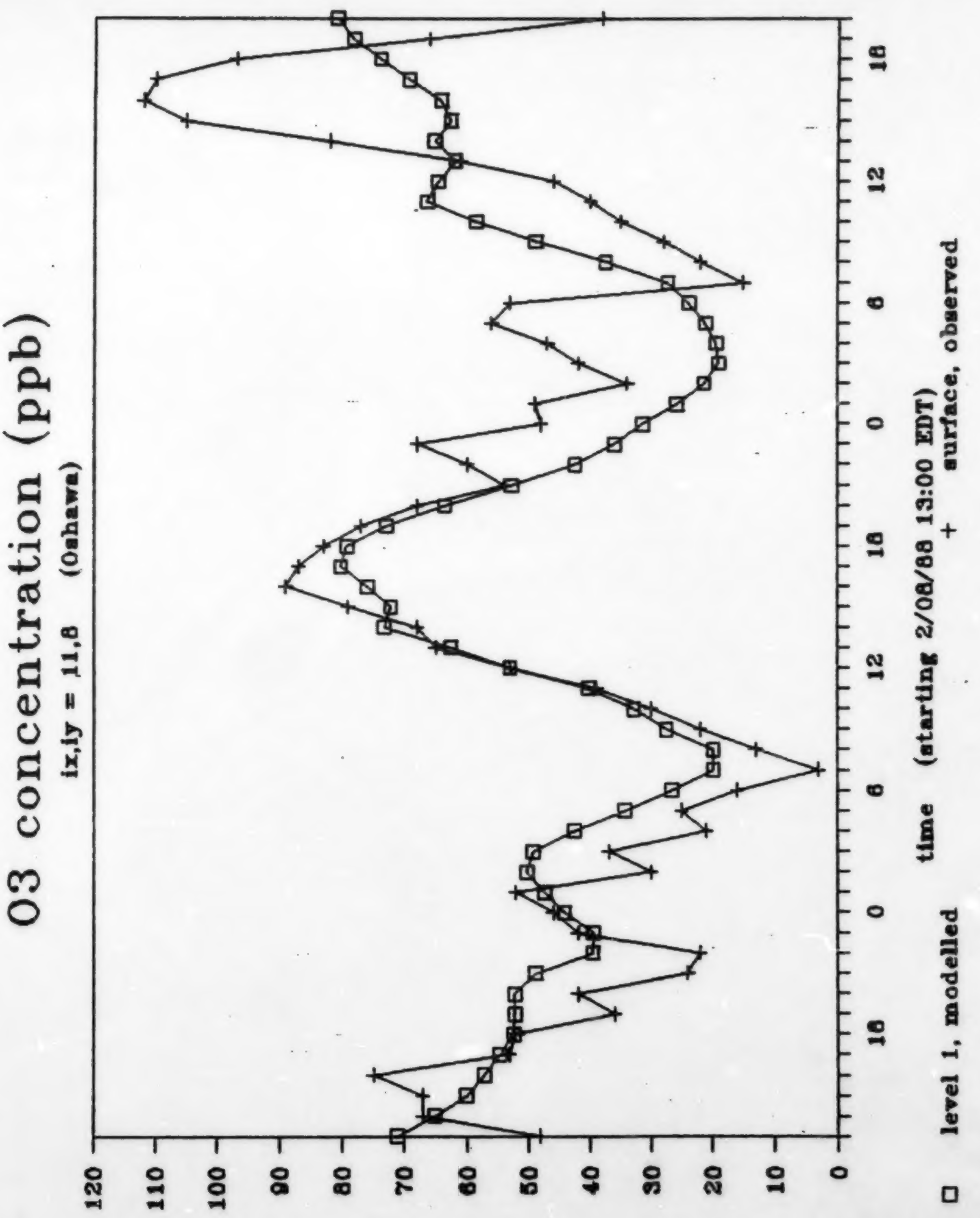
O3 concentration (ppb)
ix,iy = 11,8
(Oshawa)
120
110
100
90
80
70
60
50
40
30
20
10
0
18
0
6
12
18
0
6
12
18
time (starting 2/08/88 13:00 EDT)
□ level 1, modelled
+ surface, observed

Figure 116